Changing dynamics of Alaskan peatlands in the continuous permafrost zone

Liam Taylor

Submitted in accordance with the requirements for the degree of Master of Science by Research

The University of Leeds

School of Geography

September 2018

The candidate confirms that the work submitted is their own, except where work which has formed part of jointly authored publications has been included. The contribution of the candidate and the other authors of this work has been explicitly indicated below. The candidate confirms that appropriate credit has been given within the thesis where reference has been made to the work of others.

The work in Chapter 2 has appeared in publication as follows, with additions for the format of the thesis:

Taylor, L.S., Swindles, G.T., Morris, P.J. and Gałka, M. 2019. Ecology of peatland testate amoebae from the Alaskan continuous permafrost zone. *Ecological Indicators*. **96**(1); pp.153-162. https://doi.org/10.1016/j.ecolind.2018.08.049

In this study, LST performed all laboratory and statistical analysis under supervision from GTS and PJM. LST, GTS and PJM designed the research. GTS and MG performed the fieldwork. MG identified contemporary plant species. LST wrote the final manuscript, with contributions from all other authors.

The work in Chapter 3 has been submitted for publication as follows, with additions for the format of the thesis:

Taylor, L.S., Swindles, G.T., Morris, P.J., Gałka, M. and Green, S.M. 2018. Evidence for ecosystem state shifts in Alaskan continuous permafrost peatlands in response to recent warming. *Quaternary Science Reviews*. Submitted; in review.

In this study, LST, GTS and PJM designed the research. GTS and MG performed the fieldwork. LST and SMG performed lead-210 analysis. LST performed all other laboratory, statistical and climate analysis under supervision from GTS and PJM. LST wrote the final manuscript, with contributions from all other authors.

Acknowledgements

I would like to thank my fantastic supervisors, Dr Graeme Swindles and Dr Paul Morris, for their invaluable support throughout my Masters by Research. Their passion for the project was infectious and I could always rely on them to re-ignite my enthusiasm for research after every supervisor meeting. I am lucky to have had their creativity, wisdom and patience to guide me through this project and to continually challenge me to achieve my best.

I am also grateful to the support of Dr Mariusz Gałka (Adam Mickiewicz University, Poland) and Dr Sophie Green (University of Exeter, UK), who it has been a pleasure to work with, and co-author publications from my research.

Thanks also to the University of Leeds Ecology and Global Change research group for a tuition fee bursary to part support my Masters by Research.

Abstract

Peatlands in the continuous permafrost region store globally important amounts of organic carbon, but the stability of this store is threatened by climate warming. Reconstructions from peatlands using sensitive indicators of environmental change, such as testate amoebae, offer insight into the way these ecosystems have responded to past climate changes throughout the late-Holocene. This thesis aims to use palaeoenvironmental reconstructions from two peatlands in the Alaskan North Slope, adjacent to Toolik Lake, to understand their recent past and predict future dynamics to projected warming. To do so, the ecology of testate amoebae from peatlands across the Alaskan North Slope was explored to identify the controlling variables in their distribution. Multivariate statistical analysis shows that pore water electrical conductivity (EC), a proxy for peatland trophic status, was the primary control on testate amoeba distribution, with water table depth (WTD) the secondary control. Two transfer functions were produced to reconstruct EC and WTD with good predictive power. Reconstructions identified that both peatlands at Toolik Lake were mostly moderately-wet, minerotrophic rich fens throughout the late-Holocene, but have undergone a rapid transition to dry, oligotrophic poor fens with post-1850 CE warming. Alongside this ecosystem state shift, there has also been a three-fold increase in carbon accumulation rate post-1850 CE. Overall, this thesis extends the utility of testate amoebae as hydrological indicators into continuous permafrost peatlands; and suggests that rapid ecosystem state shifts may have occurred with recent climatic warming, which may indicate increased rates of carbon sequestration in the future.

LIST OF FIGURES

LIST OF TABLES

1. INTRODUCTION

Global mean temperatures have risen by 0.85˚C from 1880 (Stocker et al., 2013). This warming is twice as fast in the Arctic compared to the global mean due to polar amplification mechanisms (Cohen et al., 2014), such as diminishing sea-ice and snow cover (Kirtman et al., 2013). By the end of the 21st Century, temperatures in the Arctic are projected to have risen by between 2.2 and 8.3°C (from a 1986-2005 baseline) as a result of anthropogenic activity (Collins et al., 2013). The impacts of a warmer Arctic include the irreversible loss of summer sea-ice (Wang and Overland, 2009), the northwards movement of ecosystems (Myers-Smith et al., 2011), and thawing of permafrost (ground that remains frozen for at least two consecutive years) (Camill, 2005; Jorgenson et al., 2006; Schuur and Abbott, 2011). Carbon stored in permafrost soils could be released with increased warming (Schuur et al., 2009), potentially contributing to a positive feedback mechanism of greenhouse gas release. In 2015, 196 countries pledged to match man-made carbon emissions to terrestrial carbon uptake in the Paris Agreement (United Nations, 2015), but the release of carbon from permafrost regions could compromise this balance. The Paris Agreement also aims to limit warming to 2˚C above pre-industrial temperatures by 2100. However, this may still commit to the loss of up to 40% of permafrost area (Chadburn et al., 2017).

1.1 – Permafrost peatlands

Permafrost regions in the Northern Hemisphere store approximately 1672 Pg (~ 50%) of global belowground organic carbon; of which 277 Pg is stored in peatlands (Tarnocai et al., 2009). Peatlands are landscapes primarily

composed of partially decomposed organic matter resulting from high water tables. In discontinuous, sporadic, and isolated permafrost, the insulating effect of peat allows the establishment of permafrost beneath them (Brown, 1968), where the presence of peat initiates permafrost aggradation (Zoltai, 1995). In the continuous permafrost zone, harsher conditions and extreme cold temperatures mean that peatlands are rarer. The full areal extent of Northern Hemisphere circumpolar peatlands in permafrost regions is approximately 1,378,222 km^2 (Table 1.1; Figure 1.1), with the majority (39%) in continuous permafrost. This is likely an underestimation of permafrost peatlands given the difficulty in classifying peat in this region with remote sensing (Xu et al., 2018).

Region	Permafrost Zone				Total (km^2)
	Continuous	Discontinuous	Sporadic	Isolated	
Alaska	6,395	34,332	15,444	0	*56,171*
Canada	114,693	94,573	112,589	32,303	*354,158*
Europe	928	7,248	1,650	40,794	*50,620*
Siberia	418,223	189,537	148,902	160,611	*917,273*
Total	*540,239*	*325,690*	*278,585*	*233,708*	***1,378,222***

Table 1.1 – Peatland extent (km^2) in each permafrost zone in the Northern Hemisphere circumpolar region. Peatland extent data is from Xu et al. (2018) and permafrost zones from Jorgenson et al. (2008). Continuous permafrost represents 90-100% coverage, discontinuous 50-90%, sporadic 10-50% and isolated 0-10% coverage.

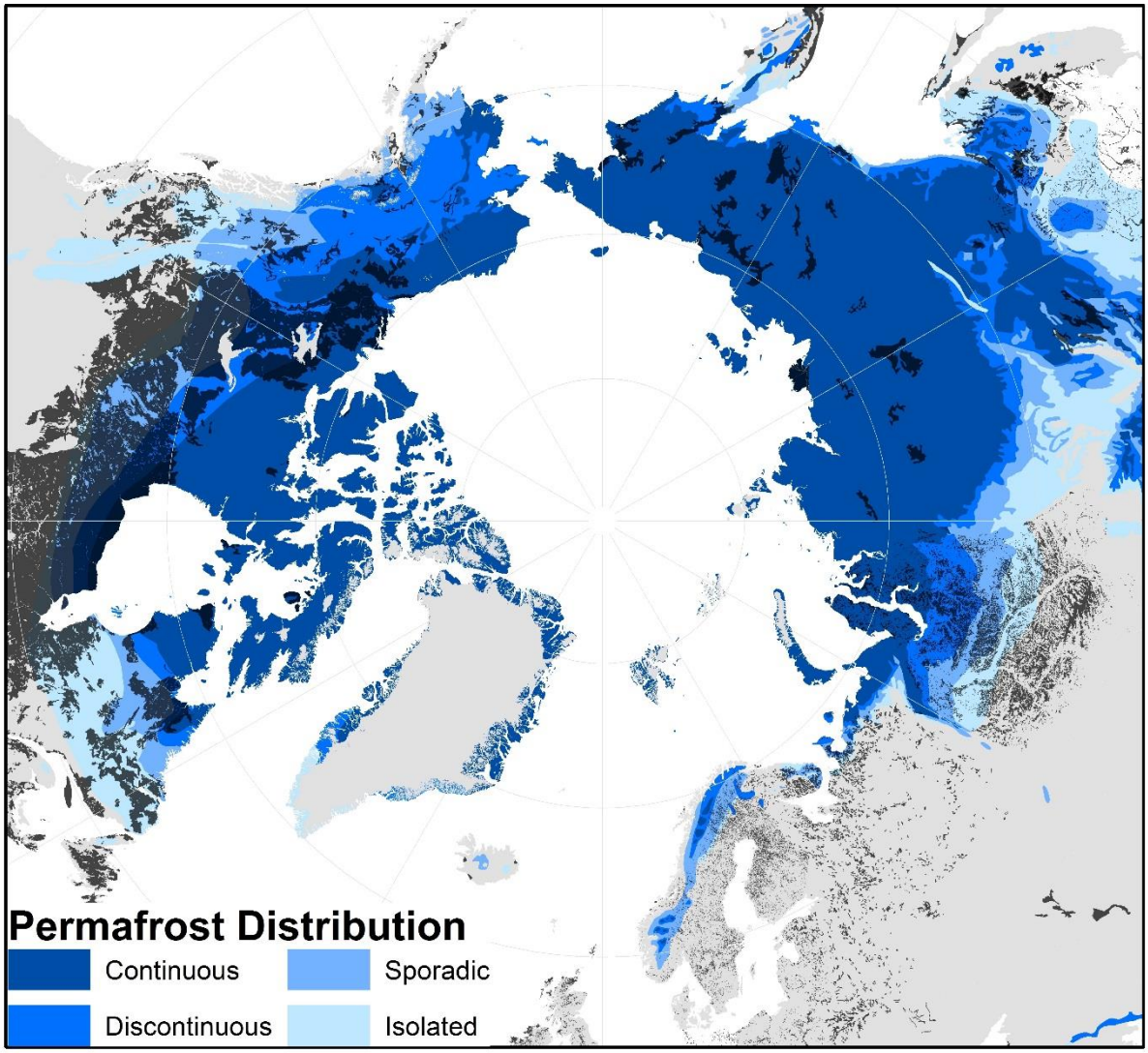

Figure 1.1 – Peatlands (black) in each permafrost zone in the Northern Hemisphere circumpolar region. Peatland extent data is from Xu et al. (2018) and permafrost zones from Jorgenson et al. (2008). Black shaded regions from Canada contain peatlands, but are not the sole land cover.

1.2 – Permafrost and Climate Change

Thaw in discontinuous permafrost regions leads to active layer (uppermost section of permafrost that thaws seasonally) thickening, thermokarst (landscape formed from permafrost thaw) expansion, tilted trees

and above-ground engineering problems in built structures (Osterkamp and Romanovsky, 1999; Osterkamp et al., 2000; Cooper et al., 2017). However, continuous permafrost responds differently to climate warming. While thermokarst lakes are expanding in Siberian continuous permafrost, they are declining in number in discontinuous, sporadic, and isolated permafrost regions (Smith et al., 2005). Furthermore, despite the larger extent of continuous permafrost, short-term carbon emissions are likely to be greater from discontinuous and sporadic permafrost (Schuur et al., 2013).

Future projections remain unclear as to whether the rate of permafrost degradation will continue to accelerate. In an extreme scenario, Lawrence and Slater (2005) hypothesise that up to 90% of near-surface permafrost area in the Northern hemisphere circumpolar region could have thawed by 2100, although the coupled global climate model they used has been criticised for over-exaggerating permafrost temperature increase (Burn and Nelson, 2006) and not accounting for high peat porosity (Yi et al., 2007). Delisle (2007) suggests that permafrost thaw will accelerate during the 21st century, but that this acceleration will largely be concentrated in discontinuous permafrost. Guo et al. (2018) show that permafrost degradation may be limited in forested regions compared to steppe ecosystems. Permafrost degradation therefore appears to be inevitable under continued warming, but the exact location and severity are still under debate.

Degradation of both permafrost and peatlands has been observed across the Arctic. Permafrost thaw is particularly concerning for the stability of

peatlands because it is likely to lead to a decreased areal extent of wetlands as a result of increased drainage (Avis et al., 2011). Canadian permafrost peatlands have changed rapidly since the end of the Little Ice Age (LIA), thawing at an accelerated rate (Camill, 2005), which has resulted in elevated release of carbon dioxide (CO_2) and methane (CH_4) (Turetsky et al., 2002). Wildfire in western Canada has also led active layer thickening, permafrost thaw, and the expansion of thermokarst bogs (Gibson et al., 2018). In Siberia, permafrost thaw is particularly concerning as CH_4 release from thermokarst lakes (Walter et al., 2006) following continued permafrost thaw (Pokrovsky et al., 2011) directly contributes to strengthening the greenhouse effect. These studies provide evidence that rapid warming of permafrost peatlands is occurring across the Arctic and the subsequent degradation is already having implications for their carbon budgets.

1.2.1 – Implications for the global carbon budget

Climate warming and permafrost thaw expose deep-carbon stores that may subsequently be released to the atmosphere. Once thawed, organic carbon from permafrost peatlands begins to decompose rapidly (Zimov et al., 2006) and is released to the atmosphere. The shallow water table of peatlands, combined with soil saturation from thaw, leads to anaerobic decomposition, which may result in the release of CH_4 – which has a greenhouse warming potential (over 100 years) that is 28 times greater than CO_2 (Myhre et al., 2013). CH_4 is released if the water table of permafrost peatlands rises, as decomposition of the active layer takes place anaerobically. Conversely, if the water table becomes deeper and decomposition is aerobic, CO_2 is released.

CH_4 production is therefore considered to be a function of thaw-induced wetland extent (Cooper et al., 2017). Under future warming, there is therefore the potential for a significant, positive feedback mechanism of irreversible CO_2 or CH_4 release from degrading permafrost peatlands.

However, other evidence may be used to paint a more optimistic picture. Peatlands are expanding northwards into the high-Arctic and experimental studies show that peat-building *Sphagnum* will enhance biomass production in response to warming (Dorrepaal et al., 2003). The enhancement of surface vegetation has caused rapid increases in carbon accumulation in northern peatlands in response to warming events throughout the Holocene (Yu et al., 2009). Payette et al. (2004) notes that increased productivity in peatland ecosystems following permafrost thaw offsets the carbon released to balance the carbon budget, although their study only observed discontinuous permafrost peatlands in Alaska. In a modelled study of all IPCC Representative Concentration Pathways (RCPs), Gallego-Sala et al. (2018) project that permafrost peatlands will become stronger carbon sinks with warming, although they acknowledge that this may be offset by carbon release from newly exposed organic matter. More biomass in high-latitude peatlands and drying due to climate change increases the susceptibility of these ecosystems to fire, and subsequently carbon release (Turetsky et al., 2015). As a result, there is no clear consensus as to whether Arctic peatlands will become net sources, or sinks, of carbon with projected climatic warming (Figure 1.2). There are also few palaeo or observational studies, particularly in continuous permafrost, to understand the dynamics of these systems.

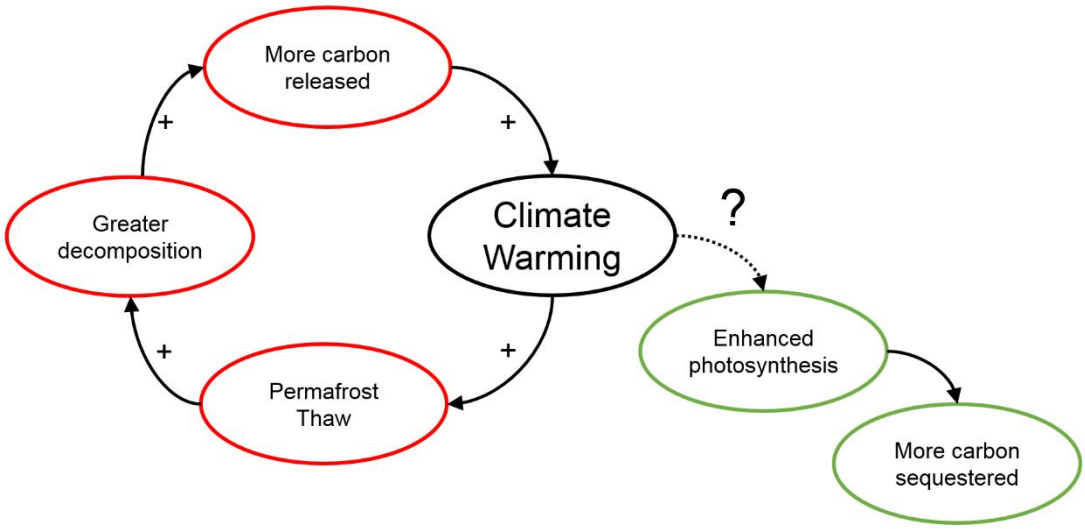

Figure 1.2 – Conceptual diagram of possible climate feedbacks relating to permafrost peatlands.

1.2.2 – Alaskan permafrost peatlands

Alaskan permafrost peatlands are degrading rapidly as a result of changing climate (Payette et al., 2004), which is believed to reduce their efficacy as a carbon sink (O'Donnell et al., 2012). Peatlands are found across Alaska, in a variety of trophic statuses. Ombrotrophic bogs and minerotrophic fens are found in the south, the Aleutian Arc, and across the North Slope (Rooney-Varga et al., 2007; Treat et al., 2014). Most Alaskan peatlands initiated during a Holocene warm period around 8,600 years ago, with rapid carbon accumulation (Jones and Yu, 2010). The landscape of the Alaskan North Slope is dominated by thermokarst (Figure 1.3).

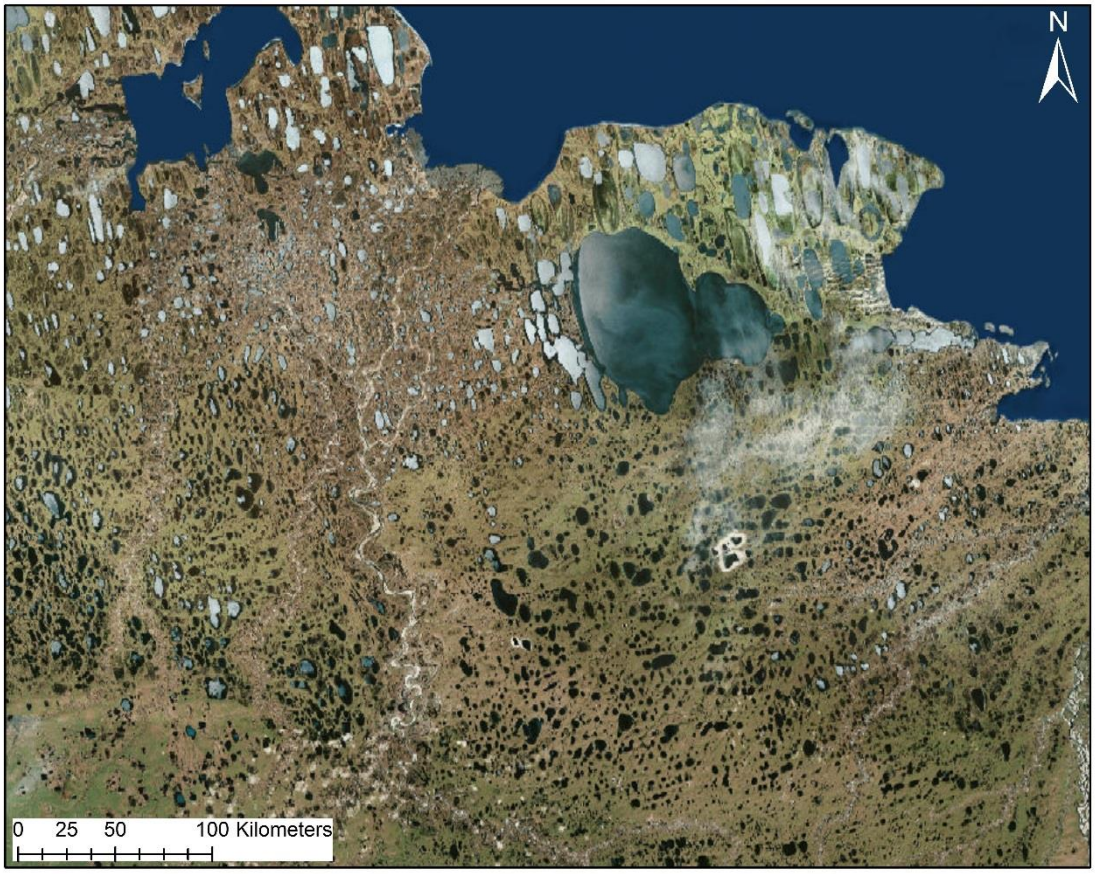

Figure 1.3 – Thermokarst landscape of the Alaskan North Slope.

1.3 – Climate drivers of change

The influence of the climate on peatlands is complex, and there is a relatively small body of literature focussed on understanding the way that peatlands have responded to past changes in the climate. Charman et al. (2009) examined the response of bog surface wetness with temperature and precipitation records from the UK, identifying that bog surface wetness is primarily driven by precipitation and forced by oceanic and atmospheric changes in the North Atlantic. The most important driver of carbon accumulation rate in peatlands from North America is temperature, with vegetation succession also a key influence over short time scales in localised areas (Charman et al., 2015). In discontinuous permafrost peatlands from

Abisko, Sweden, Gałka et al. (2017) note that long-term carbon accumulation rates are driven by local vegetation changes, which may in turn be linked to the climate.

While temperature has been shown to drive carbon accumulation rate (CAR), Zhang et al. (2018a) note the importance of precipitation and evapotranspiration that also arises from recent climate change. They suggest one of two possible likelihoods of future hydrology whereby either permafrost thaw leads to wetter surface conditions (also proposed by Swindles et al., 2015a), or increased evapotranspiration will cause drying. Winter precipitation and snow depth positively correlates with the ground temperature of permafrost peatlands (Sannel et al., 2016), which may further exacerbate permafrost thaw as high-latitude regions can be expected to receive more precipitation with future climate change (Trenberth, 2011). Given how important hydrology is to the CO_2 or CH_4 production from decomposition, and the ability for these systems to sequester carbon, the future carbon budget of permafrost peatlands is intricately linked to their hydrology.

1.4 – Reconstructing changing dynamics of permafrost peatlands during the Holocene

Peatlands can provide detailed records of Holocene ecosystem change, owing to anoxic conditions that allow for the preservation of sub-fossilised organic matter. From a peat core, it is possible to reconstruct palaeohydrology and palaeoenvironmental change, sometimes back to the initiation of the peatland. This is possible due to a number of biological (plant macrofossils,

testate amoebae), organic (peat humification, CAR), and inorganic (loss-on-ignition, geochemical composition) proxies.

Down-core changes in peatlands can typically be dated by using a combination of radiocarbon (^{14}C), lead-210 (^{210}Pb) and tephrochronology. Accelerator Mass Spectrometry (AMS) improves the precision of ^{14}C dating by using ultrafiltration to remove contaminants, allowing high temporal resolution chronologies of Holocene peat cores. The 5,730 year half-life of ^{14}C allows a maximum reliable dating range of around 50,000 years. Tephra (volcanic ash) can also be used to date peat cores (e.g. Payne and Blackford, 2008; Payne et al., 2008), using the unique chemical fingerprint of each tephra to establish precise markers based on known volcanic events in the wider region. ^{210}Pb provides precision analysis of how peatlands have responded to climate warming over the last few decades, due to its short (22.3 year) half-life. While there are some issues regarding the mobility of lead in peat (Urban et al., 1990), this is likely limited in continuous permafrost.

Most northern hemisphere permafrost peatlands initiated following the recession of glaciers and ice sheets after the Last Glacial Maximum in response to warming temperatures (Morris et al., 2018). This means that these peatlands contain potential archives of palaeoenvironmental and palaeoclimatological change from initiation in the Early Holocene to the present day.

1.5 – Testate amoebae

Testate amoebae are single-celled protists that form a hard shell (test) around their living cell, with an aperture that allows exchange with the external environment. Testate amoebae are found in soils, peats, vegetation and water bodies across Earth. Over 2000 species of testate amoebae have been officially classified (Mitchell et al., 2008a), each unique in morphology, colour, size and other visual characteristics. This makes it easy to identify one species from another under a high powered light microscope at 200–400 × magnification. Most species occupy a narrow range of environmental and hydrological tolerances. In some regions, testate amoebae distribution is sensitive to the depth of the water-table (e.g. eastern North America (Booth, 2008), Northern Ireland (Swindles et al., 2009) and New Zealand (Wilmshurst et al., 2003)), and in others, variables such as pH also have a large influence on distribution (e.g. Jura mountains (Mitchell et al., 1999); Lake Superior (Booth, 2001), and Florida Lakes (Escobar et al., 2008)). Testate amoebae have a lifespan of only a few days (Wilkinson and Mitchell, 2010), but their test allows them to be preserved in peats for millennia (Hendon and Charman, 1997).

Given the ease of identification, narrow environmental tolerances and long preservation in peat, testate amoebae are a popular method to reconstruct palaeohydrological conditions of peatlands across the world. Testate amoeba-based reconstructions have predominantly taken place in temperate and tropical regions due to their relative ease of access, but can theoretically be used anywhere they are found. In the tropics, testate amoebae have been used to reconstruct WTD largely in Amazonian peatlands (Swindles et al., 2014) identifying ecosystem state shifts towards ombrotrophy (Swindles et al., 2018).

The application of testate amoebae is more widespread in temperate regions, such as China (Qin et al., 2013), the UK (Turner and Swindles, 2012) and America (Charman and Warner, 1992).

A transfer function is required in order to use testate amoebae to quantitatively reconstruct palaeohydrological change. The input to a transfer function is contemporary testate amoeba abundance data and peat hydrological conditions from a variety of peatlands across the wider region. The output is an optimum and tolerance breakdown of each species against each measured environmental variable. This technique therefore relies on the principle of uniformitarianism, assuming that modern species-environment relationships are representative and reflective of past relationships (Mitchell et al., 2008a). Taking contemporary samples from a wide spatial area, which encompasses a broad range of taxa, makes it more useful to apply to the fossil record (Charman et al., 2007; Booth, 2008). When performing a palaeo reconstruction, the selected statistical model weights each taxa in a sample on abundance to reconstruct environmental variables per sample. However, while they are an accurate tool to reconstruct palaeoenvironmental change, Väliranta et al. (2012) stress the importance of multi-proxy reconstructions to reduce uncertainties from a single technique.

1.5.1 – Application to permafrost peatlands

Recently, testate amoebae have been used to reconstruct palaeohydrology in peatlands from permafrost regions. Existing studies of contemporary testate amoeba ecology are limited to discontinuous and sporadic permafrost. There have been a small number of investigations into

the ecology of testate amoebae in continuous permafrost peatlands. Mitchell (2004) identified that testate amoebae at Toolik Lake, Alaska, are highly sensitive to nitrogen and phosphorus fertilisation. Gałka et al. (2018) attempted to use testate amoebae to reconstruct palaeohydrology in continuous permafrost, using wetness indicators as a measure of change. They identify a transition at ~1950 CE from *Centropyxis aerophila* domination to *Hyalosphenia elegans*, indicating wetter conditions. Since ~2000 CE, *Corythion dubium* has become the dominating taxa, indicating a rapid recent transition back to dryness.

Two testate amoeba-based transfer functions currently exist from permafrost peatlands – in isolated and sporadic permafrost in northeast Canada (Lamarre et al., 2013), and discontinuous permafrost in sub-Arctic Sweden (Swindles et al., 2015b). Both studies identify that the dominant control on testate amoeba distribution in their respective regions is water-table depth (WTD). There is currently no method to quantitatively reconstruct palaeohydrology using testate amoebae in any continuous permafrost region, nor any variable other than WTD in any permafrost peatlands.

1.6 – Research Aims

This study was driven by a number of research questions that arose from gaps in the literature. Existing studies show that continuous and discontinuous permafrost peatlands differ in many important ways, yet there have been no regional scale investigations into testate amoeba ecology in continuous permafrost. Additionally, there have been no studies into how

palaeohydrological changes in continuous permafrost are influenced by the climate, nor whether these ecosystems will sequester more carbon with future warming. This thesis therefore aims to address the following research questions:

- What are the dominant environmental controls on the distribution of testate amoebae across the Alaskan North Slope?
- Are testate amoebae effective indicators of palaeohydrological change in the continuous permafrost zone?
- How have Alaskan peatlands in the continuous permafrost zone changed in response to late-Holocene climate change?

1.7 – Research Strategy

To be able to quantify palaeoenvironmental peatland change in the Alaskan continuous permafrost zone throughout the late-Holocene, it is first necessary to develop transfer functions that are appropriate to the environment. This study will therefore begin by exploring the ecology of testate amoebae from peatlands across the Alaskan North Slope, producing transfer functions from hydrological variables that are most significant in controlling their distribution. From this, it is then possible to quantify palaeoenvironmental change in the variables from the transfer functions, in addition to dry bulk density, loss-on-ignition and carbon accumulation to infer how hydrological changes affect the ability of the peatland to sequester carbon. To identify whether any palaeoenvironmental changes were driven by the climate, ^{14}C and ^{210}Pb dating will be performed and the resulting age profile correlated against temperature and precipitation records over the late-Holocene.

2. ECOLOGY OF PEATLAND TESTATE AMOEBAE FROM THE ALASKAN CONTINUOUS PERMAFROST ZONE

2.1 - Introduction

Climate warming over the last century has been most rapid at high-latitudes (Stocker et al., 2013). Permafrost temperatures in the Northern Hemisphere have increased by as much as 2°C since 1850, with the continuous permafrost zone warming most rapidly (Vaughan et al., 2013). Peatlands in permafrost areas are especially vulnerable to rapid change and anthropogenic warming (Minayeva et al., 2016) and there is evidence that they are thawing at an accelerating rate (Payette et al., 2004). Arctic peatlands are a major global carbon store of ~277 PgC and occupy 18.9% of Northern circumpolar permafrost area (Tarnocai et al., 2009). Concern exists that as permafrost peatlands thaw, a large proportion of their carbon stock may become unstable and return to the atmosphere (Routh et al., 2014; Schuur et al., 2009). Alternatively, surface peat may insulate permafrost below and limit such degradation (Mann et al., 2010). Palaeoecological approaches have been used to identify recent hydrological changes in domed permafrost peatlands, including transition to inundated Arctic fen systems (Swindles et al., 2015a; Gałka et al., 2017). The associated changes in vegetation structure (Christensen et al., 2004) and hydrology (Quinton et al., 2011), combined with continued warming, are likely to promote elevated CH_4 release from degrading permafrost peatlands, with feedbacks to the global climate system.

Permafrost peatlands are predominantly found in Eurasia and Canada, but remain relatively unstudied given their remoteness. In Alaska, peatlands cover at least 78,000 km^2 (Xu et al., 2018) and are found across the Pacific coast, Aleutian Arc and North Slope. Alaskan peatlands hold around 1% of carbon stored in Arctic peatlands (Tarnocai et al., 2009), but are rapidly warming owing to rising air temperatures. This has caused a 1-2°C warming of surface permafrost in the Northern Brooks Foothills since 1977 (Osterkamp, 2007; Osterkamp, 2005; Osterkamp and Romanovsky, 1999). Warming and degradation of Alaskan permafrost peatlands may be broadly similar to changes observed in peatlands across the wider Arctic, yet reliable proxy methods to reconstruct past changes are incomplete for continuous permafrost regions. Indeed, no such contemporary proxy record to reconstruct palaeohydrology exists in any continuous permafrost peatlands globally, despite their vital role in the carbon cycle and the importance of hydrology in carbon accumulation (Charman et al., 2013; Holden, 2005; Belyea and Malmer, 2004).

Testate amoebae are single-celled protists that have been used extensively to reconstruct peatland palaeohydrology in many regions of the world (e.g. Amesbury et al., 2016; Swindles et al., 2015a; Swindles et al., 2014; Lamentowicz et al., 2008; Payne and Mitchell, 2007; Wilmshurst et al., 2003). Testate amoebae form hard shells (tests) that are often well preserved in Holocene peats (Mitchell et al., 2008a). Species-level associations with a limited range of environmental and hydrological conditions (Charman and Warner, 1992) mean that subfossil testate amoeba assemblages have been

widely utilised in palaeoenvironmental reconstructions, particularly for water-table depth (WTD). Although testate amoebae have been used to reconstruct hydrological change in discontinuous permafrost peatlands across Europe (Zhang et al., 2017; Swindles et al., 2015b) and Canada (Lamarre et al., 2013), little is known about their ecology and effectiveness as ecological indicators in continuous permafrost. Previous studies have reported the presence of testate amoebae in both the contemporary and fossil record of continuous permafrost (e.g. Müller et al., 2009; Mitchell, 2004). However, the potential to use testate amoebae as part of a multi-proxy study in palaeohydrological reconstruction has not yet been fully developed in the continuous permafrost zone.

Our aim is to conduct the first detailed study of testate amoeba ecology in continuous permafrost peatlands. In this investigation, we:

i. Examine the ecology of testate amoebae in continuous permafrost peatlands from the North Slope, Alaska;
ii. Produce transfer functions that can be used to reconstruct the most important environmental driver(s) of testate amoeba distribution and;
iii. Test the hypothesis that WTD is the primary control on the distribution of testate amoebae species in continuous permafrost peatland ecosystems.

2.2 - Study Sites

Our study comprises five sites across the Alaskan North Slope, within a 55 km radius of Toolik Field Station (Figure 2.1; Table 2.1), and encompasses a range of ecological and hydrological conditions. The five sites span a large

trophic gradient, from ombrotrophic bogs to minerotrophic fens, with pore water electrical conductivity (EC) ranging from 37 µS cm^{-1} to 1176 µS cm^{-1}. The landscape is Arctic acidic tundra, with thermokarst lakes and palaeoglaciological features remnant of the last ice age (Gałka et al., 2018; Hinkel et al., 1987; Hamilton, 1986). Active layer (seasonally thawed permafrost) thickness of the continuous permafrost at Toolik is between 40 and 50 cm (Brown, 1998). Air temperature is a key control on seasonal permafrost thaw in the Alaskan North Slope, although topography can create local spatial variability between sites (Hinkel and Nelson, 2003).

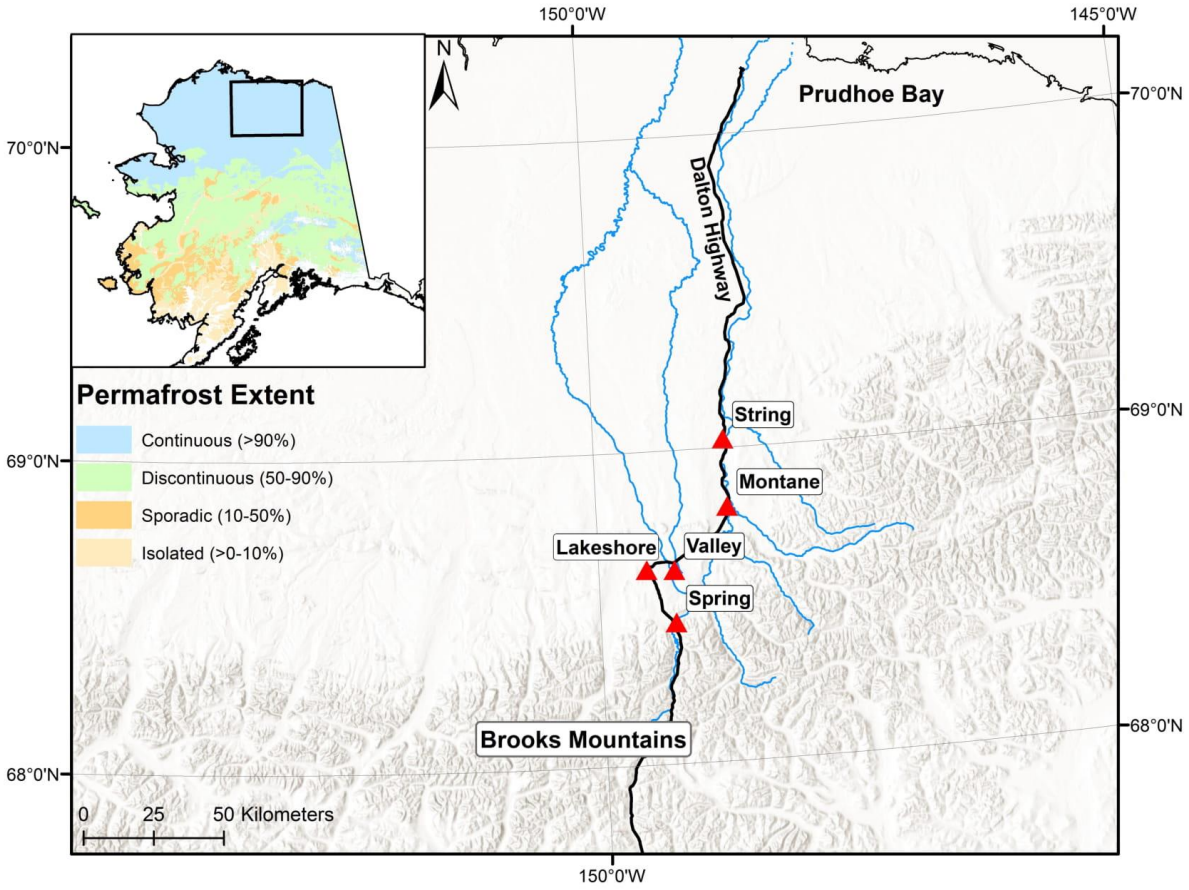

Figure 2.1 – Map outlining the five sites studied on the Northern Brooks foothills, Alaska. All sites are peatlands within the continuous permafrost zone (Jorgenson et al., 2008).

Site	Latitude (°N)	Longitude (°W)	Elevation (m)	WTD range (cm)	pH range	EC range (µS cm^{-1})	Most common plant species (% abundance)
Montane	68.814	148.841	451	16 – 56	5.82 – 6.50	224 – 509	*T. nitens* (70%)
Spring	68.452	149.346	804	0 - 25	6.96 – 7.95	257 – 505	*T. nitens* (45%)
Valley	68.620	149.338	864	4 - 53	5.41 – 6.66	595 – 1176	*S. terres/squarrosum* (85%)
String	69.029	148.839	405	0 - 54	6.40 – 6.95	881 – 1124	*A. glaucophylla* / *S. scorpioides* (35%)
Lakeshore	68.624	149.580	753	0 - 30	5.17 – 6.84	37 – 156	*S. cossoni* (45%)

Table 2.1 – Site overview and hydrological conditions. Full details of plant species are given in Appendix A.

Peatlands around Toolik Lake initiated between 8 and 10 kyr in the Brooks foothills (Reyes and Cooke, 2011; Jones and Yu, 2010) as a result of rapid warming (Mann et al., 2010; Morris et al., 2018). Palaeoecological studies have used macrofossil and pollen records to identify the vegetation succession in this region (Gałka et al., 2018). Gałka et al. (2018) also used outline testate amoeba data to infer palaeohydrological changes. However, no quantitative reconstruction of past conditions was possible because no suitable transfer function existed at the time.

2.3 - Methods

We collected 100 surface moss samples, 20 each from five peatlands across the Alaskan North Slope, reflecting a range of hydrological conditions. A well was augered at each sampling point and water level measured at regular intervals until it equalised to determine depth to water table. pH and EC of pore water from each well were measured using calibrated field meters. Approximately 5 g of each sample was weighed, dried at 105°C overnight, re-weighed to determine gravimetric moisture content (MC), and ignited in a muffle furnace at 550°C for at least 4 hours to determine loss-on-ignition (LOI)

(Chambers et al., 2011). We used the EC of pore water as a proxy for peatland nutrient status (following Lamentowicz et al., 2013).

We isolated testate amoebae following Booth et al. (2010). Approximately 2 cm^3 of each moss sample was placed in boiling water for 15 minutes, shaken, passed through a 300 µm sieve and back-sieved through a 15 µm mesh before being stored in a 4°C cold store. Sub-samples were taken and used to prepare microscope slides which were subsequently examined under a high-power transmitted light microscope at 200 and 400 x magnification. We aimed to count at least 100 individuals per sample, in addition to *Euglypha* sp., *Trinema* sp., and *Tracheuglypha* sp., as these species do not preserve well in the subfossil peat record (Swindles and Roe, 2007a; Mitchell et al., 2008b). Four samples had fewer than 100 individuals (*n* = 97, 96, 88, 41), but we retained samples with counts 50-100 as they have been deemed statistically reliable when diversity is low (Swindles et al., 2007b). Individuals were catalogued to species level or 'type' (lowest division possible) using identification keys from Charman et al. (2000), Booth and Sullivan (2007) and online guides (Siemensma, 2018).

Statistical analysis was performed in R version 3.4.1. (R Core Team, 2014), using the *vegan* (Oksanen et al., 2017) and *analogue* (Simpson and Oksanen, 2016) packages. Taxa were selected to isolate those that appear in abundance (≥ 2%) in any one sample to reduce the influence of rare taxa (following Swindles et al., 2009). Detrended Correspondence Analysis (DCA) revealed that the data are characterised by long axis gradient length (axis 1 =

4.19, axis 2 = 3.13), which means that an individual testate amoeba species will likely favour one end of the gradient over the other. Therefore Canonical Correspondence Analysis (CCA) was subsequently performed on the 100 samples. Given the conflicting criticisms of CCA surrounding its slight bias towards rare taxa (see Greenacre, 2013), we also performed ordination with non-metric multidimensional scaling (NMDS) with the Bray-Curtis dissimilarity index and redundancy analysis (RDA) with Hellinger transformed taxon data.

Transfer functions were developed using C2 version 1.7.5 (Juggins, 2007). Weighted Averaging (WA), Weighted Averaging Partial Least Squares (WAPLS) and Maximum Likelihood (ML) transfer functions were developed and tested with the full dataset to identify the best performing method. R^2, RMSEP, and maximum bias values were used as metrics of performance. ML was dismissed due to relatively poor performance. WA and WAPLS were selected as the best performing models and cross-validated with the 'leave-one-out' method and sites with residual values ≥ 20% of the range (EC: 228 μS cm^{-1}; WTD: 11 cm) removed. The ≥ 20% threshold is used as the standard cut-off in the development of testate amoeba-based transfer functions (e.g. Charman et al., 2007; Payne and Mitchell, 2007; Swindles et al., 2015b; Amesbury et al., 2016). Optima and tolerance statistics for each taxa were calculated through WA.

We also explored how the host vegetation at each site was influenced by contrasting environmental conditions in our peatlands. Additional sub-samples were suspended in deionised water and the host vegetation was

identified with light microscopy at 200 × magnification. Individuals were catalogued to species or 'type' level using identification guides from Flora of North America North of Mexico (2007, 2014), Hedenäs (2003) and Smith (2004). Nomenclature follows Walker et al. (1994) for vascular plants and Flora of North America North of Mexico (2007, 2014) for bryophytes.

2.4 - Results

2.4.1 - Relationship between environmental variables and species distribution

We identified 94 testate amoebae taxa from 29 genera and a total count of 15,723 individuals (examples are given in Figure 2.2). The most abundant species were *Centropyxis aerophila*, *Euglypha* degraded (individuals from the *Euglypha* genus that were not sufficiently well preserved for species-level identification), *Cyclopyxis eurystoma*, *Phryganella acropodia*, *Trinema lineare* and *Centropyxis ecornis*. CCA shows that EC, LOI and WTD are the most important variables in controlling the distribution of testate amoebae species in these sites ($p < 0.001$) (Figure 2.3; Table 2.2). NMDS supports this, also identifying EC as the dominant control on testate amoebae distribution (Figure 2.4; Table 2.2). Partial CCAs show that EC explains 25.0% of data variance ($p < 0.001$), WTD explains 16.5% ($p < 0.001$) and MC explains 13.3% ($p < 0.001$). RDA further supports the premise that the trophic gradient (for which EC is a proxy) is controlling species distribution. We also found a significant correlation between pH and EC ($r = 0.499$, $p < 0.1$), which is not unexpected as pH is also indicative of peatland trophic status (Gorham et al., 198

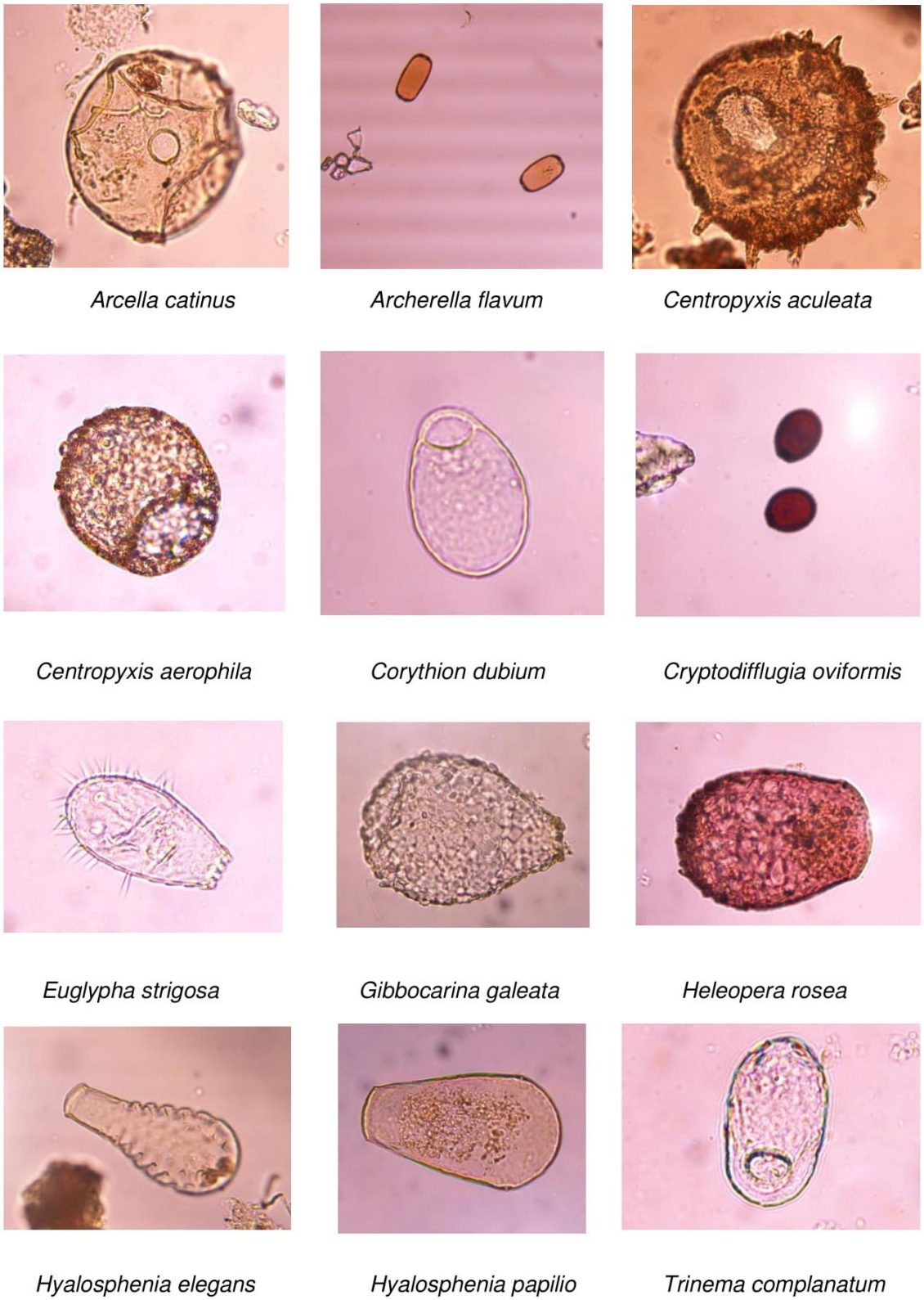

Figure 2.2 – Examples of identified testate amoebae individuals from peatlands on the Alaskan North Slope.

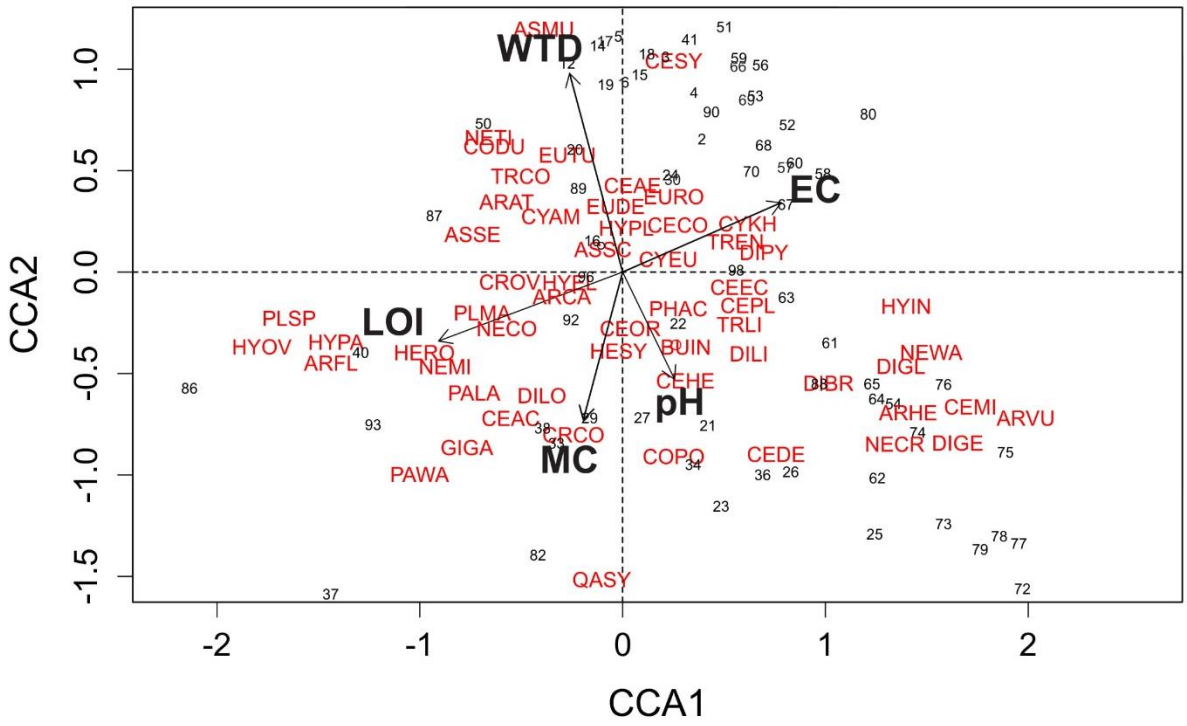

Figure 2.3 – CCA plot highlighting key controls on testate amoebae distribution. The environmental controls are EC (electrical conductivity), WTD (water table depth), LOI (loss-on-ignition), MC (moisture content) and pH. Species codes are given in Table 2.4.

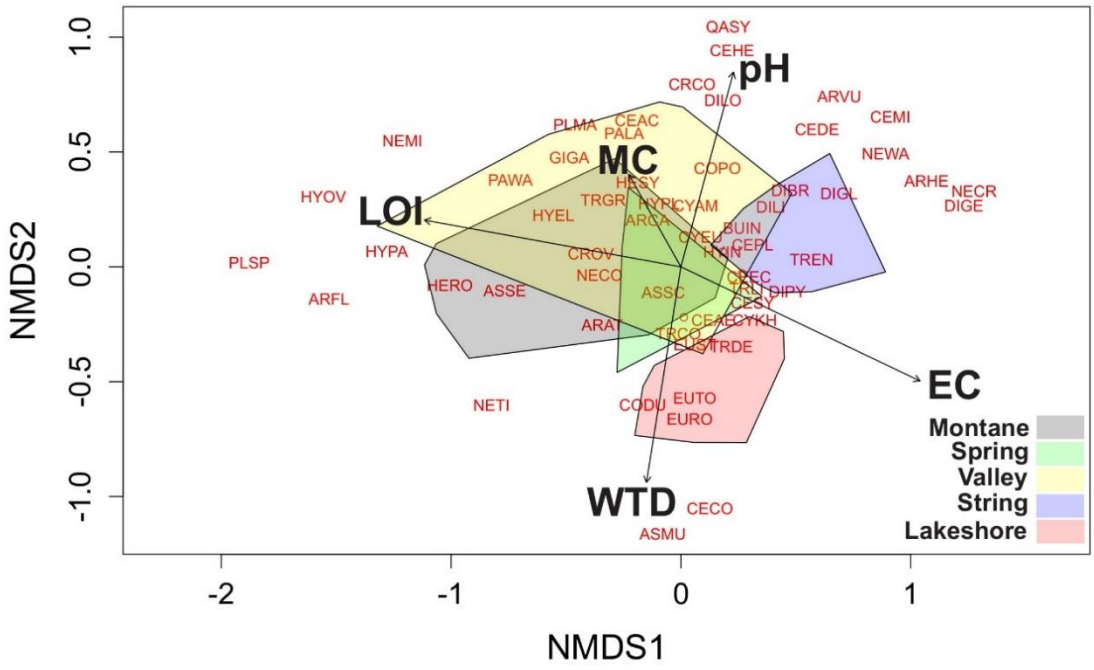

Figure 2.4 – NMDS plot highlighting key controls on testate amoebae distribution. The environmental controls are EC (electrical conductivity), WTD (water table depth), LOI (loss-on-ignition), MC (moisture content) and pH. Species codes are given in Table 2.4.

Variable	**NMDS**				**pCCA**	
	NMDS1	NDMS2	R^2	Significance	Variance explained	Significance
pH	0.261	0.966	0.289	$p < 0.001$	10.07%	$p = 0.005$
EC	0.902	-0.431	0.499	$p < 0.001$	24.98%	$p < 0.001$
WTD	-0.158	-0.988	0.339	$p < 0.001$	16.54%	$p < 0.001$
MC	-0.491	0.871	0.080	$p = 0.021$	13.26%	$p < 0.001$
LOI	-0.984	0.179	0.483	$p < 0.001$	8.93%	$p = 0.04$

Table 2.2 – Ordination statistics of environmental variables.

The most abundant plant species at sampling sites included *Warnstorfia cf. exannulata*, *Andromedia glaucophylla*, *Campylium stellatum*, *Cinclidium stygium*, *Scorpidium cossoni, Tomentypnum nitens, Sphagnum teres,* and

Andromedia glaucophylla (Appendix A). Forty plant taxa were identified from a total of 27 genera. Partial CCAs show that all variables are highly significant ($p < 0.001$). The most important variables are wetness indicators, as partial CCAs show that MC explains 5.23% of data variance and WTD explains 3.02%. There is a significant correlation (Pearson's $r = 0.197$, $p = 0.0497$, $n = 100$) between the species richness of testate amoebae and plants.

Mean EC at each sampling location is strongly correlated (Pearson's $p < 0.001$) with LOI, and WTD with MC (Pearson's $p < 0.001$), emphasising two strong hydrological gradients of trophic status and wetness in our sites. We identified a statistically significant difference in testate amoebae communities (ANOSIM $r = 0.428$, $p < 0.001$; PERMANOVA $r = 0.303$, $p < 0.001$) and plant communities (ANOSIM $r = 0.730$, $p < 0.001$; PERMANOVA $r = 0.757$, $p < 0.001$) among sites (Appendix B).

2.4.2 - Transfer function development

Transfer functions were developed for WTD (TF_{WTD}) and EC (TF_{EC}), because both variables were highly significant in ordination. R^2_{JACK} and $RMSEP_{JACK}$ values were used to identify the best performing models. For TF_{WTD}, WAPLS component 2 performed better than WA.inv (Table 2.3) after removing large residuals (> 11 cm). WA.inv did not perform well at either end of the WTD range, with high residuals at extreme wet and dry sites. We removed 31 samples to improve performance ($R^2_{JACK} = 0.842$, $RMSEP_{JACK} = 6.66$ cm, Maximum bias = 14.30 cm, $n = 69$). One species (*Arcella vulgaris*), present in one sample at 2.44% abundance, was also removed due to its high

residual value. Key dry indicator species include *Assulina muscorum*, *Nebela tincta*, *Corythion dubium* and *Euglypha spp.* Wet indicator species include *Netzelia corona*, *Centropyxis declivistoma*, *Conicocassis pontigulasiformis* and *Difflugia bryophila* (Figure 2.5). Optimum and tolerance statistics can be found in Figure 2.6.

	TF_{WTD}			TF_{EC}		
Model	R^2_{JACK}	$RMSEP_{JACK}$	Max Bias	R^2_{JACK}	$RMSEP_{JACK}$	Max Bias
Initial transfer function performance						
WAPLS	0.414	14.76	17.56	0.493	249.69	331.68
WA.inv	0.414	14.76	17.60	0.382	273.61	444.14
ML	0.471	16.20	19.38	0.452	269.63	478.26
After removing high residual sites (< 20%)						
WAPLS	0.842	6.66	14.30	0.756	146.04	188.82
WA.inv	0.734	9.36	14.18	0.680	151.52	606.32

Table 2.3 – Transfer function performance metrics. WAPLS statistics are all reported from the second component, as this was the best performing.

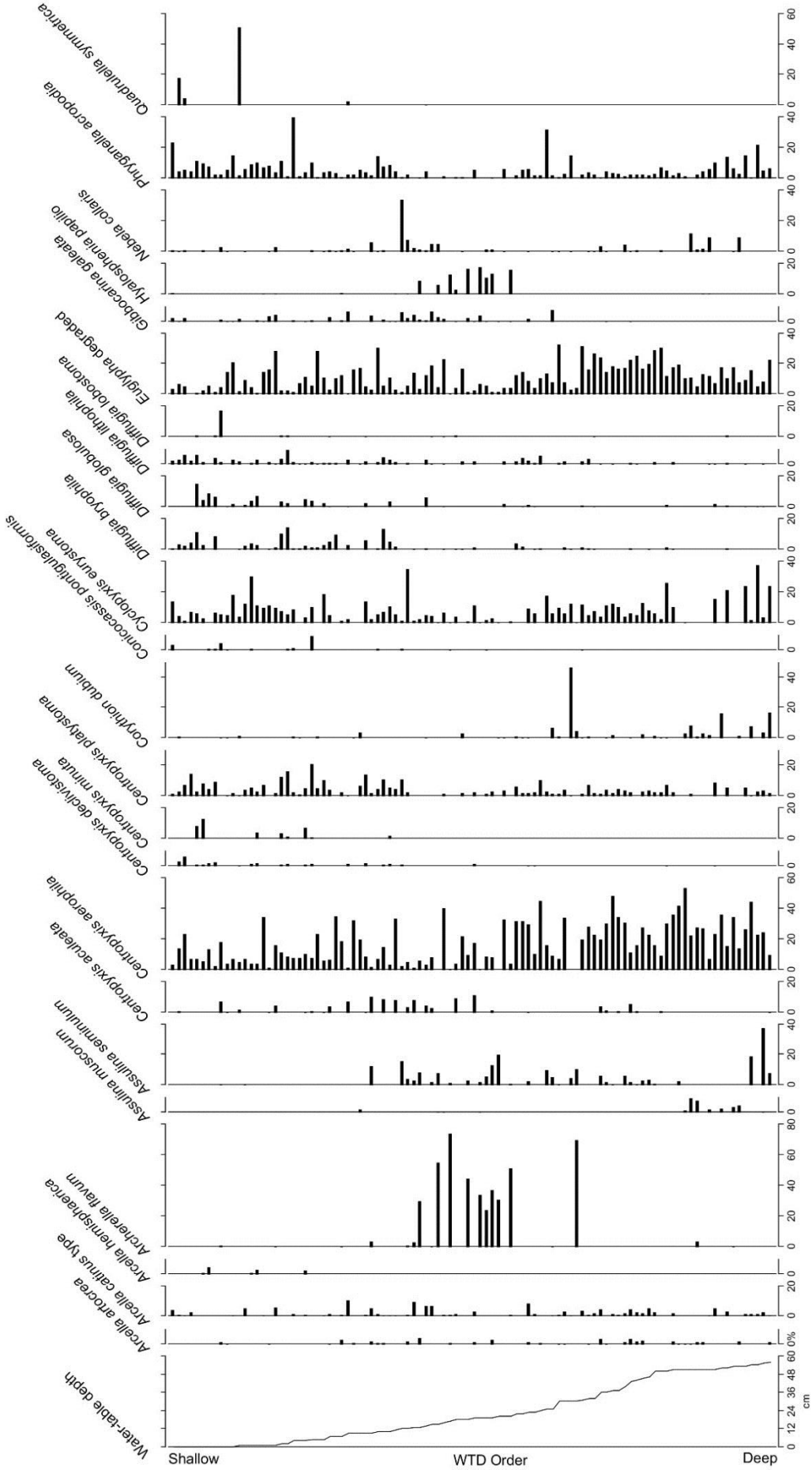

Figure 2.5 – Percentage abundance of selected testate amoebae taxa that indicate a range of WTD conditions, ranked by observed WTD.

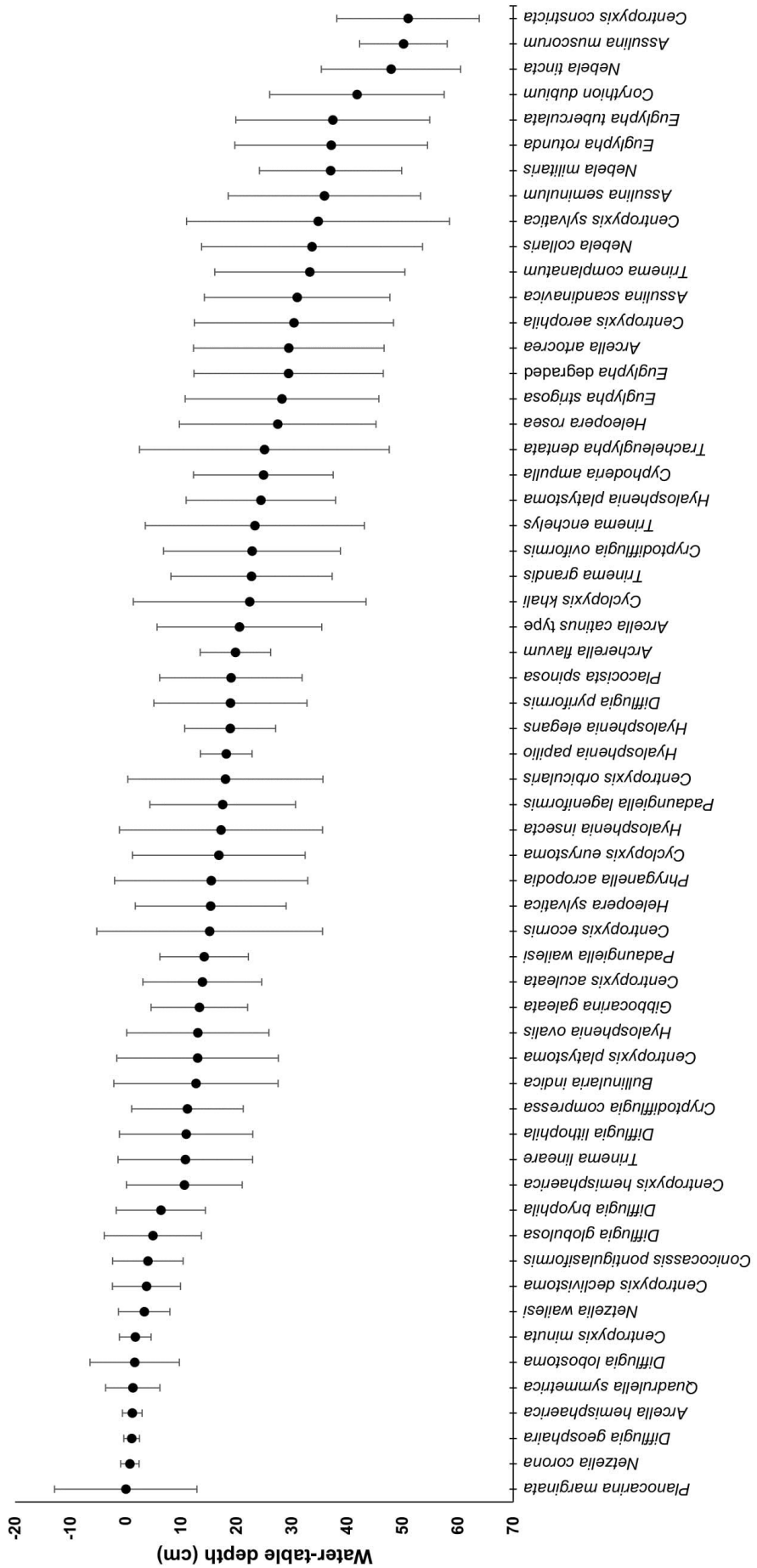

Figure 2.6 – WTD tolerance and optima statistics for testate amoebae calculated through Weighted Averaging.

TF_{EC} is also based on the second component of a WAPLS regression. ML appears to perform well prior to residual removal (Table 2.3). However, almost all of the large residuals that needed to be removed to use ML were in low-EC sites. Removing the majority of low-EC sites would yield a transfer function with low skill in oligotrophic conditions, biased towards minerotrophic sites. As a result, ML was not pursued further. WA and WAPLS represented the full gradient, with WAPLS outperforming WA. We removed 23 samples with large residuals (residuals > 228 µS cm^{-1}) from the transfer function to improve performance (after removal: R^2_{JACK} = 0.756, $RMSEP_{JACK}$ = 146 µS cm^{-1}, maximum bias = 189 µS cm^{-1}, *n* = 77). Key minerotrophic habitat indicator species include *Cyclopyxis kahli*, *Centropyxis ecornis*, *Phryganella acropodia* and *Difflugia globulosa*. Oligotrophic habitat indicator species include *Archerella flavum*, *Hyalosphenia papilio*, *Gibbocarina galeata* and *Centropyxis aculeata* (Figure 2.7).

2.4.3 - Removing high conductivity sites

We removed the 35 samples with the greatest (top 50%) EC values (≥600 µS cm^{-1}) from the full dataset. This allows us to test whether the control of trophic status on the distribution of testate amoebae species was being affected by sites that are unusually nutrient rich. NMDS continued to show EC as the primary control on species distribution, while MC, LOI, and WTD also remained highly significant ($p < 0.001$). CCA showed WTD as the primary control, with MC, EC and organic matter content also highly significant ($p < 0.001$).

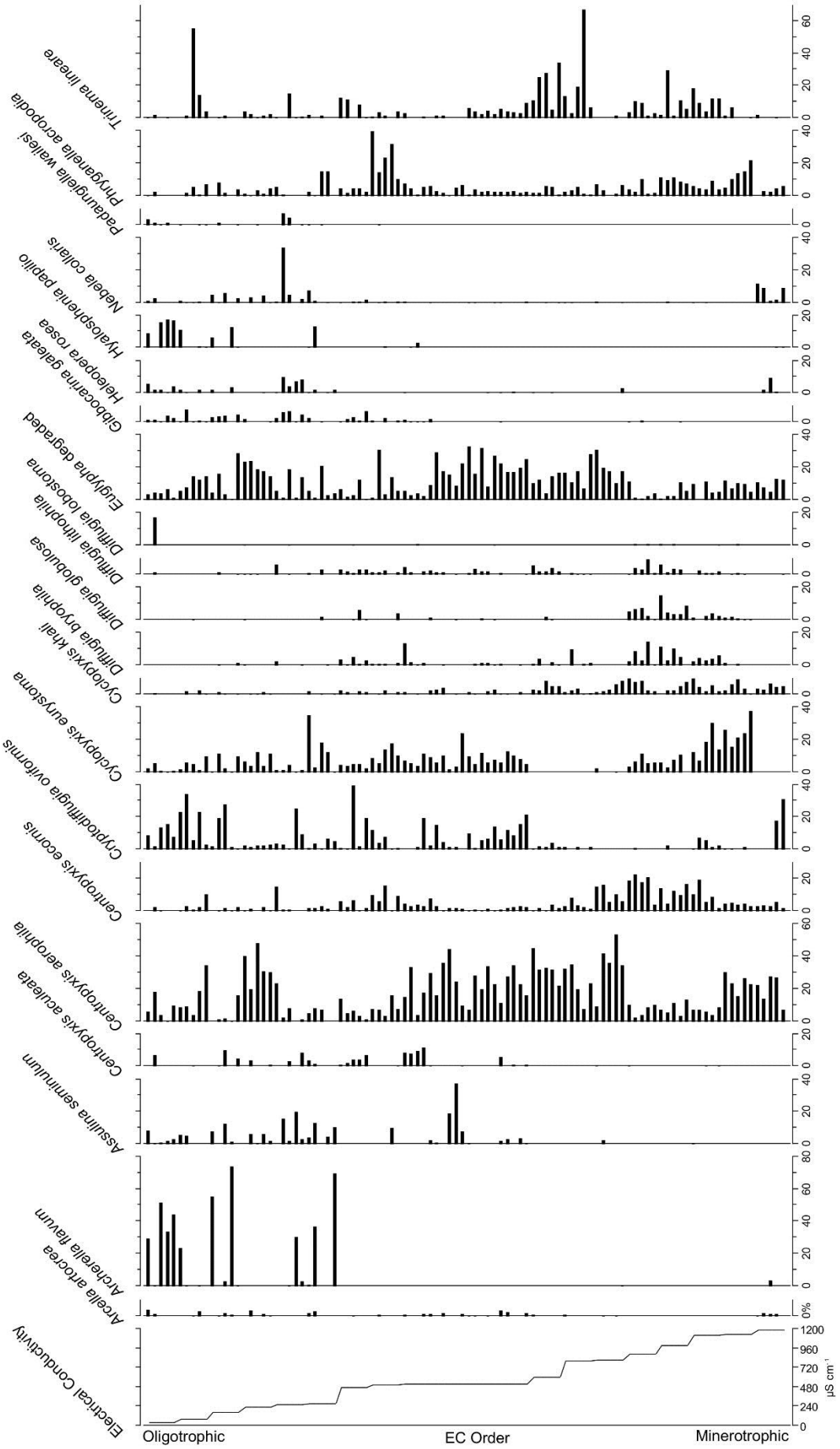

Figure 2.7 – Percentage abundance of selected testate amoebae taxa that indicate a range of EC conditions, ranked by observed EC.

2.4.4 - Transfer function performance

Both transfer functions perform well in terms of performance statistics (Table 2.3, Figure 2.8), offering the ability to provide quantitative reconstruction of WTD and EC. TF_{WTD} performs well (R^2_{JACK} = 0.84) compared to Lamarre et al. (2013) and Swindles et al. (2015b) (R^2 = 0.80 and 0.87 respectively), although tends to underestimate slightly at deeper WTDs. There is no existing comparison for the performance of TF_{EC} as it is the first EC transfer function, but also has high performance statistics (R^2_{JACK} = 0.76). TF_{EC} performs well across the trophic gradient, but has more samples at the oligotrophic end which will improve performance. Both are the first transfer functions to exist from the continuous permafrost zone.

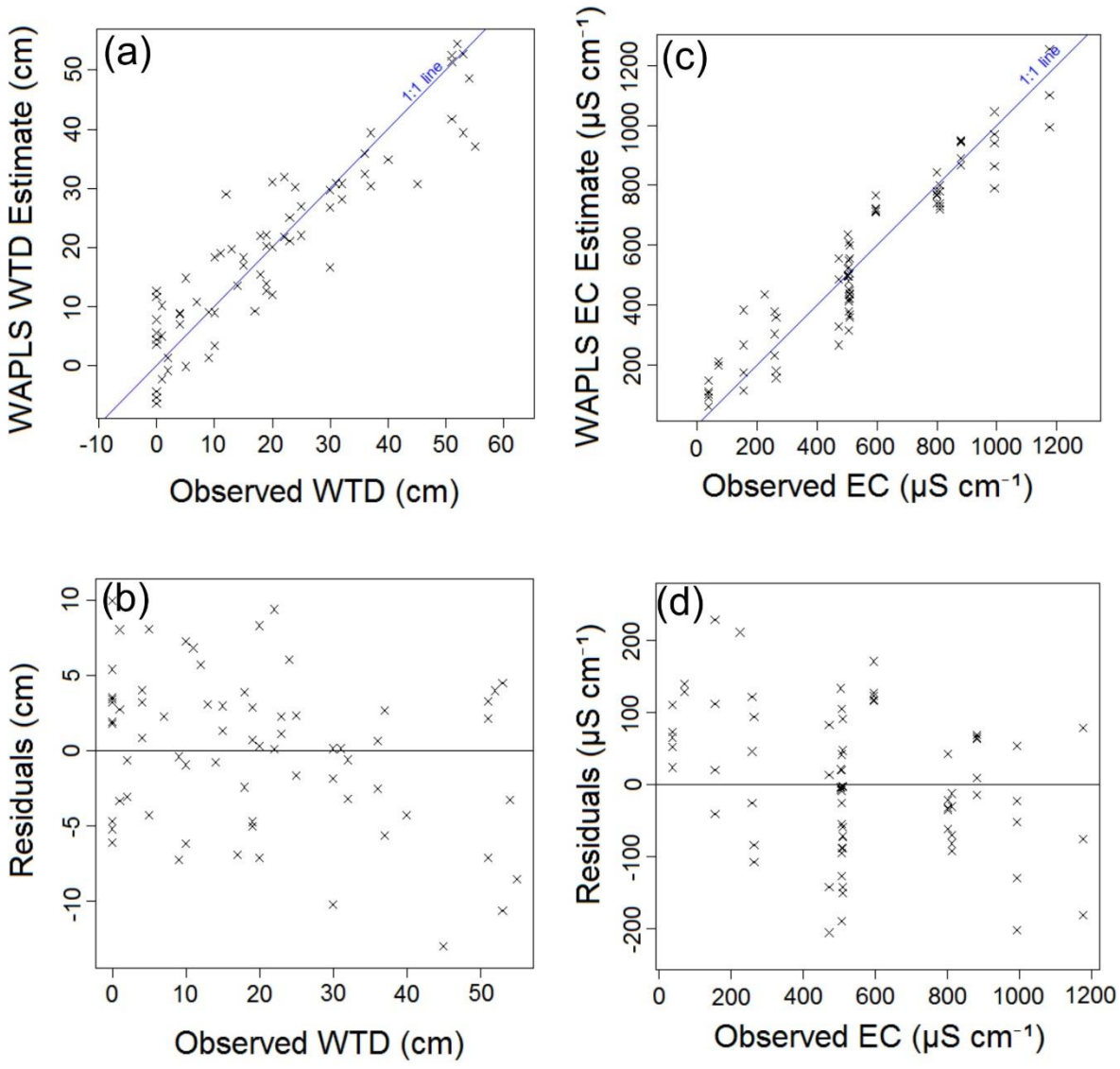

Figure 2.8 – Transfer function performance. (a) TF_{WTD} estimates of each site against observations and (b) residuals of each site against observed WTD. (c) TF_{EC} estimates of each site against observations and (d) residuals of each site against observed EC.

Code	Taxa name	In *n* samples	Maximum abundance (%)	Code	Taxa name	In *n* samples	Maximum abundance (%)
ARAT	*Arcella artocrea*	33	4.2	DIPY	*Difflugia pyriformis*	15	6.8
ARCA	*Arcella catinus* type	56	10.6	EUDE	*Euglypha* degraded	99	33.3
ARHE	*Arcella hemisphaerica*	5	4.5	EURO	*Euglypha rotunda*	51	20.7
ARFL	*Archerella flavum*	20	74.1	EUST	*Euglypha strigosa*	47	8.1
ASMU	*Assulina muscorum*	12	9.4	EUTU	*Euglypha tuberculata*	30	4.7
ASSC	*Assulina scandinavica*	40	10.9	GIGA	*Gibbocarina galeata*	40	8.1
ASSE	*Assulina seminulum*	35	37.7	HERO	*Heleopera rosea*	30	10.3
BUIN	*Bullinularia indica*	37	6.4	HESY	*Heleopera sylvatica*	61	10.4
CEAC	*Centropyxis aculeata*	30	11.8	HYEL	*Hyalosphenia elegans*	21	4.4
CEAE	*Centropyxis aerophila*	96	53.8	HYIN	*Hyalosphenia insecta*	7	3.8
CECO	*Centropyxis constricta*	3	7.1	HYOV	*Hyalosphenia ovalis*	1	5.4
CEDE	*Centropyxis declivistoma*	23	6.3	HYPA	*Hyalosphenia papilio*	17	18.1
CEEC	*Centropyxis ecornis*	92	22.6	HYPL	*Hyalosphenia platystoma*	27	4.7
CEHE	*Centropyxis hemisphaerica*	13	3.3	NECO	*Nebela collaris*	48	34.1
CEMI	*Centropyxis minuta*	8	13.1	NEMI	*Nebela militaris*	4	2.4
CEOR	*Centropyxis orbicularis*	48	6.7	NETI	*Nebela tincta*	17	33.3
CEPL	*Centropyxis platystoma*	75	20.8	NECR	*Netzelia corona*	4	4.5
CESY	*Centropyxis sylvatica*	11	2.9	NEWA	*Netzelia wailesi*	8	5.2
CODU	*Corythion dubium*	39	47.0	PALA	*Padaungiella lageniformis*	20	4.0
CRCO	*Cryptodifflugia compressa*	24	55.7	PAWA	*Padaungiella wailesi*	16	7.1
CROV	*Cryptodifflugia oviformis*	77	40.0	PHAC	*Phryganella acropodia*	88	39.8
COPO	*Conicocassis pontigulasiformis*	14	9.6	PLSP	*Placocista spinosa*	1	2.8
CYEU	*Cyclopyxis eurystoma*	81	37.7	PLMA	*Planocarina marginata*	2	3.2
CYKH	*Cyclopyxis kahli*	73	9.8	QASY	*Quadrulella symmetrica*	5	51.7
CYAM	*Cyphoderia ampulla*	10	2.5	TRDE	*Tracheleuglypha dentata*	31	9.5
DIBR	*Difflugia bryophila*	49	14.5	TRCO	*Trinema complanatum*	60	10.5
DIGE	*Difflugia geosphaira*	2	2.7	TREN	*Trinema enchelys*	2	53.5
DIGL	*Difflugia globulosa*	3	15.5	TRGR	*Trinema grandis*	11	2.1
DILI	*Difflugia lithophila*	58	9.7	TRLI	*Trinema lineare*	73	67.1
DILO	*Difflugia lobostoma*	12	17.5				

Table 2.4 - Overview of testate amoebae identified in abundances greater than 2% in any one sample.

2.5 - Discussion

Our new transfer functions can be used for palaeoenvironmental reconstruction in permafrost peatlands to understand both long-term and recent changes in wetness and hydrochemistry. This is the first study examining testate amoebae as environmental indicators in continuous permafrost peatlands. This study supports existing research that suggests testate amoebae are a useful way to reconstruct palaeohydrology in permafrost peatlands (Gałka et al., 2017; Swindles et al., 2015b; Lamarre et al., 2013, 2012; Bunbury et al., 2012). Testate amoeba-based reconstructions can form part of a multi-proxy toolkit to better understand the changing nature of peatlands in the continuous permafrost zone through the Holocene. The ecology of testate amoebae in continuous permafrost is similar to those found in discontinuous permafrost, although the key hydrological control on species distribution is different. EC plays a more important role in continuous permafrost, suggesting a strong trophic gradient may dominate Alaskan North Slope peatlands. Our results also show that the peatlands in this region are a mixture of both ombrotrophic and minerotrophic systems, and contain variability between these categories within-site. Therefore, a transfer function encompassing the entire nutrient-status gradient is more appropriate than splitting the model into individual ombrotrophic and minerotrophic models.

2.5.1 - Species diversity

Testate amoeba diversity is high (96 taxa identified from 15,723 classified individuals across 5 sites), which gives us confidence that they are robust hydrological indicators as they are found across the permafrost zone.

Most testate amoebae studies are performed exclusively in either oligotrophic or eutrophic environments, rather than across a trophic gradient. Studies of testate amoebae and vegetation diversity across trophic gradients produce conflicting results. The study carried out by Lamentowicz et al. (2010) in a temperate zone in sub-alpine peatlands of the Upper Engadine (Swiss Alps) identified a weak correlation in the fen-bog gradient between testate amoebae and moss diversity, while research by Opravilova and Hajek (2006), in a mountain peatland located in the Western Carpathians, found no correlation. We find that WTD is the only significant variable influencing the species richness of testate amoebae ($r = -0.324$, $p < 0.001$). EC shows a very weak ($r = -0.177$, $p = 0.078$) correlation. MC is the most important influence on testate amoebae species diversity.

2.5.2 - Nutrient level as the dominant factor

This study is one of the first where the trophic gradient is the primary controlling factor on testate amoeba distribution, across a full range of peatlands from bogs to fens. This accurately represents our observations of peatlands in this region, as varying significantly in their trophic status. As a result, this has allowed us to produce a transfer function to reconstruct EC throughout the Holocene, which can allow future studies to better identify the timing of fen-bog transitions or ecosystem state shifts in a peatlands' nutrient status. This can directly influence the net ecosystem productivity and subsequent carbon sequestration of Arctic peatlands (Bubier et al., 1999). This distribution of testate amoebae along the oligotrophic-eutrophic gradient has also been observed in aquatic ecosystems (e.g. Beyens et al., 1986a; Qin et

al., 2009; Ju et al., 2014). The observed trophic gradient does not affect surface vegetation though, as proxies for moisture (WTD, MC) controlled their distribution. As WTD is a statistically significant second-order control on species distribution from sites across a long trophic gradient, our transfer functions can be applied to reconstruct ecosystem change across the Holocene (such as a fen-bog transition), which contrasts findings from Payne (2011) from the Mediterranean.

The response of particular testate amoebae species to the trophic gradient closely matches an existing study from a peatland adjacent to Toolik Lake (Mitchell, 2004), where species diversity of testate amoebae was examined in response to increased nitrogen and phosphorus levels. We confirm results from Mitchell (2004) that *Archerella flavum* and *Hyalosphenia papilio* are indicators of nutrient-poor peatlands, while *Centropyxis aerophila* and *Phryganella acropodia* indicate minerotrophic conditions. However, unlike Mitchell (2004), we found that *Assulina muscorum* was indicative of minerotrophy in our dataset. We identified *Centropyxis aerophila* as a dominant species, which has also been observed in Arctic lakes (Beyens et al., 1986a). However, Beyens et al. (1986a) describe *Centropyxis aerophila* as a low-conductivity indicator, whereas we find this species across the trophic gradient and in greater abundance in higher EC sites.

2.5.3 - Reconstructing water-table depth

We also present the first testate amoeba-based transfer function to reconstruct WTD in continuous permafrost peatlands. This increases the global

extent of testate amoebae as palaeohydrological indicators and opens opportunities to better understand how high-latitude ecosystems have responded to a changing climate throughout the Holocene. Individual taxa behave broadly as expected, comparing results to other studies in discontinuous permafrost (Amesbury et al., 2013; Swindles et al., 2015b; Zhang et al., 2017). Our largest anomaly was *Archerella flavum*, which we observe to be an intermediate indicator with an optimum WTD of around 19 cm. While the presence of *A. flavum* at this WTD has been observed in the compared studies, it is generally an indicator of much wetter conditions. Conversely, we do not observe *A. flavum* in abundance (≥ 2%) drier than 9 cm WTD. This could be because of the observed strong control of low nutrient status on this taxon.

2.5.4 - Future applications

Testate amoebae can be used to investigate environmental change across Arctic peatlands, as they respond to changes in climate throughout the Holocene. This, in combination with other testate amoeba records from the Arctic (e.g. Müller et al., 2009), expands the potential for using testate amoebae as palaeoenvironmental indicators around the world. There is now the opportunity to apply our transfer functions to a fossil record from the continuous permafrost zone to investigate WTD and ombrotrophic-minerotrophic transitions since peatlands first began to develop in this area.

2.6 - Conclusions

1. We present the first testate amoeba-based transfer functions for reconstruction of water-table depth and electrical conductivity in peatlands from the Alaskan continuous permafrost zone.
2. Testate amoebae are valuable environmental indicators in continuous permafrost peatlands.
3. Pore water electrical conductivity is the primary control on the distribution of testate amoeba species in these sites. Electrical conductivity is a proxy for the nutrient status of peatlands, suggesting that testate amoebae can be used as reliable indicators of trophic status in peatlands of the North Brooks foothills, Alaska.
4. The species richness of contemporary plants and testate amoebae taxa are significantly correlated to each other, and independently to water-table depth.
5. Our new transfer functions may be valuable components of multi-proxy investigations into the responses of Arctic permafrost peatlands to climate change over the Holocene and in recent centuries.

3. EVIDENCE FOR ECOSYSTEM STATE SHIFTS IN ALASKAN CONTINUOUS PERMAFROST PEATLANDS IN RESPONSE TO RECENT WARMING

3.1 - Introduction

Peatlands in the continuous permafrost zone are globally-important stores of ~144 Pg of organic carbon (Tarnocai et al., 2009). The stability of this carbon store is thought to be threatened by current and future warming of the high-latitudes (Khvorostyanov et al., 2008; Schuur et al., 2008; Schuur et al., 2013), although the ultimate fate of permafrost peatlands and their ability to sequester carbon under future warming are uncertain. Under projected warming, land surface models suggest that the Arctic will become a net carbon source by the mid-2020s as a direct result of the degradation of permafrost and subsequent release of carbon (Schaefer et al., 2011). The potential for greenhouse gas production from peatlands is likely to increase under future climate change (Hodgkins et al., 2014), particularly during dry periods when falling water tables are likely to expose peat to rapid, aerobic decomposition, leading in turn to elevated CO_2 release (Ise et al., 2008). However, permafrost thaw may instead lead to wetter surface conditions, thereby releasing more CH_4 from anaerobic decomposition (Moore et al., 1998). Net primary productivity in peatlands is likely to rise due to longer, warmer growing seasons, and shifts towards more productive vegetation, which would enhance carbon accumulation (Natali et al., 2012), leading to a negative climate feedback. At present there remains no consensus on whether permafrost peatland carbon budgets will have net warming or cooling effects under future climate change.

Palaeoecological approaches have been used to identify how peatlands have responded to climate change during the late-Holocene, albeit predominantly in temperate regions (Langdon and Barber, 2005; Sillasoo et al., 2007; Swindles et al., 2007, 2010; Gałka et al., 2017). It is sometimes possible to identify correlations between reconstructed hydrology and climate variables (e.g. temperature and precipitation), where there is precise chronological control for the recent (~1850 CE) part of the peat profile. In studies from the UK (Charman et al., 2004) and Estonia (Charman et al., 2009), precipitation has been shown to exert the strongest control on reconstructed water table, with temperature a second-order influence. Reconstructions over the late-Holocene also show that carbon accumulation is likely to increase with rising temperatures as a result of improved net primary productivity (Charman et al., 2013). Despite the importance of continuous permafrost peatlands as a carbon store, there have been no quantitative reconstructions to identify how the carbon dynamics of these systems have responded to Holocene climate change. Furthermore, there is a dearth of long-term monitoring of peatlands in the continuous permafrost zone. As a result, peatland response to recent warming is poorly understood in the high-latitudes.

Testate amoebae are well preserved in peatlands, so can be used to reconstruct palaeohydrological metrics such as water table depth (WTD) over Holocene timescales. Testate amoeba-based reconstructions have been used in permafrost regions of Canada (Lamarre et al., 2012), Sweden (Swindles et al., 2015a), Finland and Siberia (Zhang et al., 2017), but their use has been limited to discontinuous and sporadic permafrost. Transfer functions in

peatlands from discontinuous permafrost peatlands (Swindles et al., 2015b) are not suitable as there are several non-analogue taxa. We recently developed two new transfer functions from continuous permafrost peatlands across the Alaskan North Slope, which facilitate reconstruction of both WTD and pore water electrical conductivity (EC) during the Holocene, where EC can be used as a proxy for a peatland's trophic status along the fen-bog gradient (Taylor et al., 2019). By reconstructing Holocene hydrological change and calculating the carbon accumulation rate (CAR), we can begin to identify the environmental controls on these important variables in continuous permafrost peatlands. By doing so we seek to improve predictions about the likely future response of continuous permafrost peatlands, particularly the vulnerability of their carbon stores, to projected climatic warming.

3.1.2 - Aims

Our aim is to reconstruct palaeoenvironmental variables of two Alaskan peatlands in the continuous permafrost zone. In this investigation, we:

i. Examine the palaeoecology of testate amoebae through the late-Holocene from two peatlands beside Toolik Lake, North Slope, Alaska;
ii. Reconstruct WTD and EC, and determine rates of carbon accumulation, and;
iii. Test the relationships between CAR, WTD, and EC, with temperature and precipitation

3.2 - Methods

3.2.1 - Study Area

Our study examines two cores (TFS1 and TFS2; Table 3.1), one each from the deepest peat in each of the two study sites, which extend to the bottom of the active layer. The cores come from two distinct peatlands approximately 250 metres apart and adjacent to Toolik Lake on the Alaskan North Slope. A bedrock high separates the watersheds of the two peatlands (Figure 3.1). The study area sits within the continuous permafrost region, with an active layer thickness of between 40 and 50 cm (Brown, 1998), and is surrounded by Arctic acidic tundra. Toolik Lake is situated in the northern foothills of the Brooks Mountains, at an elevation of approximately 712 m above sea level and is subject to a continental climate. Mean daily temperature ranges from 11°C in the summer to -23°C in winter with annual precipitation of ~250 mm (Environmental Data Center Team, 2018; averaging period 1988–2017). The region is snow free from early June to mid-September. Mean annual air temperature at Toolik has increased by more than 2°C from 1901 (Appendix C).

Core	Co-ordinates	Core Length (cm)	Distance to lake shore (m)	Elevation above sea-level (m)	Approximate oldest age (cal CE)	Dominant surface vegetation
TFS1	68.62475, -149.59639	45	51	715	800	*Sphagnum fuscum*, *Sphagnum capillifolium, Andromeda poligolia, Betula nana*
TFS2	68.62276, -149.60028	50	222	724	0	*Sphagnum capillifolium, Aulacomnium turgidum, Salix reticulata*

Table 3.1 – Information on cores TFS1 and TFS2. Ages are from the age-depth model presented in Figure 3.2.

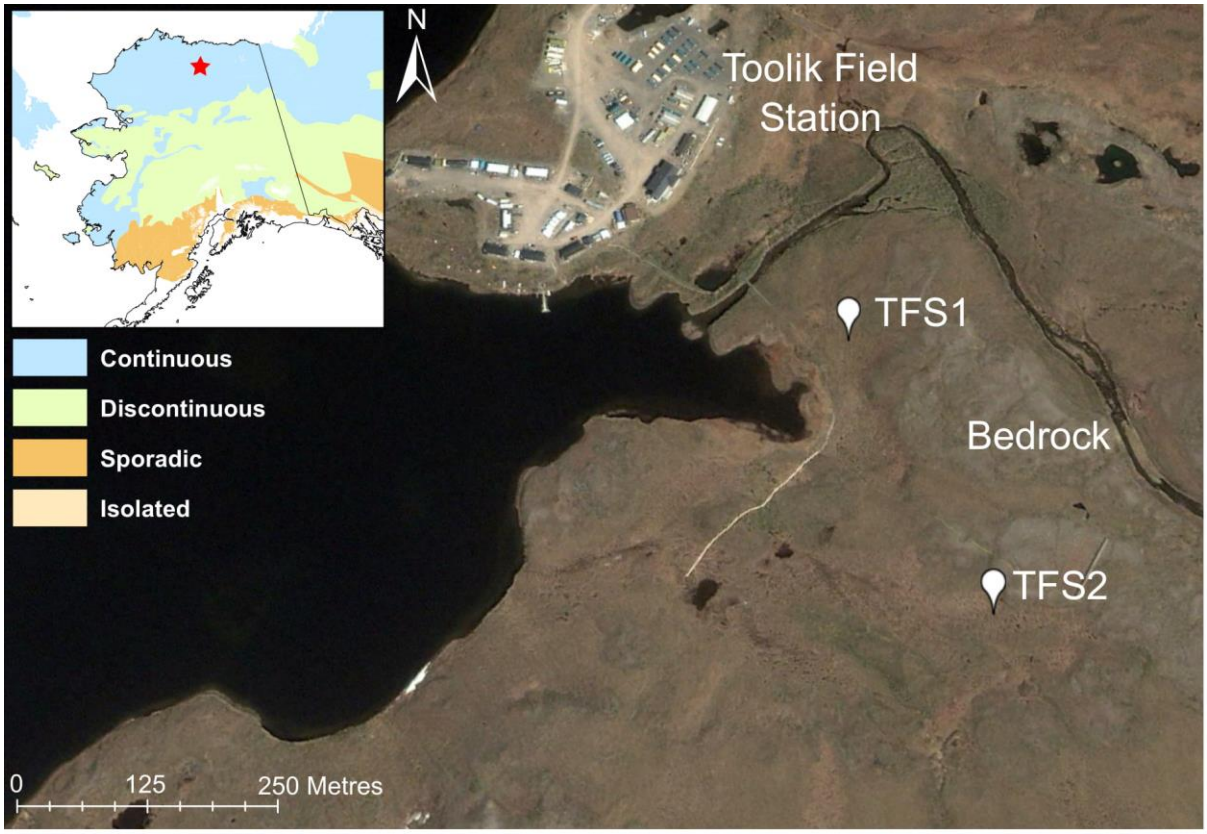

Figure 3.1 – Site Map. TFS1 and TFS2 are situated in peatlands to the south of Toolik Field Station, approximately 250 metres apart and separated by a bedrock high.

3.2.2 - Peat sampling and dating

We studied two short peat cores, TFS1 and TFS2, collected in July 2015 as 8 cm x 8 cm monoliths. For additional details on sampling, see Gałka et al. (2018). We sub-sampled both cores at 1 cm depth increments and created a chronology using radiocarbon dates previously reported by Gałka et al. (2018), with additional ^{210}Pb dating. Gałka et al. (2018) carried out AMS ^{14}C dating on a combination of macrofossils and bulk peat, from five samples in each core. They used OxCal 4.1 software and the IntCal13 curve to calibrate the

radiocarbon dates. We used the same ^{14}C dates as Gałka et al. (2018), with the exception of two dates that we omitted (TFS1 18-19 cm and TFS2 13-14 cm) because they fall within the range covered with our more precise ^{210}Pb dating (post-1900 CE).

We measured ^{210}Pb activity at 1 cm depth increments using alpha spectrometry by measuring the alpha decay of polonium-210 (^{210}Po), a daughter-product of ^{210}Pb decay. Sub-samples of 0.5 g of peat were freeze-dried, ground and homogenised, and spiked with a ^{209}Po chemical yield tracer. We extracted ^{210}Po from the peat samples using a sequential HNO_3:H_2O_2:HCl (1:2:1) acid digestion, then electroplated onto silver planchets (based on Flynn, 1968). We measured the ^{209}Po and ^{210}Po activities using Ortec Octête Plus alpha spectrometers at the University of Exeter's Radiometry Laboratory. We calculated ages using the Constant Rate of Supply (CRS) model (Appleby and Oldfield, 1978; Appleby, 2001). The main assumptions of the CRS model are: (1) a constant supply of ^{210}Pb to the peat surface; (2) rapid transfer of ^{210}Pb to peat; and (3) post-depositional immobility (Appleby, 2001).

We combined ^{14}C and ^{210}Pb age determinations and used them to create a Bayesian age model for each core using R version 3.4.1 (R Core Team, 2014), and the *rbacon* package (version 2.3.4; Blaauw et al., 2018) (Figures 3.2a, b). We modelled both cores with *a priori* information to determine the maximum age probability to a maximum of 50 cm depth. Hereafter, all references to ages or years refer to the maximum age probability at a given depth, as determined from the age model, unless otherwise specified.

3.2.3 - Carbon accumulation analysis

Sub-samples were examined at 1 cm depth increments, using samples of 2 cm^3. We measured and weighed each sub-sample, oven-dried overnight at 105°C, and re-weighed to determine gravimetric moisture content and dry bulk density (BD); and then ignited at 550°C for at least 4 hours, and re-weighed again to determine organic matter content through loss-on-ignition (LOI). We used the assumption that the carbon content of peat is 50% of organic matter (measured by LOI; following Bellamy et al., 2005). CAR for each 1 cm interval was subsequently calculated as follows:

$$CAR = \frac{z}{T_a} \times BD \times C_c \times 100$$

Where CAR is carbon accumulation rate (g C m^{-2} yr^{-1}), z is depth (cm), T_a is age difference between the 1 cm interval and the sub-sample below, BD is dry bulk density (g cm^{-3}) and C_c is carbon content (%).

3.2.4 - Testate amoeba analysis

We isolated testate amoebae for analysis following Booth et al. (2010). Approximately 2 cm^3 of each sub-sample (at 1 cm intervals) was placed in freshly boiled water for 10 minutes, shaken, passed through a 300 µm sieve and back-sieved through a 15 µm mesh. We aimed to count at least 100 individuals at 200–400 × magnification under a high-power transmitted light microscope. Eleven samples from TFS1 had fewer than 100 individuals (min n = 81), while seven samples in TFS2 had fewer than 100 individuals (min n = 66). We omitted the deepest two samples in TFS2 from further analysis due to particularly low counts (n = 22 and 9 respectively), resulting from poor preservation. Testate amoebae were identified with the assistance of published

guides (Charman et al., 2000; Booth and Sullivan, 2007; Siemensma, 2018). For the first time, we apply two modified transfer functions from continuous permafrost peatlands across the Alaskan North Slope (Taylor et al., 2019) to reconstruct WTD and EC.

3.2.5 - Climate data

We downloaded monthly temperature and precipitation records from 1901 to present from the CRU TS v. 4.01 dataset (Harris et al., 2014) for the grid cell centred on 68.75°N, 149.75°W. This dataset utilises 22 stations from across Alaska to interpolate climate data to half degree spatial resolution. All stations are land-based, with the nearest station to Toolik Lake being 217 km away at Bettles. This dataset performs very well compared to equivalent data sources for Alaska (Harris et al., 2014). We used the PAGES2k Consortium (2017) Arctic database to reconstruct annual temperatures from 0 CE. PAGES2k is a multi-proxy dataset, predominantly using tree rings, marine sediments and glacier ice that range in temporal coverage. Tree rings make up the majority of the most recent temporal coverage, while marine sediments and glacier ice are used to reconstruct temperature back to 0 CE. For more details, see PAGES2k Consortium (2017). Change point analysis was performed on these climate data using the R *changepoint* package (version 2.2.2; Killick et al., 2016), following Amesbury et al. (2017). We used the cpt.mean function to identify the primary change of the mean within each time series. The time series of each variable was the full error range (min–max) of the date at the sub-sample interval from the respective age model. Climate data from PAGES2k and CRU TS is displayed in Appendix C.

3.3 - Results

3.3.1 - Age-depth model

The bottom of the active layer in TFS1 begins at *c.* 800 CE, while in TFS2 it is much older, dating to *c.* 0 CE (Figure 3.2). High resolution ^{210}Pb data mean that the error in reconstructing change from 1900 CE is on average ± 2-3 years. Before 1900, error increases beyond the range of ^{210}Pb dating, when ^{14}C dates are used. We follow Gałka et al. (2018) in rejecting a ^{14}C date of bulk peat at the bottom of TFS2 (AMS dated to 950 ± 30 ^{14}C BP), but this does introduce large uncertainty in the true age of peatland initiation in this core. Peat accumulation rate is slow (as expected in permafrost environments) throughout both cores, rapidly accelerating from the start of the industrial revolution (which we define as 1850 CE). Mean long-term rate of peat accumulation across the full cores were 20 yr cm^{-1} in TFS1, and 50 yr cm^{-1} in TFS2.

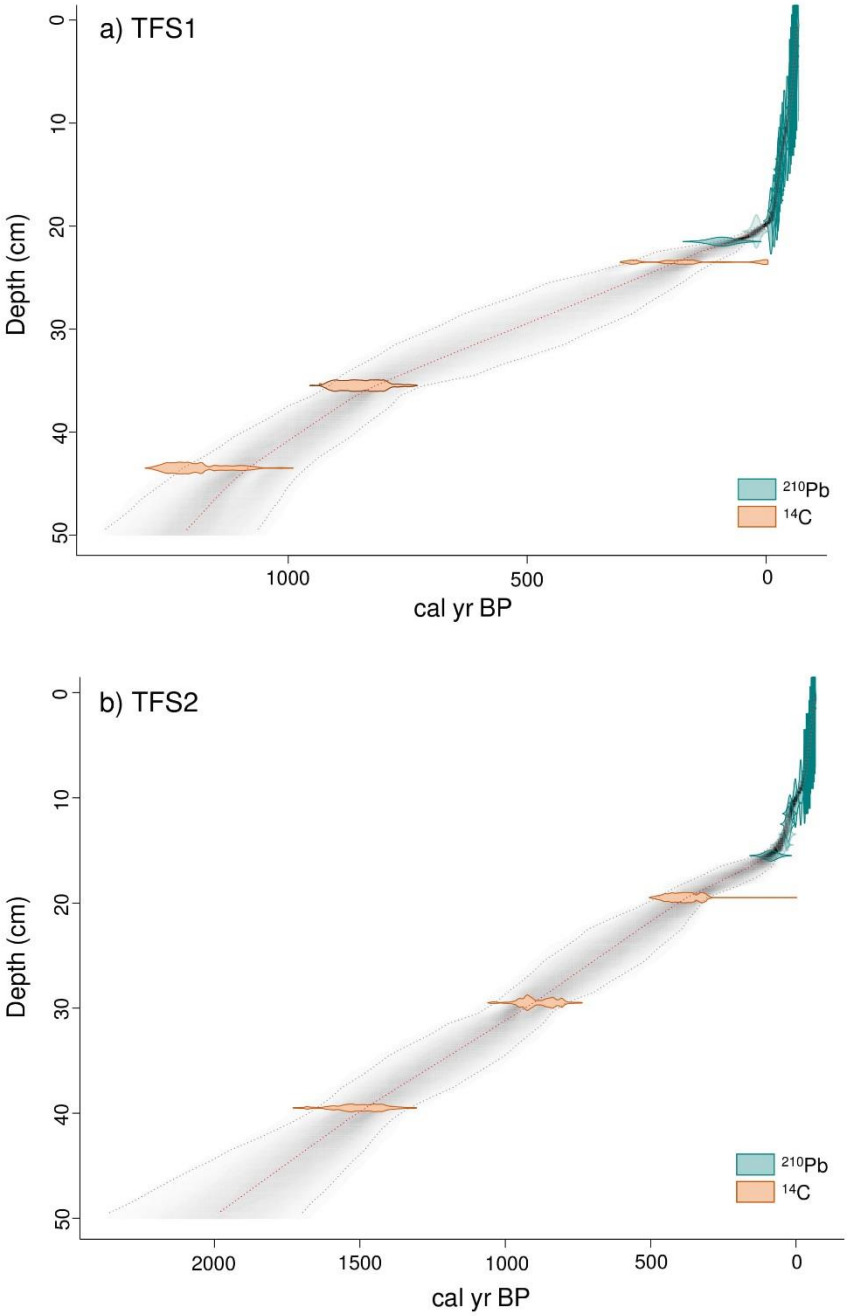

Figure 3.2 – Bayesian age models of (a) TFS1 and (b) TFS2.

3.3.2 - Testate amoeba-based reconstructions

We use the Weighted Averaging Partial Least Squares (WAPLS) second component model presented by Taylor et al. (2019) to reconstruct WTD

in both cores. Reconstructions with errors are shown alongside testate amoebae assemblages in Figures 3.3 and 3.4. TFS1 began as a wet peatland (Figure 3.5) with a mean WTD of around 4 cm, but a rise in *Centropyxis aerophila* during the LIA indicates a rapid transition to dryness (peaking at WTD of 44 cm from 1721-1888). In the last few centuries, the peatland has been dominated by *Archerella flavum* and *Hyalosphenia papilio* which indicates a moderately-wet ecosystem. TFS2 also began as wet peatland (Figure 3.6), but then dried rapidly as indicated by an increasing dominance of *C. aerophila*. Only TFS2 shows evidence of peatland initiation, given the rapid increase in organic content from LOI and transition to dryness that occurs at *c.* 200 CE. A *Conicocassis pontigulasiformis* phase from *c*. 500–1000 CE indicates a period of wetter conditions. TFS2 remained fairly steady with a moderate water table for much of the past few centuries, but begun rapidly drying from *c*. 1850 CE, as indicated by a gradually increasing abundance of *Corythion dubium*, *Cryptodifflugia oviformis* and *Assulina seminulum*.

To reconstruct EC, we used a weighted averaging model with inverse deshrinking (WA_inv), which is a different statistical approach than the WAPLS model used by Taylor et al. (2019). This is because we found that the application of the WAPLS model led to erroneous results regarding *C. pontigulasiformis*, which suggested that this species was indicative of ombrotrophic conditions. Relatively little is known about this rare species, and it was not found regularly in contemporary samples (but, where present, indicated minerotrophy). As *C. pontigulasiformis* dominates at one point in both cores, we felt it was necessary to use a model that better predicted this species

and opted for WA_inv, despite it having slightly lower performance (R^2_{BOOT} = 0.67, $RMSEP_{BOOT}$ = 158 µS cm^{-1}) than the WAPLS (Component 2) model by Taylor et al. (2019) (R^2_{JACK} = 0.76, $RMSEP_{JACK}$ = 146 µS cm^{-1}). TFS1 remains minerotrophic for much of the duration of the core, before transitioning rapidly to oligotrophy around 1950 CE. TFS2 is more varied and appears to include two short-lived shifts to more oligotrophic states (*c*. 400 CE and *c*. 1300 CE), both followed quickly by returns to minerotrophic conditions, before the full transition to the peatland's current oligotrophic state at ~1850 CE.

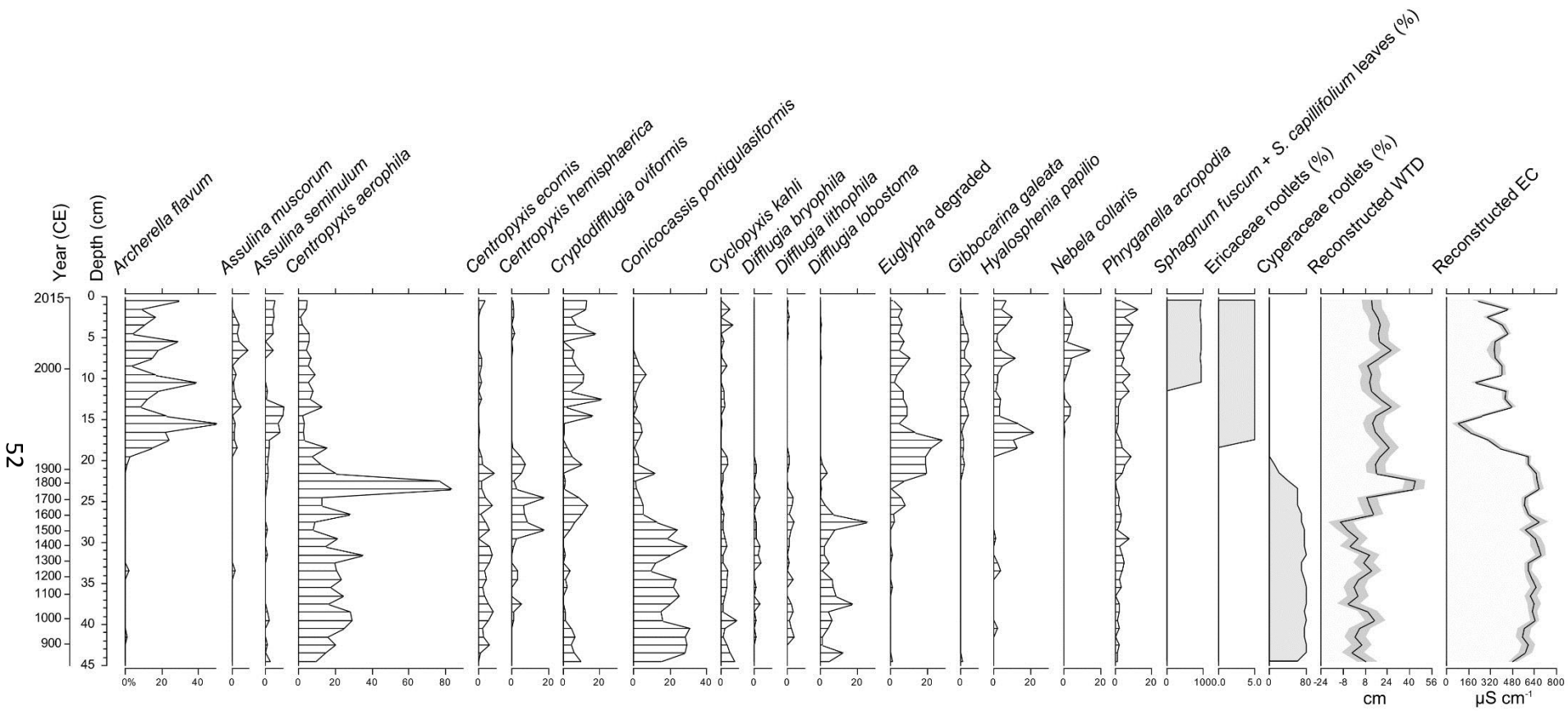

Figure 3.3 - Testate amoebae assemblages of TFS1, with selected macrofossil assemblages from Gałka et al. (2018). WTD and EC reconstructions with standard errors (shown in grey shading) are also presented.

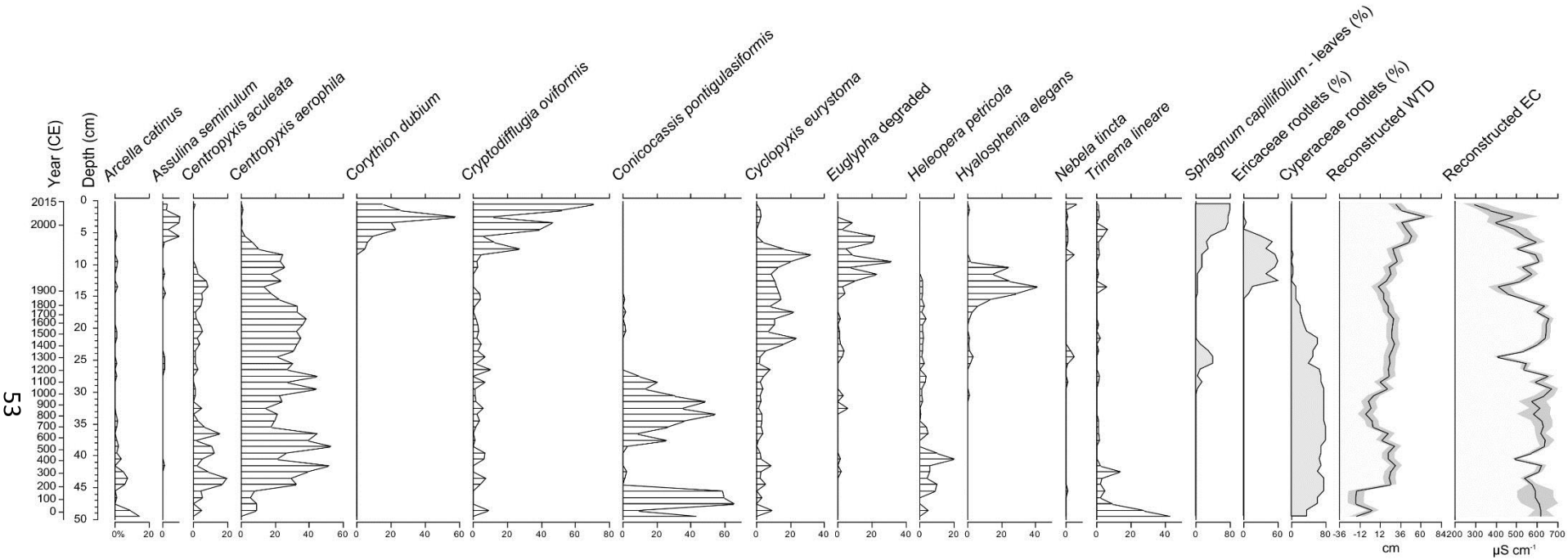

Figure 3.4 - Testate amoebae assemblages of TFS2, with selected macrofossil assemblages from Gałka et al. (2018). WTD and EC reconstructions with standard errors (shown in grey shading) are also presented.

3.3.3 - Bulk density, loss-on-ignition and carbon accumulation

At the base of TFS1, BD is high (0.27 g cm^{-3}) and LOI is low (69%). A rapid increase in BD to 0.38 g cm^{-2} and a decrease in LOI to 32% between 32.5 and 29.5 cm (corresponding to 1250–1400 CE) reflects an anomalously large amount of fine-grained minerogenic material. BD and LOI return to their previous levels after this event, before BD declines rapidly and LOI increases rapidly in the early 1950s. CAR was low throughout most of the core, slightly decreasing throughout the late-Holocene before rapid acceleration in the early 1900s and a more recent slight decline (Figure 3.5).

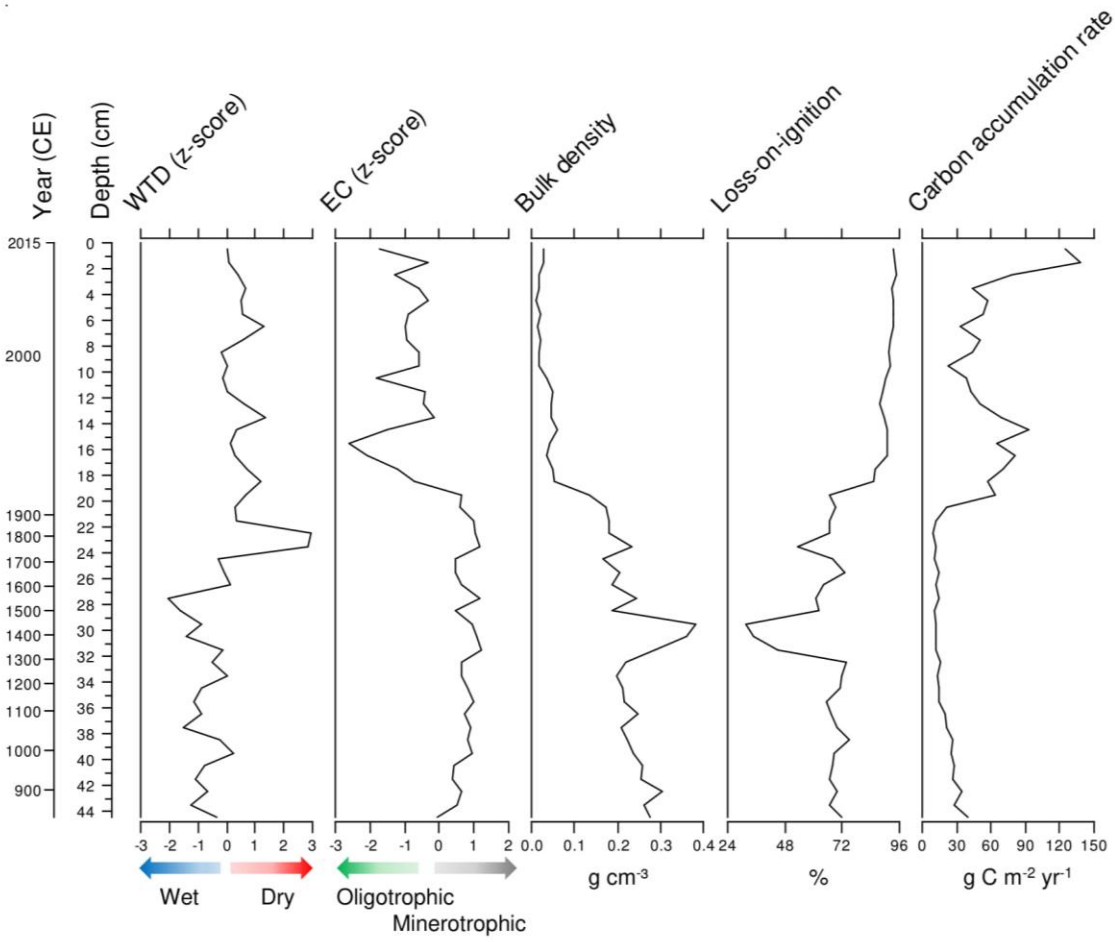

Figure 3.5 – Full reconstruction of palaeoenvironmental variables for TFS1.

In TFS2, a rapid increase in LOI (representing a rise in estimated carbon content; from 34% to 52%) at around 200 CE is a clear indication of peatland initiation. An anomalous peak in BD of 1.05 g cm^{-3} at 46.5 cm corresponds to a rock clast within the peat matrix, possibly derived from the basal glacial sediments. As with TFS1, BD and LOI remain fairly constant throughout the late-Holocene, with carbon accumulation decreasing very gradually over time. The transition to more rapid carbon accumulation, low BD and rising LOI comes earlier in TFS2, at ~1850 CE (Figure 3.6). CAR increases rapidly from 1850 CE before a more recent slight decline.

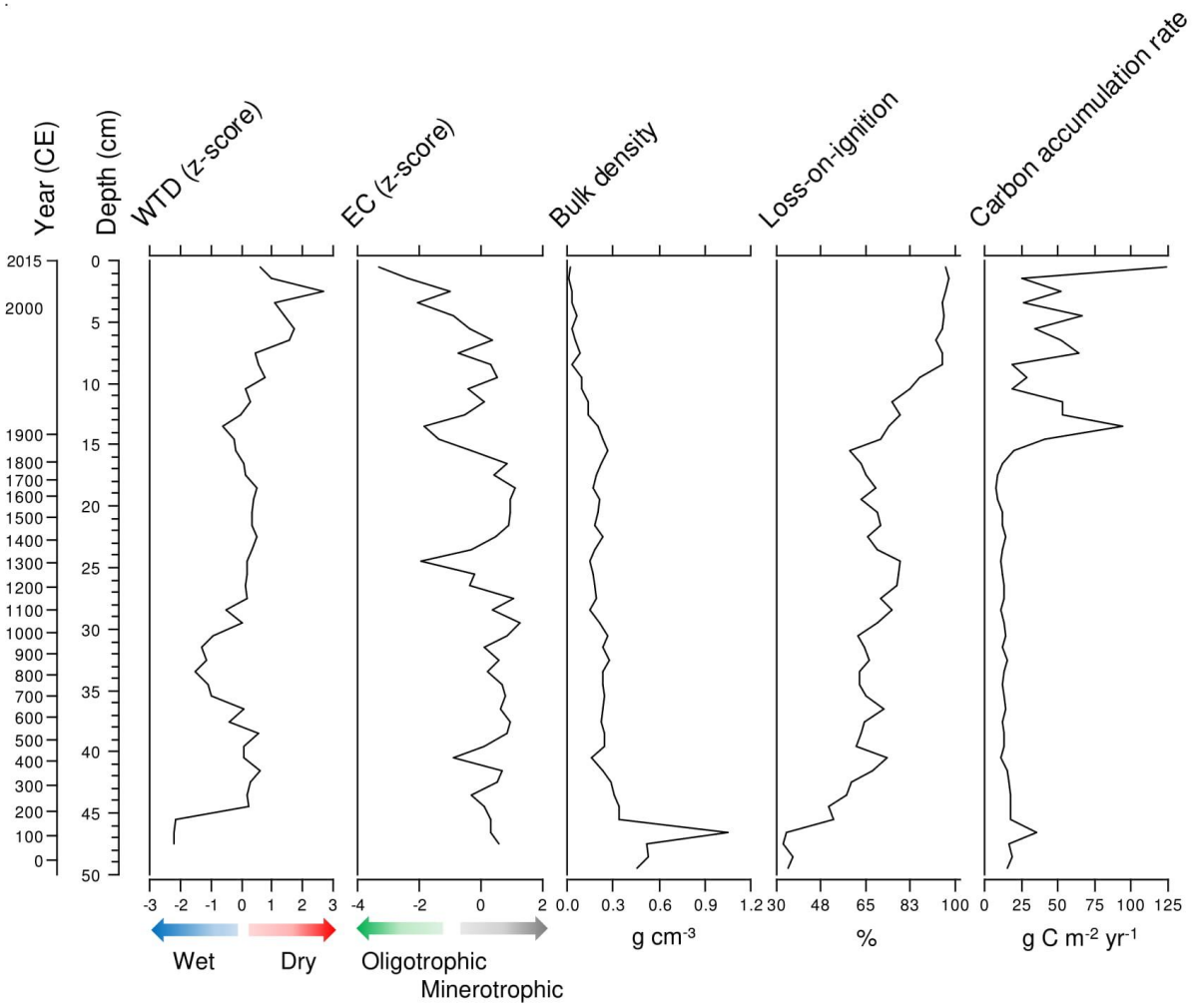

Figure 3.6 – Full reconstruction of palaeoenvironmental variables for TFS2.

3.3.4 - Relationship to climate data

High-resolution ^{210}Pb analysis allows us to investigate if there has been any correlation between recent changes (from 1901 CE; the temporal range of CRU TS) in the peatland and shifts in the climate. We tested the correlations between WTD, EC and CAR against annual and seasonal temperature and precipitation records. TFS1 showed a strong positive correlation between CAR and annual, summer and autumn precipitation ($p < 0.01$; $r = 0.623$, 0.552 and 0.701 respectively); no other relationships were significant in TFS1. TFS2 showed significant positive correlations between WTD and annual, summer, spring and July temperature ($r = 0.673$, 0.771, 0.678 and 0.804 respectively; $p < 0.01$ in all cases). Although these climate variables correlate with observed changes in the peatlands, this does not necessarily infer they are the primary drivers of change, given the complex connectivity of peatland drivers.

We also investigated whether these relationships had remained stationary through time. Increasing chronological errors in deeper layers of both cores prevented the meaningful application of correlation analyses along their entire lengths. Instead we use a change point analysis to identify when the biggest transitions of WTD, EC, LOI and CAR occurred. This allows us to evaluate whether sudden, rapid warming has given rise to similar transitions in the dynamics of the peatlands. The most significant change in EC, LOI and CAR occurred after 1850 CE (Table 3.2; Appendix D). In TFS1, the most significant WTD change occurs during the LIA as the peatland rapidly dries, while in TFS2, the most significant WTD change point occurred as the peatland dried during its early development.

	TFS1			TFS2		
	Change point Depth (cm)	Year (CE) (min-max range)	Transition Description	Change point Depth (cm)	Year (CE) (min-max range)	Transition Description
WTD	27.5	1555 (1383–1702)	Drier	45.5	164 (-137–393)	Drier
EC	19.5	1959 (1952–1965)	Towards ombrotrophy	4.5	1997 (1993–2001)	Towards ombrotrophy
LOI	19.5	1959 (1952–1965)	Increase	11.5	1930 (1922–1938)	Increase
CAR	20.5	1930 (1916–1944)	Increase	15.5	1853 (1816–1886)	Increase

Table 3.2 - Change point analysis showing timing of the most significant changes in each reconstructed variable in the two cores.

3.4 - Discussion

This study highlights the usefulness of testate amoeba-based reconstructions to identify ecosystem state shifts of peatlands in the continuous permafrost zone. Our results are similar to the observed increase in carbon accumulation of other permafrost peatlands post-1850 CE (Yu et al., 2009; Lamarre et al., 2012; Loisel and Yu, 2013), in addition to identifying an ecosystem state shift in both peatlands towards a dry, oligotrophic state.

3.4.1 - Testate amoebae analysis

Our 1 cm resolution testate amoeba analysis is comparable to the lower resolution (4 cm) study on core TFS2 by Gałka et al. (2018). Their study comprised of a semi-quantitative analysis of wetness indicators, as no suitable transfer function existed at that time. While our analysis largely agrees with theirs, there are notable differences in taxa in the deepest sections, and throughout the core for small taxa (e.g. *C. oviformis*). We attribute these

differences to the methods used to isolate the tests. We placed peat sub-samples in freshly boiled water which was allowed to cool for 10-minutes, compared to Gałka et al. (2018) placing sub-samples in continuously boiling water. We believe this degraded their tests and contributed to lower observed species diversity, particularly in the deepest samples. We identified *C. pontigulasiformis* at significant abundance (max. 65.2%) in both fossil records, with a trend of increasing abundance with depth. This contrasts with the contemporary counts of this species, which are limited (Taylor et al., 2019). Similar records of *C. pontigulasiformis* also show this species to be relatively rare in the contemporary record (Beyens et al., 1986b; Beyens and Chardez, 1995; Gavel et al., 2018), but have been reported in sub-Arctic lakes (Nasser and Patterson, 2015).

3.4.2 - Peatland initiation

Peatlands across the Alaskan North Slope began to initiate around 8,600 years ago (Jones and Yu, 2010), likely during warm periods (MacDonald et al., 2006; Gorham et al., 2007) as a result of increased plant productivity (Morris et al., 2018). Only TFS2 shows evidence of peat initiation at the base of the core, corresponding to ~200 CE. Hu et al. (2001) note that Alaska experienced a warm period between 0 and 300 CE, which we hypothesise initiated peat accumulation in TFS2. Initiation in TFS2 is also identified in macrofossil analysis (Gałka et al. 2018), with Cyperaceae (mainly *Carex* species) and herb rootlets increasing steadily between 48.5 and 46.5 cm, during the 0-300 CE warm period.

3.4.3 - Post-initiation development

The presence of *Difflugia lobostoma* gradually increases in TFS1 between 800 CE and 1600 CE, indicating WTD becoming steadily shallower during this period. Between 32.5 and 29.5 cm (corresponding to ~1250-1400 CE), LOI dramatically falls (from 73% to 32%), BD rises (from 0.22 to 0.38 g cm^{-3}) and a large quantity of quartz and feldspar are found in the samples. TFS1 was extracted close to Toolik Lake and is 9 m lower in elevation than TFS2. We hypothesise that this anomaly is a result of the lake briefly rising to flood the peatland before settling back down. Given the 150-year time range that this event corresponds to, this could signify lake level change over a number of decades, or a shorter event that resulted in greater sediment deposition. We do not observe any change in testate amoebae distribution, so we hypothesise that this was caused by a much shorter event that briefly raised lake level than a longer-term, multi-decadal rise (as testate amoebae have a life span of a matter of days; Wilkinson and Mitchell, 2010).

In TFS2, a period of wetter, minerotrophic conditions centres on 800 CE. This period is indicated by a peak in *C. pontigulasiformis*, which is also observed at the same time in TFS1 (although *C. pontigulasiformis* remains present for longer in TFS1). Climate drivers may have been responsible for bringing the peatland back to a drier state, as the region experience a warm period from 850-1200 (Hu et al., 2001) which corresponds to steadily drier conditions in TFS2, although this is not observed in TFS1. The transition back to dryness is indicated by a resurgence of *C. aerophila* and an increasing abundance of *Phryganella acropodia*.

3.4.4 - Little Ice Age (LIA)

In TFS1, there is a notable shift towards drier conditions beginning approximately 1550 CE, corresponding to the LIA (Mann et al., 2009). This dry shift is indicated by a large spike in *C. aerophila* (peaking at 83% abundance). During this period, LOI, BD and CAR remain steady and both peatlands are minerotrophic. TFS2 does not exhibit a shift towards dryness during the LIA, likely because this peatland was already dry (as indicated by *Centropyxis platystoma* and *C. aerophila*). However, both cores exhibit a wetting trend at the end of the LIA. Testate amoeba-based reconstructions from permafrost peatlands in Canada (Lamarre et al., 2012), Finland and Russia (Zhang et al., 2018a) also show drier conditions during the LIA. A $\delta^{18}O$ record from the south-central Brooks Range indicates that the LIA caused an increase in winter precipitation and a decrease in summer (Clegg and Hu, 2010), allowing the water table to fall and the peat to dry during the growing season.

3.4.5 - Post-1850 Warming

As TFS1 recovers from the LIA in the late 1800s, WTD remains relatively steady at a moderate depth, with increasing oligotrophy and carbon accumulation. This is evidenced by a switch towards dominance by *A. flavum*, *H. papilio* and *Nebela collaris* among others. CAR rapidly accelerates at the start of the twentieth century. Change point analysis shows that the most notable shift in CAR occurs after 1850 CE, from a mean of 18.4 g C m^{-2} yr^{-1} before, to a mean of 59.5 g C m^{-2} yr^{-1}, corresponding to temperatures rising across the region.

In TFS2, CAR begins to rapidly increase at *c*. 1850 CE, as the peatland shifts to become gradually drier and more oligotrophic. *C. dubium*, *C. oviformis* and *Assulina* sp. are most prevalent after 1850 CE. CAR in the top of the core is highly variable between samples. CAR changes from a mean of 14.2 g C m^{-2} yr^{-1} to a mean of 48.2 g C m^{-2} yr^{-1} after 1850 CE, with the most significant change point occurring at the very beginning of post-1850 warming. This supports the suggestion of an ecosystem state shift in this period.

It is not unexpected for peatland reconstructions to show CAR accelerating towards the top of the core, as the acrotelm (the uppermost layer that remains oxic) remains actively decomposing (Roulet et al., 2007). However, our peatlands both become drier and more oligotrophic at the same time that CAR accelerates. This is not characteristic of the acrotelm (Ingram, 1978), and indicates that there has been a fundamental ecosystem state shift in these peatlands in response to recent warming. Furthermore, the rapid increase in CAR that is observed in both peatlands prior to 1900 CE, alongside a decline in EC, is not within the range of the acrotelm, further supporting the suggestion of an ecosystem state shift.

Macrofossil and pollen analysis performed on both cores (Gałka et al., 2018) also support our findings. Using the chronology presented here, we find that a large rise in *Sphagnum* begins in the 1940s in TFS1 and in the late 1800s in TFS2. Ericaceae rootlets also dramatically increase at a similar time, further supporting their transition to oligotrophic poor fen status (Pancost et al., 2003). Throughout late-Holocene warm periods, Gałka et al. (2018) note an increase

in shrub species (Ericaceae, *Andromeda polifolia* and *Empetrum nigrum*), supporting the hypothesis that Arctic peatlands may become more productive under future warming. This has been evidenced in studies from discontinuous permafrost peatlands (e.g. Turetsky et al., 2007; Natali et al., 2012), including shrub expansion and local plant succession in sub-arctic Sweden (Gałka et al., 2017) although the long-term lasting effect of accelerated carbon accumulation has been questioned (Dise, 2009).

3.4.6 - Permafrost Peatlands and Climate Change

Given that ours is the first study to quantitatively reconstruct peatland dynamics in continuous permafrost, it is challenging to identify synergy between our findings and previous works. Charman et al. (2009) identified that bog surface wetness was primarily driven by precipitation in bogs from the UK and Estonia, but they did not investigate CAR. Charman et al. (2013) found that temperature changes across the late-Holocene drive changes in CAR from a range of peatlands across Europe, but they did not investigate precipitation changes. Zhang et al. (2018a) also found increasingly dry conditions in discontinuous and sporadic permafrost peatlands from across Finland and Siberia, noting that this is indicative of increased evapotranspiration. The differences in the influence of climate on TFS1 and TFS2 may be due to the short analysis period (1900 - 2015 CE; compared to Charman et al. (2013) over two millennia), and slow peat accumulation rate of permafrost peatlands. Alternatively, as both peatlands are sloping, microtopography at the site may regulate the extent to which precipitation influences CAR.

Warming temperatures as a result of anthropogenic activity have led to increased productivity in these Arctic peatlands, which directly enhanced their recent carbon sequestration rates. However, it is unclear whether this enhanced sink can be maintained under further warming, or whether respiration will come to dominate peatland-atmosphere fluxes, causing carbon release to increase (Dorrepaal et al., 2009; Hodgkins et al., 2014; Comyn-Platt et al., 2018). Adding to the complexity of the system, the uncertainty of future permafrost peatlands and their role in the carbon cycle will be complicated by hydrological changes that result from collapse (Swindles et al., 2015b), as well as changes in vegetation, peat chemistry and organic matter quality (Treat et al., 2014). If, as seems likely, the active layer of permafrost peatlands continues to thicken, this may result in the release of carbon as CH_4, rather than CO_2, from thermokarst features (Kirkwood et al., 2018). Further analysis should now seek to identify whether our findings are representative of Arctic permafrost peatlands more generally.

3.5 - Conclusions

1. We reconstruct late-Holocene environmental changes in two continuous permafrost peatlands from Toolik Lake, Alaska, applying two testate amoeba-based transfer functions to reconstruct water table depth and pore water electrical conductivity.
2. One of these peatlands likely initiated during a warm period between 0 and 300 CE.

3. Prior to 1850 CE, both peatlands remained as minerotrophic with low carbon accumulation rates that reflect the slow formation of peat in permafrost regions.
4. There has been a rapid transition towards oligotrophy and a three-fold increase in mean carbon accumulation rate since 1850 CE that may be attributed to rising temperatures.
5. As the Arctic continues to warm, peatlands in the continuous permafrost zone may become an increasingly important carbon sink.

4. DISCUSSION

In this thesis, I have begun to explore the changing dynamics of Alaskan peatlands in the continuous permafrost zone. This is the first such study in continuous permafrost peatlands that includes quantitative testate amoeba-based reconstructions, despite the large (> 500,000 km^2) extent of these ecosystems. This study proves the efficacy of testate amoebae as hydrological indicators in continuous permafrost peatlands. Using these new transfer functions, this study has identified the transition of two Alaskan peatlands towards a drier, oligotrophic state with rising carbon accumulation rates as a result of warming from ~1850 CE.

4.1 – Peatland nutrient status

Throughout this investigation, the trophic status of Alaskan peatlands has been an important factor, both in controlling the distribution of testate amoebae and the recent transition to oligotrophy with recent warming. Trophic status has been the dominant control on testate amoeba distribution in similar studies. For example, Tolonen et al. (1992) note that EC and peatland trophic status were controlling factors in testate amoebae distribution in Southern Finland. This may result from the availability of specific nutrients along the trophic gradient and their role in test development. Some testate amoeba genera (including *Centropyxidae* and *Arcellidae*) incorporate iron into their test (Payne, 2011), so would have an optimum in nutrient rich environments with greater iron availability.

Kurina and Li (2018) were able to identify key indicators of trophic status by classifying testate amoebae into qualitative categories of ‘ombrotrophic’ or ‘minerotrophic’. They found that in transfer functions that span a large trophic gradient, WTD measurements are less reliable than if they had been taken from exclusively ombrotrophic or minerotrophic environments. Zhang et al. (2018b) also note the complexity of environmental controls on testate amoebae in minerotrophic peatlands. Contrary to Kurina and Li (2018), this study produces a WTD transfer function that has high predictive power, despite being from peatlands across a range of trophic statuses. This may be because of the high species diversity of testate amoebae taxa that were identified, which produced enough taxa that were influenced by WTD from across the trophic gradient to be used for reconstruction purposes of both variables.

Payne (2011) suggests that poor preservation of tests in fens may not allow for palaeoecological reconstruction, but this was not a problem in TFS1 or TFS2. This allowed me to produce, and apply, accurate transfer functions for reconstructing WTD in the late-Holocene. However, Amesbury et al. (2018) argue that transfer functions should encompass a greater number of taxa from much larger spatial areas, over a wider range of hydrological conditions. Furthermore, hydrological conditions from Alaska were examined over a single week in July 2015 and repeat measurements should be taken to ensure that the WTD and EC reported are representative of the site, and not of short-term weather conditions. Taking far more contemporary samples from a wider area, although time and resource intensive, would decrease the influence of weather conditions as a potential limitation.

While the trophic gradient heavily influences testate amoeba distribution, it does not appear to affect surface vegetation, which is instead controlled by proxies of moisture. Mitchell et al. (2000) note that this could be due to testate amoebae being much more sensitive to water chemistry, while surface vegetation is more closely regulated by factors such as local topography and shading. Camill (1999) also suggests that local scale vegetation assemblages are often controlled by community composition and microtopography in continuous permafrost peatlands, although hydrology (including WTD) remains important (Churchill et al., 2015). This explains why the most important measured variable in controlling surface vegetation (MC) only explained 5.23% of variance in this study.

While we have been able to observe a transition in the trophic status of TFS1 and TFS2, it is not possible to attribute this to a fen-to-bog transition as there is inconclusive evidence to suggest a transition of primary water sources from groundwater to atmospheric. Poor fens typically have a lower EC than rich fens (Vitt et al., 1995), so there is high confidence in inferring a transition to oligotrophic poor fens in TFS1 and TFS2. This may mean that the future for these peatlands are as bogs, following a typical fen-to-bog transition, especially as *Sphagnum fuscum*, which dominates surface vegetation in both cores, is more typical of bog environments than fens (Granath et al., 2010). Alternatively, Swindles et al. (2015a) propose that permafrost peatlands have an ecohydrological end point of inundated Arctic fen with wet surface conditions and high carbon accumulation. However, this may not be an applicable model

in continuous permafrost, as they also suggest that this occurs alongside the disappearance of underlying permafrost. Mean annual air temperature at Toolik remains well below 0˚C, and we observe TFS1 and TFS2 to both become drier, not wetter, with recent warming.

4.2 – Climate influence

Peatlands preserve records of large-magnitude changes in temperature and precipitation (Morris et al., 2015). In this study, both peatlands showed a drying trend with recent climate warming, which may increase their susceptibility to fire. This may have a large impact on carbon loss, especially resulting from the additional thaw of underlying permafrost (Turetsky et al., 2015). This drying trend has also been observed in sporadic and discontinuous permafrost peatlands in Western Canada from testate amoeba reconstructions (van Bellen et al., 2018), which has been attributed to climate warming in the region. Over long-time scales, vegetation changes that are driven by peatland drying can influence the return interval for fires (Camill et al., 2009).

Drying that was observed in TFS1, and to a lesser extent in TFS2, during the LIA may also be due to climate influence. Zoltai (1993) found that permafrost aggradation in Canadian peatlands caused uplift of the overlying peat by up to 1 metre and subsequent drying. As ice lenses grow during colder climate periods, this may have caused the peatland to become domed and the surface peat to dry. This has also been observed in Siberia, where permafrost aggradation also reduced peat accumulation rates (Routh et al., 2014), although there was no effect on CAR in TFS1 or TFS2.

Both TFS1 and TFS2 showed more than three-fold increases in rates of apparent carbon accumulation as a result of post-1850 warming, due to increased net primary productivity of surface vegetation (also observed by Lamarre et al., 2012). If a similar magnitude response is seen across all 540,239 km^2 of peatlands in continuous permafrost, this could result in a globally significant enhanced short-term sink for anthropogenic carbon emissions. Given there are criticisms that Earth system models may not accurately reflect the carbon balance in permafrost regions (Wania et al., 2009), including the models used for IPCC AR5 (Schuur et al., 2015), there exists a need to integrate observational data from permafrost peatlands into such models to make accurate projections of future carbon budgets.

Precipitation may become a larger influence in the dynamics of TFS1 and TFS2 as high-latitude regions are expected to become wetter in the future (Trenberth, 2011). While Sannel et al. (2016) identify that winter precipitation has large influence on permafrost thaw, TFS1 showed a strong positive correlation between CAR and annual, summer and autumn precipitation with TFS2 showing no response. As the majority of precipitation at Toolik is received during the summer months, precipitation during this period likely enhances productivity in surface vegetation and subsequently increase carbon accumulation. It is not currently possible to test the hypothesis proposed by Sannel et al. (2016) that snow depth is correlated to ground temperature and productivity at Toolik, as snow depth measurements began in 2016.

In order to attribute changes in the climate to observed environmental changes in both peatlands, a good dating record is essential. This study improves upon Gałka et al. (2018) by including ^{210}Pb dates, however more work could be done to improve dating lower in each core. We suggest that TFS2 shows evidence of initiation during a warm period from 0-300 CE between 50 and 46 cm depth in the core, however the rejection of the ^{14}C date at 50 cm means that this relies on a ^{14}C date from 39-40 cm and the Bayesian age model. While this is a robust method, examining tephra or re-running the ^{14}C date on a different sub-sample within this initiation period would be preferable in identifying the true date of initiation, to be able to attribute this to a warming period.

4.3 – Results in the broader context of the Arctic

Peatlands are found across the Alaskan North Slope as a mixture of ombrotrophic and minerotrophic systems (Jones and Yu, 2010). TF_{WTD} and TF_{EC} are applicable across the entire North Slope in continuous permafrost, and perhaps broader. They should be tested in other continuous permafrost peatlands to validate their applicability in the wider Arctic, particularly in similar systems in Canada and eastern Siberia. TF_{WTD} and TF_{EC} were both tested on a peat core from a discontinuous permafrost peatland in Abisko, Sweden (Swindles et al., 2015b), but there were too many missing analogues to make for a meaningful reconstruction, primarily due to the lower diversity in the Swedish site. This was useful to highlight the differences between peatlands as different systems in continuous permafrost to other permafrost regimes,

which reinforces the need for further studies, and transfer functions, that are unique to continuous permafrost.

The changing dynamics of TFS1 and TFS2 match existing studies from permafrost peatlands across the Arctic, with regards to increased carbon accumulation (Yu et al., 2009; Lamarre et al., 2012), increasing oligotrophy (Loisel and Yu, 2013) and rapid dryness (Klein et al., 2015; van Bellen et al., 2018; Zhang et al., 2018a) with recent warming. However, this is the only of such studies to come from continuous permafrost, and, while representing the significant carbon store of Alaskan peatlands, these results may not necessarily be representative of Arctic-wide change in the continuous permafrost zone. Furthermore, although testate amoeba-based transfer functions provide a method to quantitatively reconstruct hydrological changes in a peat core, they should be one component of a wider multi-proxy study to identify ecosystem state shifts. In addition to the methods presented in this thesis, reconstructions could include a number of additional proxies, such as plant macrofossils, pollen analysis and C/N ratios.

Across the Arctic, Gallego-Sala et al. (2018) show that peatlands are likely to become stronger carbon sinks with future warming, with tropical and temperate peatlands becoming net carbon sources under high-emission trajectories. Carbon sequestration is also likely to increase greatest in continuous permafrost regions (Chaudhary et al., 2017). Further research is needed to identify if carbon may be released from permafrost soils, but some research suggests that high-latitude wetlands and peatlands will become net

carbon sources rather than sinks with warming (Sullivan et al., 2008), although there remains significant uncertainty.

4.4 – Future Research

Given this thesis represents the first study of the ecology of testate amoebae in continuous permafrost, future research should strive to ascertain whether the findings presented here are ubiquitous across the Arctic. Similarly, evaluating the applicability of TF_{WTD} and TF_{EC} in other regions should be a priority. The first of such follow-on studies should take place in Canada or Siberia, given they together represent 98.6% of the aerial extent of peatlands in continuous permafrost. Future studies should also seek to encompass a full range of peatlands from across the trophic gradient and measure proxies of nutrient status (such as EC), as this was found to have significant influence in Alaskan peatlands. With additional EC data, it may be possible to present two transfer functions that separate oligotrophic and minerotrophic sites, which was not possible in this study owing to a statistically insignificant number of samples at either end of the trophic gradient. It would also be interesting to explore the ecological reasons of why certain testate amoebae species prefer minerotrophic or oligotrophic environments, as this is still relatively unknown.

A dearth of long-term climate and weather monitoring in continuous permafrost creates difficulty in attributing changing peatland dynamics to climatic drivers. Even at Toolik, where a field station has been present since 1976, important variables of climate (such as snow-depth) have only recently begun being measured. Future research campaigns that are seeking to use

long-term records of climate data should identify nearby weather stations that can provide the required data to answer the research questions. For time series going back to 1901 CE, or 0 CE, this study shows that the CRU TS v. 4.01 and PAGES2k datasets respectively can provide good insight across the Arctic.

When attempting to link changes in peatlands to possible climate drivers, it is important to have a good chronology to be able to reliably attribute these drivers. The timing of the bottom of the cores in this study has a relatively large error, resulting from a limited number of ^{14}C dates (due to the high financial cost of this technique) and the need to exclude an erroneous result at the bottom of TFS2. Evaluating the potential for further dating techniques, such as tephrochronology, may provide a more accurate age model for future palaeo studies.

This study evaluates well the impact that post-1850 warming has had on carbon sequestration in two Alaskan peatlands, concluding that CAR will likely increase with future warming. However, to understand the full dynamics of the permafrost peatland carbon budget, it is important to also monitor the outward fluxes of carbon from these ecosystems. In TFS1 and TFS2, warming has led to drying, which results in a larger oxic active layer (owing to deepening WTD) and CO_2 release from decomposition. Drying also increases the susceptibility of fire, which can release large amounts of CO_2 in a single event. However, if high-emission RCPs are followed, increased permafrost thaw may drastically alter the hydrology of peatlands in continuous permafrost as they become wetter, resulting in CH_4 release instead. There is no literature

consensus on the future carbon balance of permafrost peatlands, and existing studies tend to either focus on carbon sequestration or carbon release in isolation. Future research should examine the pan-Arctic response of permafrost peatlands to recent warming, evaluating both carbon sequestration and carbon flux together to finally answer the question of the role of permafrost peatlands in future global carbon budget.

5. CONCLUSION

This thesis has demonstrated that testate amoebae are valuable environmental indicators in continuous permafrost peatlands. The ecology of testate amoebae in continuous permafrost is broadly similar to previous observations in discontinuous regions, with a number of notable exceptions (e.g. *Archerella flavum* occupying a drier hydrological niche). A strong trophic gradient exists in peatlands across the Alaskan North Slope, which has allowed for the development of two new transfer functions. It is now possible to reconstruct water table depth and pore water electrical conductivity (a proxy for peatland nutrient status) in Alaskan peatlands from the continuous permafrost zone. Contemporary plant species are not affected by this trophic gradient and are instead controlled by proxies of moisture and other, non-measured, variables such as local microtopography.

These transfer functions were subsequently applied to two cores from Toolik Lake, Alaska. By reconstructing water table depth and electrical conductivity, in addition to loss-on-ignition and carbon accumulation rate, it has been possible to attribute initiation in one of these peatlands to a warm period between 0 and 300 CE. Permafrost aggradation may have caused a small drying trend during the Little Ice Age, but both peatlands remained largely moderately-wet and minerotrophic throughout the late-Holocene. Since ~1850 CE, there has been a rapid transition towards drier, oligotrophic poor fens with an associated three-fold increase in mean carbon accumulation rate. Using reconstructed climate data from the same time period, we are able to attribute this transition, and the increased carbon sequestration, to recent warming.

As the Arctic continues to warm, peatlands in the continuous permafrost zone may become increasingly important carbon sinks. Further research now needs to take place across the continuous permafrost zone to test the applicability of TF_{WTD} and TF_{EC}, and identify whether post-1850 warming has caused similar ecosystem state shifts across the Arctic.

COMPILED REFERENCES

Amesbury, M.J., Booth, R.K., Roland, T.P., Bunbury, J., Clifford, M.J., Charman, D.J., Elliot, S., Finkelstein, S., Garneau, M., Hughes, P.D.M., Lamarre, A., Loisel, J., Mackay, H., Magnan, G., Markel, E.R., Mitchell, E.A.D., Payne, R.J., Pelletier, N., Roe, H., Sullivan, M.E., Swindles, G.T., Talbot, J., van Bellen, S. and Warner, B.G. 2018. Towards a Holarctic synthesis of peatland testate amoeba ecology: Development of a new continental-scale palaeohydrological transfer function for North America and comparison to European data. *Quaternary Science Reviews*. **201**; pp.483-500.

Amesbury, M.J., Roland, T.P., Royles, J., Hodgson, D.A., Convey, P., Griffiths, H. and Charman, D.J. 2017. Widespread Biological Response to Rapid Warming on the Antarctic Peninsula. *Current Biology*. **27**; pp.1616-1622.

Amesbury, M.J., Swindles, G.T., Bobrov, A. Charman, D.J., Holden, J., Lamentowicz, M., Mallon, G., Mazei, Y., Mitchell, E.A.D., Payne, R.J., Roland, T.P., Turner, T.E. and Warner, B.G.. 2016. Development of a new pan-European testate amoebae transfer function for reconstructing peatland palaeohydrology. *Quaternary Science Reviews*. **152**; pp.132-151.

Amesbury, M.J., Mallon, G., Charman, D.J., Hughes, P.D.M., Booth, R.K., Daley, T.J. and Garneau, M. 2013. Statistical testing of a new testate amoeba-based transfer function for water-table depth reconstruction on ombrotrophic peatlands in north-eastern Canada and Maine, United States. *Journal of Quaternary Science*. **28**(1); pp.27-39.

Appleby, P.G. 2001. Chronostratigraphic techniques in recent sediments. In W. M. Last and J. P. Smol (Eds.), *Tracking Environmental Change Using Lake Sediments Volume 1: Basin Analysis, Coring and Chronological Techniques*; pp.171-203. Dordrecht, Klower Academic Publishers.

Appleby, P.G. and Oldfield, F. 1978. The calculation of lead-210 dates assuming a constant rate of supply of unsupported ^{210}Pb to the sediment. *Catena*. **5**(1); pp.1-8.

Avis, C.A., Weaver, A.J. and Meissner, K.J. 2011. Reduction in areal extent of high-latitude wetlands in response to permafrost thaw. *Nature Geoscience*. **4**; pp.444-448.

Belyea, L.R. and Malmer, N. 2004. Carbon sequestration in peatland: patterns and mechanisms of response to climate change. *Global Change Biology*. **10**(7); pp.1043-1052.

Beyens, L. and Chardez, D. 1995. An annotated list of testate amoebae observed in the Arctic between the longitudes 27˚E and 168˚W. *Archiv für Protistenkunde*. **146**(2); pp.219-233.

Beyens, L., Chardez, D. and De Landtsheer, R. 1986a. Testate Amoebae Communities from Aquatic Habitats in the Arctic. *Polar Biology*. **6**; pp.197-205.

Beyens, L., Chardez, D. and DeBock, P. 1986b. Some new and rare testate amoebae from the Arctic. *Acta Protozoologica*. **25**; pp.81-91.

Blaauw, M., Christen, J.A., Vazquez, J.E., Belding, T., Theiler, J., Gough, B. and Karney, C. 2018. *rbacon: Age-Depth Modelling using Bayesian Statistics*, R package version 2.3.4. [Online] https://CRAN.R-project.org/package=rbacon.

Booth, R.K., Lamentowicz, M. & Charman, D.J. 2010. Preparation and analysis of testate amoebae in peatland palaeoenvironmental studies. *Mires and Peat,* **7**: Art. 2. [Online] http://www.mires-and-peat.net/pages/ volumes/map07/ map0702.php.

Booth, R.K. 2008. Testate amoebae as proxies for mean annual water-table depth in *Sphagnum*-dominated peatlands of North America. *Journal of Quaternary Science*. **23**(1); pp.43-57.

Booth, R.K. and Sullivan, M. 2007. *Key of Testate Amoebae Inhabiting* Sphagnum-*dominated Peatlands with an Emphasis on Taxa Preserved in Holocene Sediments*. Lehigh University, Bethlehem.

Booth, R.K. 2001. Ecology of testate amoebae (protozoa) in two Lake Superior coastal wetlands: Implications for paleoecology and environmental monitoring. *Wetlands*. **21**(4); pp.564-576.

Brown, J. 1998. Circumpolar Active-Layer Monitoring (CALM) Program: Description and data. In *Circumpolar active-layer permafrost system, version 2.0*. (ed.) M. Parsons and T. Zhang, (comp.) International

Permafrost Association Standing Committee on Data Information and Communication. Boulder, CO: National Snow and Ice Data Center.

Brown, R.J.E. 1968. Occurrence of permafrost in Canadian peatlands. *Proceedings of the Third International Peat Congress*. Quebec. pp.174-181.

Bubier, J.L., Frolking, S., Crill, P.M. and Linder, E. 1999. Net ecosystem productivity and its uncertainty in a diverse boreal peatland. *Journal of Geophysical Research*. **104**(D22); pp.27683-27692.

Bunbury, J., Finkelstein, S.A. and Bollmann, J. 2012. Holocene hydro-climatic change and effects on carbon accumulation inferred from a peat bog in the Attawapiskat River watershed, Hudson Bay Lowlands, Canada. *Quaternary Research*. **78**(2); pp.275-284.

Burn, C.R. and Nelson, F.E. 2006. Comment on "A projection of severe near-surface permafrost degradation during the 21st century" by David M. Lawrence and Andrew G. Slater. *Geophysical Research Letters*. **33**(21); pp.1-2.

Camill, P., Barry, A., Williams, E., Andreassi, C., Limmer, J. and Solick, D. 2009. Climate-vegetation-fire interactions and their impact on long-term carbon dynamics in a boreal peatland landscape in northern Manitoba, Canada. *Biogeosciences*. **114**; G04017.

Camill, P. 2005. Permafrost thaw accelerates in boreal peatlands during late-20th century climate warming. *Climatic Change*. **68**(1-2); pp.135-152.

Camill, P. 1999. Patterns of boreal permafrost peatland vegetation across environmental gradients sensitive to climate warming. *Canadian Journal of Botany*. **77**(5); pp.721-733.

Chadburn, S.E., Burke, E.J., Cox, P.M., Friedlingstein, P., Hugelius, G. and Westermann, S. 2017. An observation-based constraint on permafrost loss as a function of global warming. *Nature Climate Change*. **7**; pp.340-344.

Chambers, F.M., Beilman, D.W. and Yu, Z. 2011. Methods for determining peat humification and for quantifying peat bulk density, organic matter and carbon content for palaeo studies of climate and peatland carbon dynamics. *Mires and Peat*. **7**(7). [Online] http:www.mires-and-peat.net/pages/volumes/map07/map0707.php.

Charman, D.J., Amesbury, M.J., Hinchliffe, W., Hughes, P.D.M., Mallon, G., Blake, W.H., Daley, T.J., Gallego-Sala, A.V. and Mauquoy, D. 2015. Drivers of Holocene peatland carbon accumulation across a climate gradient in northeastern North America. *Quaternary Science Reviews*. **121**; pp.110-119.

Charman, D.J., Beilman, D.W., Blaauw, M., Booth, R.J., Brewer, S., Chambers, F.M., Christen, J.A., Gallego-Sala, A., Harrison, S.P., Hughes, P.D.M., Jackson, S.T., Korhola, A., Mauquoy, M., Mitchell, F.J.G., Prentice, I.C., van der Linden, M., Vleeschouwer, F.D., Yu, Z.C., Aim, J., Bauer, I.E., Corish, Y.M.C., Garneau, M., Hohl, V., Huang, Y., Karofeld, E., Le Roux, G., Loisel, J., Moschen, R., Nichols, J.E., Nieminen, T.M., MacDonalds, G.M., Phadtare, N.R., Rausch, N., Sillasoo, Ü., Swindles, G.T., Tuittila, E.-S., Ukonmaanaho, L., Väliranta, M., van Bellen, S., van Geel, B., Vitt, D.H. and Zhao, Y. 2013. Climate-related changes in peatland carbon accumulation during the last millennium. *Biogeosciences.* **10**(2); pp.929-944.

Charman, D.J., Barber, K.E., Blaauw, M., Langdon, P.G., Mauquoy, D., Daley, T.J., Hughes, P.D.M. and Karofeld, E. 2009. Climate drivers for peatland palaeoclimate records. *Quaternary Science Reviews*. **28**(19-20); pp.1811-1819.

Charman, D.J., Blundell, A. and ACCROTELM members. 2007. A new European testate amoebae transfer function for palaeohydrological reconstruction on ombrotrophic peatlands. *Journal of Quaternary Science*. **22**(3); pp.209-221.

Charman, D.J., Brown, A.D., Hendon, D. and Karofeld, E. 2004. Testing the relationship between Holocene peatland palaeoclimate reconstructions and instrumental data at two European sites. *Quaternary Science Reviews*. **23**(1-2); pp.137-143.

Charman, D.J., Hendon, D. and Woodland, W.A. 2000. The Identification of Testate Amoebae (Protozoa: Rhizopoda) in Peats*, Quaternary Research Association*, Oxford.

Charman, D.J. and Warner, B.G. 1992. Relationship between testate amoebae (Protozoa: Rhizopoda) and microenvironmental parameters on a

forested peatland in northeastern Ontario. *Canadian Journal of Zoology.* **70**(12); pp.2474-2482.

Chaudhary, N., Miller, P.A. and Smith, B. 2017. Modelling past, present and future peatland carbon accumulation across the pan-Arctic region. *Biogeosciences*. **14**; pp.4023-4044.

Christensen, T.R., Johansson, T., Åkerman, H.J., Mastepanov, M., Malmer, N., Friborg, T., Crill, P. and Svensson, B.H. 2004. Thawing sub-arctic permafrost: Effects on vegetation and methane emissions. *Geophysical Research Letters.* **31**(4); pp.1-4.

Churchill, A.C., Turetsky, M.R., McGuire, A.D. and Hollingsworth, T.N. 2015. Response of plant community structure and primary productivity to experimental drought and flooding in an Alaskan fen. *Canadian Journal of Forest Research*. **45**(2); pp.185-193.

Clegg, B.F., and Hu, F.S. 2010. An oxygen-isotope record of Holocene climate change in the south-central Brooks Range, Alaska. *Quaternary Science Reviews*. **29**(7-8); pp.928-939.

Cohen, J., Screen, J.A., Furtado, J.C., Barlow, M., Whittleston, D., Coumou, D., Francis, J., Dethloff, K., Entekhabi, D., Overland, J. and Jones, J. 2014. Recent Arctic amplification and extreme mid-latitude weather. *Nature Geoscience*. **7**; pp.627-637.

Collins, M., Knutti, R., Arblaster, J., Dufresne, J.-L., Fichefet, T., Friedlingstein, P., Gao, X., Gutowski, W.J., Johns, T., Krinner, G., Shongwe, M., Tebaldi, C., Weaver, A.J. and Wehner, M. 2013. Long-term Climate Change: Projections, Commitments and Irreversibility, In *Climate Change 2013: The Physical Science Basis. Contribution of Working Group I to the Fifth Assessment Report of the Intergovernmental Panel on Climate Change*, [Stocker, T.F., Qin, D., Plattner, G.-K., Tignor, M., Allen, S.K., Boschung, J., Nauels, A., Xia, Y., Bex, V. and Midgley, P.M. (eds)]. Cambridge University Press, Cambridge, United Kingdom and New York, NY, USA, pp.1029-1136.

Comyn-Platt, E., Hayman, G., Huntingford, C., Chadburn, S.E., Burke, E.J., Harper, A.B., Collins, W.J., Webber, C.P., Powell, T., Cox, P.M., Gedney, N. and Sitch, S. 2018. Carbon budgets for 1.5 and 2˚C targets lowered

by natural wetland and permafrost feedbacks. *Nature Geoscience*. **11**; pp.568-573.

Cooper, M.D.A., Estop-Aragones, C., Fisher, J.P., Thierry, A., Garnett, M.H., Charman, D.J., Murton, J.B., Phoenix, G.K., Treharne, R., Kokelj, S.V., Wolfe, S.A., Lewkowicz, A.G., Williams, M. and Hartley, I.P. 2017. Limited contribution of permafrost carbon to methane release from thawing peatlands. *Nature Climate Change*. **7**; pp.507-511.

Delisle, G. 2007. Near-surface permafrost degradation: How severe during the 21st century?. *Geophysical Research Letters*. **34**(9); pp.1-4.

Dise, N.B. 2009. Peatland Response to Global Change. *Science*. **326**(5954); pp.810-811.

Dorrepaal, E., Toet, S., van Logtestijn, R.S.P., Swart, E., van de Weg, M.J., Callaghan, T.V. and Aerts, R. 2009. Carbon respiration from subsurface peat accelerated by climate warming in the subarctic. *Nature*. **460**; pp.616-619.

Dorrepaal, E., Aerts, R., Cornelissen, J.H.C., Callaghan, T.V. and van Logtestijn, R.S.P. 2003. Summer warming and increased winter snow cover affect *Spaghnum fuscum* growth, structure and production in a sub-arctic bog. *Global Change Biology*. **10**(1); pp.93-104.

Environmental Data Center Team. 2018. *Meteorological monitoring program at Toolik, Alaska*. Toolik Field Station, Institute of Arctic Biology, University of Alaska Fairbanks, Fairbanks, AK 99775. http://toolik.alaska.edu/edc/abiotic_monitoring/data_query.php

Escobar, J., Brenner, M., Whitmore, T.J., Kenney, W.F. and Curtis, J.H. 2008. Ecology of testate amoebae (thecamoebians) in subtropical Florida lakes. *Journal of Paleolimnology*. **40**(2); pp.715-731.

Flora of North America North of Mexico. 2007. Edited by Flora of North America Editorial Committee. Vol. 27. Oxford University Press, New York. p. 714.

Flora of North America North of Mexico. 2014. Edited by Flora of North America Editorial Committee. Vol. 28. Oxford University Press, New York. p. 702.

Flynn, W.W. 1968. The determination of low levels of polonium-210 in environmental materials. *Analytica Chimica Acta*. **43**; pp.221-227.

Gałka, M., Swindles, G.T., Szal, M., Fulweber, R. and Feurdean, A. 2018. Response of plant communities to climate change during the late

Holocene: Palaeoecological insights from peatlands in the Alaskan Arctic. *Ecological Indicators*. **85**; pp.525-536.

Gałka, M., Szal, M., Watson, E.J., Gallego-Sala, A., Amesbury, M.J., Charman, D.J., Roland, T.P., Turner, T.E. and Swindles, G.T. 2017. Vegetation succession, carbon accumulation and hydrological change in subarctic peatlands, Abisko, Northern Sweden. *Permafrost and Periglacial Processes*. **28**(4); pp.589-604.

Gallego-Sala, A.V., Charman, D.J., Brewer, S., Page, S.E., Prentice, I.C., Friedlingstein, P., Moreton, S., Amesbury, M.J., Beilman, D.W., Björk, S., Blyakharchuk, T., Bochicchio, C., Booth, R.K., Bunbury, J., Camill, P., Carless, D., Chimner, R.A., Clifford, M., Cressey, E., Courtney-Mustaphi, C., Vleeschouwer, F.D., de Jong, R., Fialkiewicz-Koziel, B., Finkelstein, S.A., Garneau, M., Githumbi, E., Hribjlan, J., Holmquist, J., Hughes, P.D.M., Jones, C., Jones, M.C., Karofeld, E., Klein, E.S., Kokfelt, U., Korhola, A., Lacourse, T., Le Roux, G., Lamentowicz, M., Large, D., Lavoie, M. Loisel, J., Mackay, H., MacDonald, G.M., Makila, M., Magnan, G., Marchant, R., Marcisz, K., Martínez Cortizas, A., Massa, C., Mathijssen, P., Mauquoy, D., Mighall, T., Mitchell, F.J.G., Moss, P., Nichols, J., Oksanen, P.O., Orme, L., Packalen, M.S., Robinson, S., Roland, T.P., Sanderson, N.K., Sannel, A.B.K., Silva-Sánchez, N., Steinberg, N., Swindles, G.T., Turner, T.E., Uglow, J., Väliranta, M., van Bellen, S., van der Linden, M., van Geel, B., Wang, G., Yu, Z., Zaragoza-Castells, J. and Zhao, Y. 2018. Latitudinal limits to the predicted increased of the peatland carbon sink with warming. *Nature Climate Change*. [Online] https://doi.org/10.1038/s41558-018-0271-1

Gavel, M.J., Patterson, R.T., Nasser, N.A., Galloway, J.M., Hanna, B.W., Cott, P.A., Roe, H.M. and Falck, H. 2018. What killed Frame Lake? A precautionary tale for urban planners. *PeerJ*. **6**; e4850.

Gibson, C.M., Chasmer, L.E., Thompson, D.K., Quinton, W.L., Flannigan, M.D. and Olefeldt, D. 2018. Wildfire as a major driver of recent permafrost thaw in boreal peatlands. *Nature Communications*. **9**; 3041.

Gorham, E., Lehman, C., Dyke, A., Janssens, J. and Dyke, L. 2007. Temporal and spatial aspects of peatland initiation following deglaciation in North America. *Quaternary Science Reviews*. **26**(3-4); pp.300-311.

Gorham, E., Janssens, J.A., Wheeler, G.A. and Glaser, P.H. 1987. The Natural and Anthropogenic Acidification of Peatlands. In: Hutchinson, T. C. and Meema, K. M. (eds) *Effects of Atmospheric Pollutants on Forests, Wetlands and Agricultural Ecosystems*. NATO ASI Series (Series G: Ecological Sciences), vol 16. Springer, Berlin, Heidelberg.

Granath, G., Strengbom, J. and Rydin, H. 2010. Rapid ecosystem shifts in peatlands: linking plant physiology and succession. *Ecology*. **91**(10); pp.3047-3056.

Greenacre, M. 2013. The contributions of rare objects in correspondence analysis. *Ecology.* **94**(1); pp.241-249.

Guo, W., Liu, H., Anenkhonov, O.A., Shangguan, H., Sandanov, D.V., Korolyuk, A.Y., Hu, G. and Wu, X. 2018. Vegetation can strongly regulate permafrost degradation at its southern edge through changing surface freeze-thaw processes. *Agricultural and Forest Meteorology*. **252**; pp.10-17.

Hadenäs, L. 2003. The European species of the Calliergon–Scorpidium–Drepanocladus complex, including some related or similar species. *Meylania.* **28**; pp.1–116.

Hamilton, T.D. 1986. Late cenozoic glaciation of the central brooks range. In: Hamilton, T.D., Reed, K.M., Thorson, R.M. (eds) *Glaciation in Alaska: the Geological Record*, Alaska Geological Society, Fairbanks; pp.9-49.

Harris, I., Jones, P.D., Osborn, T.J. and Lister, D. 2014. Updated high-resolution grids of monthly climatic observations- the CRU TS3.10 Dataset. *International Journal of Climatology*. **34**(3); pp.623-642

Hendon, D. and Charman, D.J. 1997. The preparation of testate amoebae (Protozoa: Rhizopoda) samples from peat. *The Holocene*. **7**(2); pp. 199-205.

Hinkel, K.M., Nelson, F.E. and Outcalt, S.I. 1987. Frost mounds at Toolik Lake, Alaska. *Physical Geography*. **8**(2); pp.148-159.

Hinkel, K.M. and Nelson, F.E. 2003. Spatial and temporal patterns of active layer thickness at Circumpolar Active Layer Monitoring (CALM) sites in northern Alaska, 1995-2000. *Climate and Dynamics*. **108**(D2); pp.1-13.

Hodgkins, S.B., Tfaily, M.M., McCalley, C.K., Logan, T.A., Crill, P.M., Saleska, S.R., Rich, V.I. and Chanton, J.P. 2014. Changes in peat chemistry

associated with permafrost thaw increase greenhouse gas production. *PNAS*. **111**(16); pp.5819-5824

Holden, J. 2005. Peatland hydrology and carbon release: why small-scale process matters. *Philosophical transactions of the Royal Society*. **363**(1837); pp.2891-2913.

Hu, F.S., Ito, E., Brown, T.A., Curry, B. and Engstrom, D.R. 2001. Pronounced climatic variations in Alaska during the last two millennia. *PNAS*. **98**(19); pp.10552-10556.

Ingram, H.A.P. 1978. Soil Layers in Mires: Function and Terminology. *Journal of Soil Science*. **29**(2); pp.224-227.

Ise, T., Dunn, A.L., Wofsy, S.C. and Moorcroft, P.R. 2008. High sensitivity of peat decomposition to climate change through water-table feedback. *Nature Geoscience*. **1**; pp.763-766.

Jorgenson, M.T. Yoshikawa, K., Kanevskiy, M. and Shur, Y. 2008. Permafrost characteristics of Alaska, *Ninth International Conference on Permafrost,* Extended Abstracts, Kane, D.L., Hinkel, K.M. (eds). Institute of Northern Engineering, University of Alaska, Fairbanks; pp.121-122.

Jorgenson, M.T., Shur, Y.L. and Pullman, E.R. 2006. Abrupt increase in permafrost degradation in Arctic Alaska. *Geophysical Research Letters*. **33**(2); L02503.

Jones, M.C. and Yu, Z. 2010. Rapid deglacial and early Holocene expansion of peatlands in Alaska. *PNAS.* **107**(16); pp.7347-7352.

Ju, L., Yang, J., Liu, L. and Wilkinson, D.M. 2014. Diversity and Distribution of Freshwater Testate Amoebae (Protozoa) Along Latitudinal and Trophic Gradients in China. *Microbial Ecology*. **68**(4); pp.657-670.

Juggins, S. 2007. *C2*, version 1.7.5. [Online] https://www.staff.ncl.ac.uk/ stephen.juggins/software/C2Home.htm.

Khvorostyanov, D.V., Ciais, P., Krinner, G. and Zimov, S.A. 2008. Vulnerability of east Siberia's frozen carbon stores to future warming. *Geophysical Research Letters*. **35**(10); pp.1-5.

Killick, R., Haynes, K., Eckley, I., Fearnhead, P. and Lee, J. 2016. *Changepoint: Methods for Changepoint Detection*, R package version 2.2.2. [Online] https://cran.r-project.org/package=changepoint.

Kirkwood, A.H., Roy-Léveillée, P., Basiliko, N., McLaughin, J. and Packalen, M. 2018. Microbial greenhouse gas production in permafrost peatlands of the Hudson Bay Lowlands, Canada. *5th European Conference on Permafrost*, Chamonix, June 2018.

Kirtman, B., Power, S.B., Adedoyin, J.A., Boer, G.J., Bojariu, R., Camilloni, I., Doblas-Reyes, F.J., Fiore, A.M., Kimoto, M., Meehl, G.A., Prather, M., Sarr, A., Schä, C., Sutton, R., van Oldenborgh, G.J., Vecchi, G. and Wang, H.J. 2013. Near-term Climate Change: Projections and Predictability. In: *Climate Change 2013: The Physical Science Basis. Contribution of Working Group I to the Fifth Assessment Report of the Intergovernmental Panel on Climate Change* [Stocker, T.F., Qin, D., Plattner, G.-K., Tignor, M., Allen, S.K., Boschung, J., Nauels, A., Xia, Y., Bex, V. and Midgley, P.M. (eds)]. Cambridge University Press, Cambridge, United Kingdom and New York, NY, USA.

Klein, E., Berg, E.E. and Dial, R. 2005. Wetland drying and succession across the Kenai Peninsula Lowlands, south-central Alaska. *Canadian Journal of Forest Research*. **35**(8); pp.1931-1941.

Kurina, I.V. and Li, H. 2018. Why do testate amoeba optima related to water table depth vary?. *Microbial Ecology*. 1432-184X. [Online] https://doi.org/10.1007/s00248-018-1202-4

Lamarre, A., Magnan, G., Garneau, M. and Boucher, É. 2013. A testate amoeba-based transfer function for paleohydrological reconstruction from boreal and subarctic peatlands in northeastern Canada. *Quaternary International*. **306**; pp.88-96.

Lamarre, A., Garneau, M., Asnong, H. 2012. Holocene paleohydrological reconstruction and carbon accumulation of a permafrost peatland using testate amoeba and macrofossil analyses, Kuujjuarapik, subarctic Québec, Canada. *Review of Palaeobotany and Palynology.* **186**; pp.131-141.

Lamentowicz, M., Lamentowicz, Ł. and Payne, R.J. 2013. Towards quantitative reconstruction of peatland nutrient status from fens. *The Holocene*. **23**(12); pp.1661-1665.

Lamentowicz, M., Lamentowicz, Ł., van der Knaap, W.O., Gabka, M. and Mitchell, E.A. 2010. Contrasting Species-Environment Relationships in

Communities of Testate Amoebae, Bryophytes and Vascular Plants along the Fen-Bog Gradient. *Environmental Microbiology*. **59**; pp.499-510.

Lamentowicz, Ł., Lamentowicz, M. and Gąbka, M. 2008. Testate amoebae ecology and a local transfer function from a peatland in Western Poland. *Wetlands.* **28**(1); pp.164-175.

Langdon, P.G. and Barber, K.E. 2005. The climate of Scotland over the last 5000 years inferred from multiproxy peatland records: inter-site correlations and regional variability. *Journal of Quaternary Science*. **20**(6); pp.549-566.

Lawrence, D.M. and Slater, A.G. 2005. A projection of severe near-surface permafrost degradation during the 21st century. *Geophysical Research Letters*. **32**(24); pp.1-5.

Loisel, J. and Yu, Z. 2013. Recent acceleration of carbon accumulation in a boreal peatland, south central Alaska. *Biogeosciences*. **118**(1); pp.41-53.

MacDonald, G.M., Beilman, D.W., Kremenetski, K.V., Sheng, Y., Smith, L.C. and Velichko, A.A. 2006. Rapid Early Development of Circumarctic Peatlands and Atmospheric CH_4 and CO_2 Variations. *Science*. **314**(5797); pp.285-288.

Mann, D.H., Groves, P., Reanier, R.E. and Kunz, M.L. 2010. Floodplains, permafrost, cottonwood trees, and peat: What happened the last time climate warmed suddenly in arctic Alaska?. *Quaternary Science Reviews*. **29**(27-28); pp.3812-3830.

Mann, M.E., Zhang, Z. and Rutherford, S. 2009. Global Signatures and Dynamical Origins of the Little Ice Age and Medieval Climate Anomaly. *Science*. **326**(5957); pp.1256-1260.

Minayeva, T., Sirin, A., Kershaw, P. and Bragg, O. 2016. Arctic Peatlands. In: Finlayson, C., Milton, G., Prentice, R., Davidson, N. (eds) *The Wetland Book*. Springer, Dordrecht.

Mitchell, E.A.D., Charman, D.J. and Warner, B.G. 2008a. Testate amoebae analysis in ecological and paleoecological studies of wetlands: past, present and future. *Biodiversity and Conservation*. **17**(9); pp.2115-2137.

Mitchell, E.A.D., Payne, R.J. and Lamentowicz, M. 2008b. Potential implications of differential preservation of testate amoeba shells for paleoenvironmental reconstruction in peatlands. *Journal of Paleolimnology.* **40**(2); pp.603-618.

Mitchell, E.A.D. 2004. Response of Testate Amoebae (Protozoa) to N and P Fertilization in an Arctic Wet Sedge Tundra. *Arctic, Antarctic, and Alpine Research*. **36**(1); pp.78-83.

Mitchell, E.A.D., Butler, A., Grosverneir, P., Rydin, H., Albinsson, C., Greenup, A.L., Heijmans, M.M.P.D., Hoosbeek, M.R. and Saarinen, T. 2000. Relationships among testate amoebae (Protozoa), vegetation and water chemistry in five *Sphagnum*-dominated peatlands in Europe. *The New Phytologist*. **145**(1); pp.95-106.

Mitchell, E.A.D., Buttler, A.J., Warner, B.G. and Gobat, J.M. 1999. Ecology of testate amoebae (Protozoa: Rhizopoda) in *Sphagnum* peatlands in the Jura Mountains, Switzerland and France. *Écoscience*. **6**(4); pp.565-576.

Moore, T.R., Roulet, N.T. and Waddington, J.M. 1998. Uncertainty in Predicting the Effect of Climatic Change on the Carbon Cycling of Canadian Peatlands. *Climatic Change*. **40**(2); pp.229-245.

Morris, P.J., Swindles, G.T., Valdes, P.J., Ivanovic, R.F., Gregoire, L.J., Smith, M.W., Tarasov, L., Haywood, A.M. and Bacon, K.L. 2018. Global peatland initiation driven by regionally asynchronous warming. *PNAS*. **115**(19); pp.4851-4856.

Morris, P.J., Baird, A.J., Young, D.M. and Swindles, G.T. 2015. Untangling climate signals from autogenic changes in long-term peatlands development. *Geophysical Research Letters*. **42**(24); pp.10788-10797.

Müller, S., Bobrov, A.A., Schirrmeister, L., Andreev, A.A. and Tarasov, P.E. 2009. Testate amoebae record from the Laptev Sea coast and its implication for the reconstruction of Late Pleistocene and Holocene environments in the Arctic Siberia. *Palaeogeography, Palaeoclimatology, Palaeoecology*. **271**(3-4); pp.301-315.

Myers-Smith, I.H., Forbes, B.C., Wilmking, M., Hallinger, M., Lantz, T., Blok, D., Tape, K.D., Macias-Fauria, M., Sass-Klaassen, U., Lévesque, E., Boudreau, S., Ropars, P., Hermanutz, L., Trant, A., Siegwart Collier, L., Weijers, S., Rozema, J., Rayback, S.A., Schmidt, N.M., Schaepman-

Strub, G., Wipf, S., Rixen, C., Ménard, C.B., Venn, S., Goetz, S., Andreu-Hayles, L., Elmendorf, S., Ravolainen, V., Welker, J., Grogan, P., Epstein, H.E. and Hik, D.S. 2011. Shrub expansion in tundra ecosystems: dynamics, impacts and research priorities. *Environmental Research Letters*. **6**; 045509.

Myhre, G., Shindell, D., Bréon, F.-M., Collins, W., Fuglestvedt, J., Huang, J., Koch, D., Lamarque, J.-F., Lee, D., Mendoza, B., Nakajima, T., Robock, A., Stephens, G., Takemura, T. and Zhang, H. 2013. Anthropogenic and Natural Radiative Forcing. In: *Climate Change 2013: The Physical Science Basis. Contribution of Working Group I to the Fifth Assessment Report of the Intergovernmental Panel on Climate Change* [Stocker, T.F., Qin, D., Plattner, G.-K., Tignor, M., Allen, S.K., Boschung, J., Nauels, A., Xia, Y., Bex, V. and Midgley, P.M. (eds)]. Cambridge University Press, Cambridge, United Kingdom and New York, NY, USA.

Nasser, N.A. and Patterson, R.T. 2015. *Conicocassis*, a new genus of Arcellinina (testate lobose amoebae). *Palaeontologia Electronica*. **18**; pp.1-11.

Natali, S.M., Schuur, E.A.G. and Rubin, R.L. 2012. Increased plant productivity in Alaskan tundra as a result of experimental warming of soil and permafrost. *Journal of Ecology*. **100**(2); pp.488-498.

O'Donnell, J.A., Jorgenson, M.T., Harden, J.W., McGuire, A.D., Kanevskiy, M.Z. and Wickland, K.P. 2012. The Effects of Permafrost Thaw on Soil Hydrologic, Thermal, and Carbon Dynamics in an Alaskan Peatland. *Ecosystems*. **15**(2); pp.213-229.

Oksanen, J., Blanchet, F.G., Friendly, M., Kindt, R., Legendre, P., McGlinn, D., Minchin, P.R., O'Hara, R.B., Simpson, G.L., Solymos, P., Stevens, M.H.H., Szoecs, E. and Wagner, H. 2017. *Vegan: Community Ecology Package*, R package version 2.4-4. [Online] https://CRAN.R-project.org/package=vegan.

Opravilová, V. and Hájek, M. 2006. The variation of testacean assemblages (Rhizopoda) along the complete base-richness gradient in fens: A case study from the Western Carpathians. *Acta Protozoologica*. **45**; pp.191-204.

Osterkamp, T.E. 2007. Characteristics of the recent warming of permafrost in Alaska. *Journal of Geophysical Research: Earth Surface*. **112**(F2); pp.1-10.

Osterkamp, T.E. 2005. The recent warming of permafrost in Alaska. *Global and Planetary Change*. **49**(3-4); pp.187-202.

Osterkamp, T.E., Viereck, L., Shur, Y., Jorgenson, M.T., Racine, C., Doyle, A. and Boone, R.D. 2000. Observation of thermokarst and its impact on boreal forests in Alaska, U.S.A. *Arctic, Antarctic, and Alpine Research*. **32**(3); pp.303-315.

Osterkamp, T.E. and Romanovsky, V.E. 1999. Evidence for warming and thawing of discontinuous permafrost in Alaska. *Permafrost and Periglacial Processes*. **10**(1); pp.17-37.

PAGES2k Consortium. 2017. A global multiproxy database for temperature reconstructions of the Common Era. *Scientific Data*. **4**, 170088.

Pancost, R.D., Baas, M., van Geel, B. and Sinninghe Damsté, J.S. 2003. Response of an ombrotrophic bog to a regional climate event revealed by macrofossil, molecular and carbon isotopic data. *The Holocene*. **13**(6); pp.921-932

Payette, S., Delwaide, A., Caccianiga, M. and Beauchemin, M. 2004. Accelerated thawing of subarctic peatland permafrost over the last 50 years. *Geophysical Research Letters*. **31**(18); pp.1-4.

Payne, R.J. 2011. Can testate amoeba-based palaeohydrology be extended to fens?. *Journal of Quaternary Science.* **26**(1); pp.15-27.

Payne, R.J. and Blackford, J.J. 2008. Peat humification and climate change: a multi-site comparison from mires in south-east Alaska. *Mires and Peat*. **3**. [Online] http://www.mires-and-peat.net/pages/volumes/map03/map0309.php.

Payne, R.J., Blackford, J.J. and van der Plicht, J. 2008. Using cryptotephras to extend regional tephrochronologies: An example from southeast Alaska and implications for hazard assessment. *Quaternary Research*. **69**(1); pp.42-55.

Payne, R.J. and Mitchell, E.A.D. 2007. Ecology of Testate Amoebae from Mires in the Central Rhodope Mountains, Greece and Development of a

Transfer Function for Palaeohydrological Reconstruction. *Protist.* **158**(2); pp.159-171.

Pokrovsky, O.S., Shirokova, L.S., Kirpotin, S.N., Audry, S., Viers, J. and Dupré, B. 2011. Effect of permafrost thawing on organic carbon and trace element colloidal speciation in the thermokarst lakes of western Siberia. *Biogeosciences*. **8**(3); pp.565-583.

Qin, Y., Mitchell, E.A.D., Lamentowicz, M., Payne, R.J., Lara, E., Gu, Y., Huang, X. and Wang, H. 2013. Ecology of testate amoebae in peatlands of central China and development of a transfer function for paleohydrological reconstruction. *Journal of Paleolimnology*. **50**(3); pp.319-330.

Qin, Y., Booth, R.K., Gu, Y., Wang, Y. and Xie, S. 2009. Testate amoebae as indicators of 20th century environmental change in Lake Zhangdu, China. *Fundamental and Applied Limnology.* **175**(1); pp.29-38.

Quinton, W.L., Hayashi, M. and Chasmer, L.E. 2011. Permafrost-thaw-induced land-cover change in the Canadian subarctic: implications for water resources. *Hydrological Processes*. **25**(1); pp.152-158.

R Core Team (2014) *R: A language and environment for statistical computing*, R Foundation for Statistical Computing, Vienna, Austria. [Online] http://www.R-project.org.

Reyes, A.V. and Cooke, C.A. 2011. Northern peatland initiation lagged abrupt increases in deglacial atmospheric CH3. *PNAS*. **108**(12); pp.4748-4753.

Rooney-Varga, J.N., Giewat, M.W., Duddleston, K.N., Chanton, J.P. and Hines, M.E. 2007. Links between archaeal community structure, vegetation type and methanogenic pathway in Alaskan peatlands. *FEMS Microbiology Ecology*. **60**(2); pp.240-251.

Roulet, N.T., Lafleur, P.M., Richard, P.J.H., Moore, T.R., Humphreys, E.R. and Bubier, J. 2007. Contemporary carbon balance and late Holocene carbon accumulation in a northern peatland. *Global Change Biology*. **13**(2); pp.397-411

Routh, J., Hugelius, G., Kuhry, P., Filley, T., Tillman, P.K., Becher, M. and Crill, P. 2014. Multi-proxy study of soil organic matter dynamics in permafrost peat deposits reveal vulnerability to climate change in the European Russian Arctic. *Chemical Geology*. **368**; pp.104-117.

Sannel, A.B.K., Hugelius, G., Jansson, P. and Kuhry, P. 2016. Permafrost Warming in a Subarctic Peatland – Which meteorological controls are most important?. *Permafrost and Periglacial Processes*. **27**(2); pp.177-188.

Schaefer, K., Zhang, T., Bruhwiler, L. and Barrett, A.P. 2011. Amount and timing of permafrost carbon release in response to climate warming. *Tellus*. **63**(2); pp.165-180.

Schuur, E.A.G., McGuire, A.D., Schädel, C., Grosse, G., Harden, J.W., Hayes, D.J., Hugelius, G., Koven, C.D., Kuhry, P., Lawrence, D.M., Natali, S.M., Olefeldt, D., Romanovsky, V.E., Schaefer, K., Turetsky, M.R., Treat, C.C. and Vonk, J.E. 2015. Climate change and the permafrost carbon feedback. *Nature*. **520**; pp.171-179.

Schuur, E.A.G., Abbott, B.W., Bowden, W.B., Brovkin, V., Camill, P., Canadell, J.G., Chanton, J.P., Chapin III, F.S., Christensen, T.R., Ciais, P., Crosby, B.T., Czimczik, C.I., Grosse, G., Harden, J., Hayes, D.J., Hugelius, G., Jastrow, J.D., Jones, J.B., Kleinen, T., Koven, C.D., Krinner, G., Kuhry, P., Lawrence, D.M., McGuire, A.D., Natali, S.M., O'Donnell, J.A., Ping, C.L., Riley, W.J., Rinke, A., Romanovsky, V.E., Sannel, A.B.K., Schädel, C., Schaefer, K., Sky, J., Subin, Z.M., Tarnocai, C., Turetsky, M.R., Waldrop, M.P., Walter Anthony, K.M., Wickland, K.P., Wilson, C.J. and Zimov, S.A. 2013. Expert assessment of vulnerability of permafrost carbon to climate change. *Climatic Change*. **119**(2); pp.359-374.

Schuur, E.A.G. and Abbott, B. 2011. Climate change: High risk of permafrost thaw. *Nature*. **480**; pp.32-33.

Schuur, E.A.G., Vogel, J.G., Crummer, K.G., Lee, H., Sickman, J.O. and Osterkamp, T.E. 2009. The effect of permafrost thaw on old carbon release and net carbon exchange from tundra. *Nature.* **459**; pp.556-559.

Schuur, E.A.G., Bockheim, J., Canadell, J.G., Euskirchen, E., Field, C.B., Goryachkin, S.V., Hagemann, S., Kuhry, P., Lafleur, P.M., Lee, H., Mazhitova, G., Nelson, F.E., Rinke, A., Romanovsky, V.E., Shiklomanov, N., Tarnocai, C., Venevsky, S., Vogel, J.G. and Zimov, S.A. 2008. Vulnerability of Permafrost Carbon to Climate Change: Implications for the Global Carbon Cycle. *BioScience*. **58**(8); pp.701-714.

Siemensma, F.J. 2018. *Microworld, world of amoeboid organisms*, Kortenhoef, Netherlands [Online] https://www.arcella.nl (accessed 8th March 2018).

Sillasoo, U., Mauquoy, D., Blundell, A., Charman, D., Blaauw, M., Daniell, J.R.G., Toms, P., Newberry, J., Chambers, F.M. and Karofeld, E. 2007. Peat multi-proxy data from Männikjärve bog as indicators of late Holocene climate changes in Estonia. *BOREAS*. **36**(1); pp.20-37.

Simpson, G.L. and Oksanen, J. 2016. *Analogue: Analogue matching and Modern Analogue Technique transfer function models*, R package version 0.17-0. [Online] http://CRAN.R-project.org/package=analogue.

Smith, L.C., Sheng, Y., MacDonald, G.M. and Hinzman, L.D. 2005. Disappearing Arctic lakes. *Science*. **308**(5727); p.1429.

Smith, A.J.E. 2004. *The Moss Flora of Britain and Ireland*. Second Edition. Cambridge University Press, Cambridge, pp.1011.

Stocker, T. F., Qin, D., Plattner, G.-K., Alexander, L.V., Allen, S.K., Bindoff, N.L., Bréon, F.-M., Church, J.A., Cubasch, U., Emori, S., Forster, P., Friedlingstein, P., Gillett, N., Gregory, J.M., Hartmann, D.L., Jansen, E., Kirtman, B., Knutti, R., Krishna Kumar, K., Lemke, P., Marotzke, J., Masson-Delmotte, V., Meehl, G.A., Mokhov, I.I., Piao, S., Ramaswamy, V., Randall, D., Rhein, M., Rojas, M., Sabine, C., Shindell, D., Talley, L.D., Vaughan, D.G. and Xie, S.-P. 2013. Technical Summary. In *Climate Change 2013: The Physical Science Basis. Contribution of Working Group I to the Fifth Assessment Report of the Intergovernmental Panel on Climate Change* [Stocker, T.F., Qin, D., Plattner, G.-K., Tignor, M., Allen, S.K., Boschung, J., Nauels, A., Xia, Y., Bex, V. and Midgley, P.M. (eds)]. Cambridge University Press, Cambridge, United Kingdom and New York, NY, USA, pp.33-115.

Sullivan, P.F., Arens, S.J.T., Chimner, R.A. and Welker, J.M. 2008. Temperature and microtopography interact to control carbon cycling in a high arctic fen. *Ecosystems*. **11**(1); pp.61-76.

Swindles, G.T., Kelly, T.J., Roucoux, K.H. and Lawson, I.T. 2018. Response of testate amoebae to a late Holocene ecosystem shift in an Amazonian peatland. *European Journal of Protistiology*. **64**; pp.13-19.

Swindles, G.T., Morris, P.J., Mullan, D., Watson, E.J., Turner, T.E., Roland, T.P., Amesbury, M.J., Kokfelt, U., Schoning, K., Pratte, S., Gallego-Sala,

A., Charman, D.J., Sanderson, N., Garneau, M., Carrivick, J.L., Woulds, C., Holden, J., Parry, L. and Galloway, J.M. 2015a. The long-term fate of permafrost peatlands under rapid climate warming. *Scientific Reports*. **5**: 17951.

Swindles, G.T., Amesbury, M.J., Turner, T.E., Carrivick, J.L., Woulds, C., Raby, C., Mullan, D., Roland, T.P., Galloway, J.M., Parry, L., Kokfelt, U., Garneau, M., Charman, D.J. and Holden, J. 2015b. Evaluating the use of testate amoebae for palaeohydrological reconstruction in permafrost peatlands. *Palaeogeography, Palaeoclimatology, Palaeoecology*. **424**; pp.111-122.

Swindles, G.T., Reczuga, M., Lamentowicz, M., Raby, C.L., Turner, T.E., Charman, D.J., Gallego-Sala, A., Valderrama, E., Williams, C., Draper, F., Honorio Coronado, E.N., Roucoux, K.H., Baker, T., Mullan, D.J. 2014. Ecology of Testate amoebae in an Amazonian Peatland and Development of a Transfer Function for Palaeohydrological Reconstruction. *Microbial Ecology*. **68**(2); pp.284-298.

Swindles, G.T., Blundell, A., Roe, H.M. and Hall, V.A. 2010. A 4500-year proxy climate record from peatlands in the North of Ireland: the identification of widespread summer 'drought phases'?. *Quaternary Science Reviews*. **29**(13-14); pp.1577-1589.

Swindles, G.T., Charman, D.J., Roe, H.M. and Sansum, P.A. 2009. Environmental controls on peatland testate amoebae (Protozoa: Rhizopoda) in the North of Ireland: Implications for Holocene palaeoclimate studies. *Journal of Paleolimnology*. **42**(1); pp.123-140.

Swindles, G.T. and Roe, H.M. 2007a. Examining the dissolution characteristics of testate amoebae (Protozoa: Rhizopoda) in low pH conditions: Implications for peatland palaeoclimate studies. *Palaeogeography, Palaeoclimatology, Palaeoecology.* **252**(3-4); pp.486-496.

Swindles, G.T., Plunkett, G. and Roe, H.M. 2007b. A multiproxy climate record from a raised bog in County Fermanagh, Northern Ireland: a critical examination of the link between bog surface wetness and solar variability. *Journal of Quaternary Science*. **22**(7); pp.667-679.

Tarnocai, C., Canadell, J.G., Schuur, E.A.G., Kuhry, P., Mazhitova, G. and Zimov, S. 2009. Soil organic carbon pools in the northern circumpolar permafrost region. *Global Biogeochemical Cycles*. **23**(2); pp.1-11.

Taylor, L.S., Swindles, G.T., Morris, P.J. and Gałka, M. 2019. Ecology of peatland testate amoebae from the Alaskan continuous permafrost zone. *Ecological Indicators*. **96**(1); pp.153-162.

Treat, C.C., Wollheim, W.M., Varner, R.K., Grandy, A.S., Talbot, J. and Frolking, S. 2014. Temperature and peat type control CO_2 and CH_4 production in Alaskan permafrost peats. *Global Change Biology*. **20**(8); pp.2674-2686.

Trenberth, K.E. 2011. Changes in precipitation with climate change. *Climate Research*. **47**; pp.123-138.

Tolonen, K., Warner, B.G. and Vasander, H. 1992. Ecology of Testaceans (Protozoa: Rhizopoda) in Mires in Southern Finland: I. Autecology. *Archiv für Protistenkunde*. **142**(3-4); pp.119-138.

Turetsky, M.R., Benscoter, B., Page, S., Rein, G., van der Werf, G.R. and Watts, A. 2015. Global vulnerability of peatlands to fire and carbon loss. *Nature Geoscience*. **8**; pp.11-14.

Turetsky, M.R., Wieder, R.K., Vitt, D.H., Evans, R.J. and Scott, K.D. 2007. The disappearance of relict permafrost in boreal North America: Effects on peatland carbon storage and fluxes. *Global Change Biology*. **13**(9); pp.1922-1934.

Turetsky, M.R., Wieder, R.K. and Vitt, D.H. 2002. Boreal peatland C fluxes under varying permafrost regimes. *Soil Biology and Biochemistry*. **34**; pp.907-912.

Turner, T.E. and Swindles, G.T. 2012. Ecology of Testate Amoebae in Moorland with a complex fire history: Implications for ecosystem monitoring and sustainable land management. *Protist*. **163**(6); pp.844-855.

United Nations. 2015. *Conference of the Parties, Twenty-first session: Adoption of the Paris Agreement*, Paris, United Nations Framework Convention on Climate Change.

Urban, N.R., Eisenreich, S.J., Grigal, D.F. and Schurr, K.T. 1990. Mobility and diagenesis of Pb and ^{210}Pb in peat. *Geochimica et Cosmochimica Acta*. **54**(12); pp.3329-3346.

Väliranta, M., Blundell, A., Charman, D.J., Karofeld, E., Korhola, A., Sillasoo, Ü and Tuittila, E.-S. 2012. Reconstructing peatland water tables using transfer functions for plant macrofossils and testate amoebae: A methodological comparison. *Quaternary International*. **268**; pp.34-43.

van Bellen, S., Magnan, G., Davies, L., Froese, D., Mullan-Boudreau, G., Zaccone, C., Garneau, M. and Shotyk, W. 2018. Testate amoeba records indicate regional 20th-century lowering of water tables in ombrotrophic peatlands in central-northern Alberta, Canada. *Global Change Biology*. **24**(7); pp.2758-2774.

Vaughan, D.G., J.C. Comiso, I. Allison, J. Carrasco, G. Kaser, R. Kwok, P. Mote, T. Murray, F. Paul, J. Ren, E. Rignot, O. Solomina, K. Steffen and T. Zhang. (2013) Observations: Cryosphere. In*: Climate Change 2013: The Physical Science Basis. Contribution of Working Group I to the Fifth Assessment Report of the Intergovernmental Panel on Climate Change* [Stocker, T.F., D. Qin, G.-K. Plattner, M. Tignor, S.K. Allen, J. Boschung, A. Nauels, Y. Xia, V. Bex and P.M. Midgley (eds.)]. Cambridge University Press, Cambridge, United Kingdom and New York, NY, USA.

Vitt, D.H., Bayley, S.E. and Jin, T-L. 1995. Seasonal variation in water chemistry over a bog-rich fen gradient in Continental Western Canada. *Canadian Journal of Fisheries and Aquatic Sciences*. **53**(3); pp.587-606.

Walker, M.D., Walker, D.A. and Auerbach, N.A. 1994. Plant communities of a tussock tundra landscape in the Brooks Range Foothills. Alaska. *Journal of Vegetation Science*. **5**; pp.843–866.

Walter, K.M., Zimov, S.A., Chanton, J.P., Verbyla, D. and Chapin III, F.S. 2006. Methane bubbling from Siberian thaw lakes as a positive feedback to climate warming. *Nature*. **443**; pp.71-75.

Wang, M. and Overland, J.E. 2009. A sea ice free summer Arctic within 30 years?. *Geophysical Research Letters*. **36**(7); L07502.

Wania, R., Ross, I. and Prentice, I.C. 2009. Integrating peatlands and permafrost into a dynamic global vegetation model: 2. Evaluation and

sensitivity of vegetation and carbon cycle processes. *Global Biogeochemical Cycles*. **23**(2); GB3015, pp.1-15.

Wilkinson, D.M. and Mitchell, E.A.D. 2010. Testate Amoebae and Nutrient Cycling with Particular Reference to Soils. *Geomicrobiology Journal*. **27**; pp.520-533.

Wilmshurst, J.M., Wiser, S.K. and Charman, D.J. 2003. Reconstructing Holocene water tables in New Zealand using testate amoebae: differential preservation of tests and implications for the use of transfer functions. *The Holocene*. **13**(1); pp.61-72.

Xu, J., Morris, P.J., Liu, J. and Holden, J. 2018. PEATMAP: Refining estimates of peatland distribution based on a meta-analysis. *CATENA*. **160**; pp.134-140.

Yi, S., Woo, M. and Arain, M.A. 2007. Impacts of peat and vegetation on permafrost degradation under climate warming. *Geophysical Research Letters*. **34**(16); pp.1-5.

Yu, Z., Beilman, D.W. and Jones, M.C. 2009. Sensitivity of Northern Peatland Carbon Dynamics to Holocene Climate Change. *Geophysical Monograph Series*. **184**; pp.55-69.

Zhang, H., Piilo, S.R., Amesbury, M.J., Charman, D.J., Gallego-Sala, A.V. and Väliranta, M.M. 2018a. The role of climate change in regulating Arctic permafrost peatland hydrological and vegetation change over the last millennium. *Quaternary Science Reviews*. **182**; pp.121-130.

Zhang, H., Väliranta, M., Amesbury, M.J., Charman, D.J., Laine, A. and Tuittila, E.-S. 2018b. Successional change of testate amoeba assemblages along a space-for-time sequence of peatland development. *European Journal of Protistology*. **66**; 36-47.

Zhang, H., Amesbury, M.J., Ronkainen, T., Charman, D.J., Gallego-Sala, A.V. and Väliranta, M. 2017. Testate amoeba as palaeohydrological indicators in the permafrost peatlands of north-east European Russia and Finnish Lapland. *Journal of Quaternary Science.* **32**(7); pp.976-988.

Zimov, S.A., Davydov, S.P., Zimova, G.M., Davydova, A.I., Schuur, E.A.G., Dutta, K. and Chapin III, F.S. 2006. Permafrost carbon: Stock and decomposability of a globally significant carbon pool. *Geophysical Research Letters*. **33**(20); pp.1-5.

Zoltai, S.C. 1995. Permafrost Distribution of Peatlands of West-Central Canada During the Holocene Warm Period 6000 Years BP. *Géographie physique et Quaternaire*. **49**(1); pp.45-54.

Zoltai, S.C. 1993. Cyclic development of permafrost in the peatlands of Northwestern Alberta, Canada. *Arctic and Alpine Research*. **25**(3); pp.240-246.

Appendix A - Details of plant species identified at each of the five sampling sites in the Alaskan North Slope.

Taxa name	In *n* samples	Percentage of samples taxa is present in				
		Montane	Spring	Valley	String	Lakeshore
Andromeda glaucophylla	23	50	5	5	35	20
Aulacomnium palustre	6	0	15	10	5	0
Aulacomnium turgidum	7	5	5	0	0	25
Betula nana	7	20	0	5	0	10
Brachythecium mildeanum	1	0	5	0	0	0
Bryum sp.	14	15	20	0	30	5
Calliergon cordifolium	2	0	0	0	0	10
Calliergon richardsonii	2	0	0	0	0	10
Campylium cf. laxifolium	1	0	5	0	0	0
Campylium stellatum	22	40	20	0	30	20
Cinclidium stygium	17	20	40	0	15	10
Cirriphyllum piliferum/cirrosum	1	0	0	0	0	5
Dicranella sp.	8	5	10	0	15	10
Dryas integrifolia	6	5	25	0	0	0
Fissidens sp.	4	20	0	0	0	0
Hylocomnium splenders	6	10	5	0	0	15
Hypnum pratense	2	0	10	0	0	0
Loeskypnum badium	1	0	0	0	0	5
Meesia triquetra	13	0	20	0	30	15
Paludella squarrosa	5	0	5	0	0	20
Pohlia sp.	2	0	0	10	0	0
Polytrichum cf. juniperinum	2	0	10	0	0	0
Polytrichum commune	12	0	0	60	0	0
Polytrichum juniperinum	4	0	0	20	0	0
Pseudocalliergon sp.	3	15	0	0	0	0
Salix reticulata	2	10	0	0	0	0
Salix sp.	5	5	20	0	0	0
Sarmentypnum sarmentosum	1	0	0	0	5	0
Scorpidium cossoni	14	0	0	0	25	45
Scorpidium cossoni/revolvens	16	55	25	0	0	0
Scorpidium scorpioides	9	0	10	0	35	0
Sparganium sp.	1	0	0	5	0	0
Sphagnum capillifolium	4	0	0	0	0	20
Sphagnum contortum	1	0	0	0	0	5
Sphagnum teres	3	0	0	0	0	15
Sphagnum teres/squarrosum	17	0	0	85	0	0
Sphagnum wahrnstorfii	7	0	15	0	0	20
Straminergon stramineum	9	0	0	30	0	15
Tomentypnum nitens	33	70	45	0	20	30
Warnstorfia cf. exannulata	7	0	0	35	0	0

Appendix B – ANOSIM (analysis of similarities) of testate amoebae and plant distribution between five peatlands across the Alaskan North Slope.

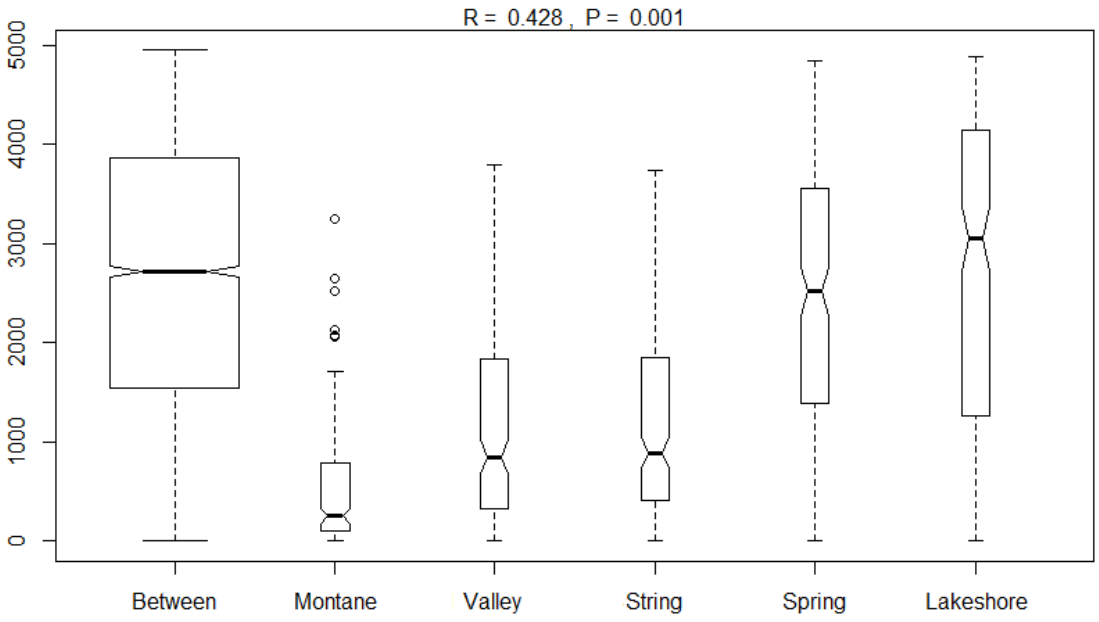

ANOSIM analysis of testate amoebae distribution between sites.

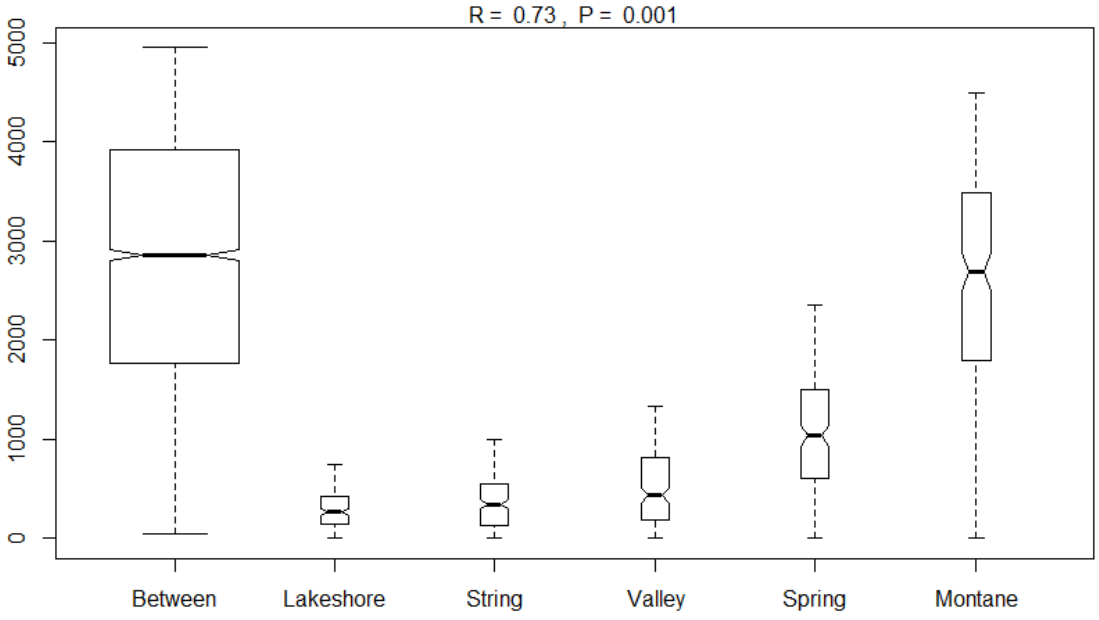

ANOSIM analysis of contemporary plant species distribution between sites.

Appendix C – Reconstructions of climate variables from the PAGES2k and CRU-TS datasets.

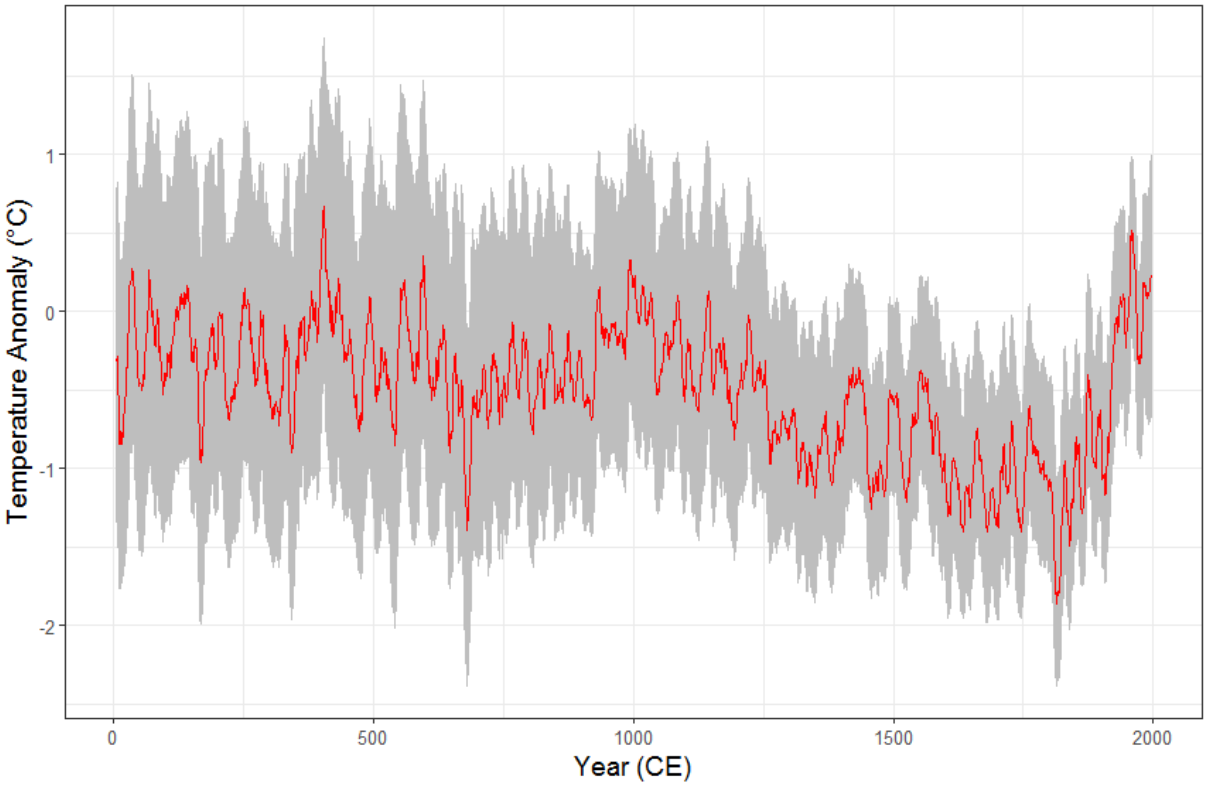

Arctic temperature reconstruction over the late-Holocene using data from PAGES2k. 10-year running mean is displayed in red, with error in grey shading. Temperatures are anomalies relative to the 1961-1990 base period.

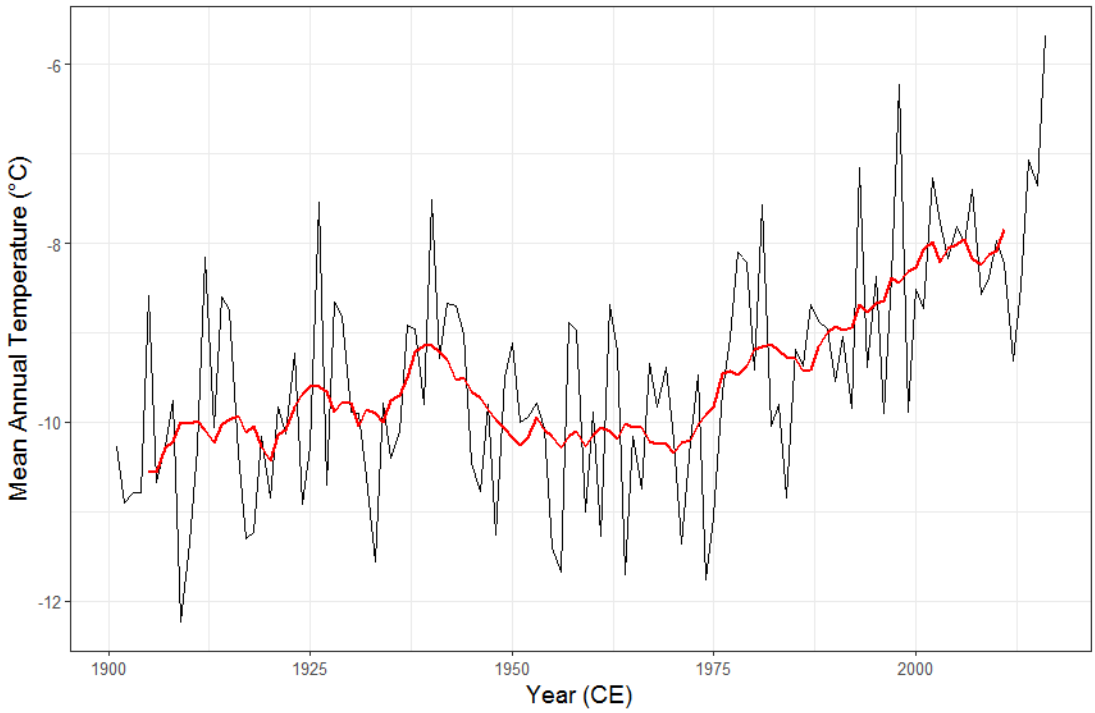

Temperature reconstruction from 1901 using CRU-TS v 4.01 dataset from the 68.75°N, 149.75°W grid cell. Black line shows mean annual temperature (°C), red line shows 10-year running mean.

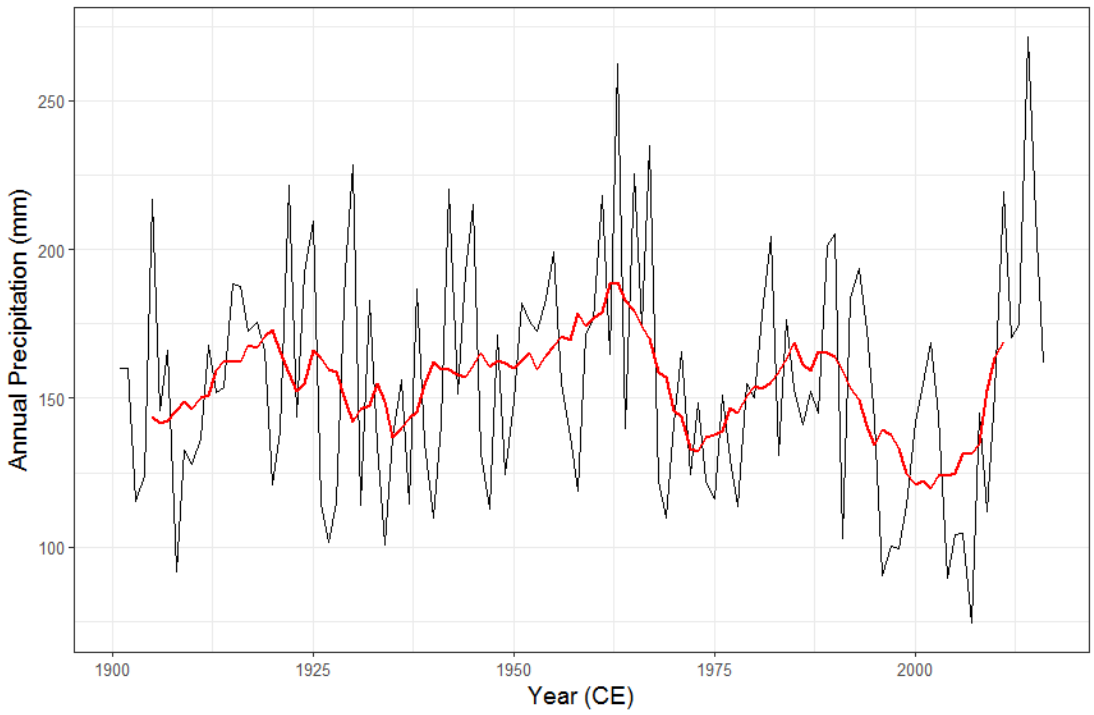

Precipitation reconstruction from 1901 using CRU-TS v 4.01 dataset from the 68.75°N, 149.75°W grid cell. Black line shows annual precipitation total (mm), red line shows 10-year running mean.

Appendix D – Box plots showing change in CAR pre- and post- 1850

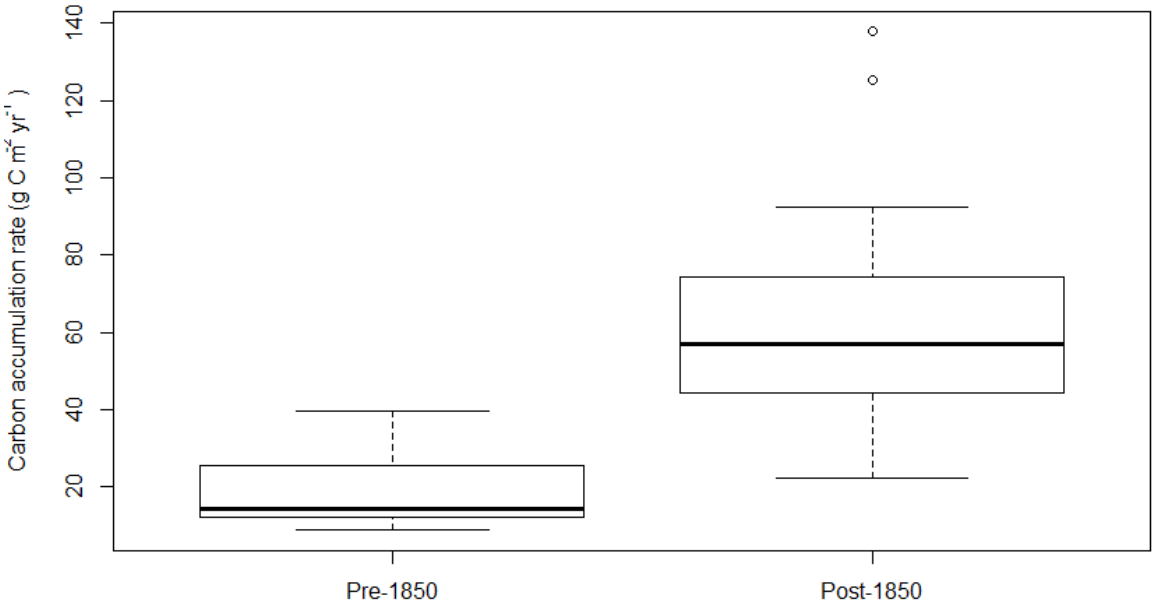

Change in CAR post-1850 in TFS1.

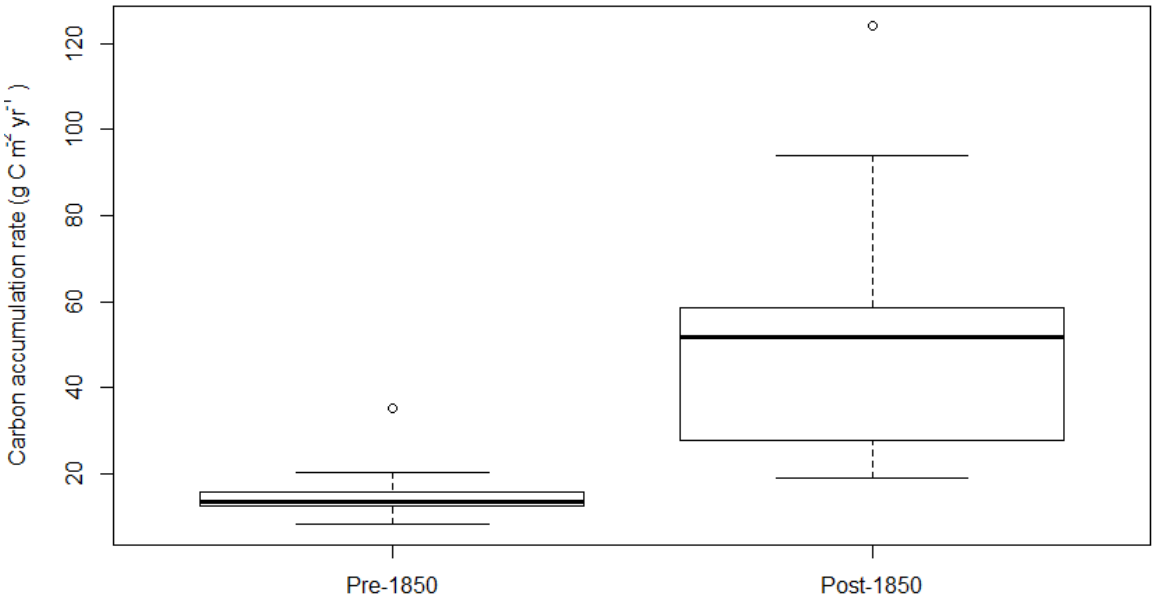

Change in CAR post-1850 in TFS2.